UNIVERSITY OF TRENTO

Doctoral School in Civil, Environmental and Mechanical Engineering

Curriculum 1. Civil and Environmental Engineering

Matteo De Vincenzi

Monitoring transport processes in slow flow inland waters

The case study of the Mantua wetland-lake system

2026 - Doctoral thesis

UNIVERSITY OF TRENTO - Italy
Department of Civil, Environmental and Mechanical Engineering

Doctoral School in Civil, Environmental and Mechanical Engineering
Topic 1. Civil and Environmental Engineering - XXXVIII cycle 2023/2025

Doctoral Thesis - April 2026

Matteo De Vincenzi

Monitoring transport processes in slow flow inland waters

The case study of the Mantua wetland-lake system

Supervisors
Marco Tubino - University of Trento
Luca Adami - University of Trento

Credits of the cover image: Matteo De Vincenzi

University of Trento
Doctoral School in Civil, Environmental and Mechanical Engineering
http://web.unitn.it/en/dricam
Via Mesiano 77, I-38123 Trento
Tel. +39 0461 282670 / 2611 - *dicamphd@unitn.it*

"I used to think that top environmental problems were biodiversity loss, ecosystem collapse and climate change. I thought that thirty years of good science could address these problems. I was wrong. The top environmental problems are selfishness, greed and apathy, and to deal with these we need a cultural and spiritual transformation. And we scientists don't know how to do that."

James Gustave Speth

Acknowledgements

I would like to thank my supervisor for recognising my passion for field measurements and for valuing it so deeply, providing me with the opportunity to give my best throughout this work. A special mention goes to the people who joined me in the hardest fieldwork: Martina Busetti, Leoluca Corello, Alice Zorzi, Matteo Giovannini, Gaia Donini, Ali Farrokhi, Francesca Hinegk, Gabriele Barile, Riccardo Salucci, Niccolò Ragno. Thanks to all my colleagues — or rather, my friends — who have shared with me not only moments of joy, but also the challenges and uncertainties along the way. Today I realise that the difficulties that once felt so overwhelming are, in truth, relatively small compared to the real challenges of life.

Abstract

Physical processes in lentic ecosystems are driven by different forcings than those in lotic environments, where hydrodynamic actions are dominant. As the flow velocity gradually decreases, other processes begin to play a significant role, such as temperature gradients, wind forcing, and the presence of vegetation. This is precisely the case in the Mincio fluvial system near the city of Mantua (Lombardy, Northern Italy), where the morphology changes from a single-thread river to a fluvial lake complex, passing through a multiple-channel transitional wetland. Most of the catchment area of this unique lake system is located within the Po Valley, specifically downstream of a heavily human-altered environment with intensive agricultural use. As a result, it suffers from many environmental problems, including eutrophication, siltation, hypoxia, and the spread of invasive macrophytes, further exacerbated by low discharge. In fact, the flow regime in the Mincio River is regulated by a complex system of hydraulic infrastructures, which have been designed to guarantee flood protection, but often in conflict with environmental conservation. The present study aims to investigate different processes (morphological evolution, dissolved oxygen dynamics, temperature-induced circulations) that characterise this lentic ecosystem, on the basis of an extensive dataset of field measurements. All of the studied aspects are related to transport processes that, given the low-energy environment, are highly sensitive to small variations in the drivers and to external forcings. For this reason, a complete understanding of these dynamics is crucial for better management of the system.

First, an analysis was conducted to identify the most effective methodology for achieving good-quality velocity measurements in slow currents ($< 10\,\mathrm{cm/s}$). The performance of different Acoustic Doppler Current Profilers (ADCP) was tested and compared, helping to fill the literature gap on ADCP application in lakes. Technical solutions were also suggested to resolve instrument-related problems. Another series of instrumentation tests was conducted as part of the setup of a low-cost sonar device designed to investigate the morphological evolution of the lake system. With this instrument, a bathymetric survey of the lake and wetland was acquired and compared

with available historical maps dating back to 2006. The evidence of a deposition trend was clear, with depth differences of the order of 1 m and a possible risk of terrestrialization. Twenty monthly field campaigns, including discharge, total suspended solids concentration and dissolved nutrients measurements, were conducted at five sections of the Mincio River and in its two main tributaries (Goldone and Osone channels). These two channels, which mainly drain agricultural areas, were identified as responsible for high nutrient and suspended solids loads after rainfall events. In addition, dissolved oxygen sensors were deployed at different depths, inside and outside vegetation patches, both in the lake and in the wetland. As a result of unfavourable ecological and hydrodynamic conditions, severe bottom anoxia problems were observed during the summer, especially under emerging macrophyte cover. Following the testing phase, an ADCP was used to monitor water circulation in Mantua's Lake Superiore. The occurrence of density-driven currents, which had been hypothesised to be due to the presence of vegetation and a sloping bottom, was confirmed by field measurements. The velocity measurements were coupled with a 2-year continuous temperature monitoring with logger chains at different locations in the lake. This allowed the quantification of the effect of dense vegetation patches on water temperature.

The present work offers a twofold contribution: it provides evidence-based management recommendations for local authorities and also makes available to the scientific community an extensive field study on key topics of freshwater lentic ecosystems, such as sedimentation, anoxia, water mixing, and the role of aquatic vegetation, which can be extended to other similar low-energy water environments.

Contents

List of Figures

List of Tables

1. Introduction

Unlike rivers, where the water current acts as the main controlling factor, slow water bodies can be affected by multiple drivers. The hydrodynamics of lakes and reservoirs is governed by different agents, including weather forcing (e.g., wind, solar radiation), the occurrence of internal waves, the presence of inflows or outflows, and the spread of aquatic vegetation. The combination of different driving forces that may potentially have the same importance increases the complexity of this kind of water bodies. For this reason, a complete study of these systems cannot rely only on a simple mono-topic investigation (i.e., a single set of field measurements or a traditional modelling approach), but requires the integration of different investigation methodologies (Salmaso and Mosello, 2022).

This integrated approach must be supported by different measurement technologies and coupled with a broad area of interdisciplinary expertise. Additionally, the balance between the drivers is highly site-specific: in a fluvial lake, for example, the through-flowing discharge can become predominant; in a shallow lake, the wind strength can be enough to mix the entire water column; in a basin colonised by macrophytes, vegetation can have a relevant effect on water temperature, circulation, and dissolved oxygen. Other examples are represented by cold environments, where the ice coverage can alter the lake's dynamics, or coastal marshes, where the tide has an important effect on water circulation. This implies that a study regarding a particular context should be focused on the specific case study of interest and can hardly be generalised, except to similar systems and only with proper caution. Anthropogenic pressures such as eutrophication, hydrological alterations, imported invasive organisms, and inefficient sediment management add further complexity to the system.

A perfect example of such environments, where an integrated approach is essential, is the Mantua lake system (Mantua, Lombardy, Northern Italy), created by the Mincio River. The Mincio River is the outflow of Lake Garda; therefore, its water is clear and has a good quality index at the beginning of its course. Around the city of Mantua there is a complex hydraulic system, which was designed primarily for flood

protection: in case of high discharge in Mincio, water is diverted into an artificial channel, called "Diversivo", bypassing the lake system to protect the city of Mantua. Due to a cautionary plan adopted by the local water management agency (AIPo), the remaining discharge in the Mincio River can be even lower than the Minimum Vital Flow of $6\,m^3/s$. Concurrently, the incoming discharge from the (not-regulated) river's tributaries is usually higher because of heavy rainfall. These tributaries collect water from agricultural drainages; as a result, they carry huge amounts of nutrients and fine sediments originating from surface runoff. This contribution to the Mincio River has a detrimental effect on water quality, further worsened by the low incoming discharge of clear water that could dilute suspended sediments and nutrients input.

Near the village of Rivalta the river forms a wetland with a complex network of secondary channels. This results in a slowdown of the water velocity, which in turn causes the settling of suspended particles. As a consequence, most of the secondary channel network is threatened by terrestrialization, with a switch from hydrophytes to helophytes and ultimately terrestrial plants. This process leads to the loss of habitats of great ecological value, listed in the NATURA2000 European protected sites.

Downstream of the wetland, a dam on the Mincio River creates Lake Superiore, an artificial shallow lake that was completely re-naturalised and is part of the lake system surrounding the city of Mantua. Similarly to the wetland, the lake is also affected by sedimentation problems, like many reservoirs in the world. Additionally, the high nutrient load, together with the increased water renewal time due to low discharges, resulted in eutrophication of the lake system, which is now classified as hypereutrophic (Pinardi et al., 2021). As a consequence, Mantua lakes are nowadays in the "Turbid-water" state (Scheffer, 2004), with Secchi disc depth of around 50 cm during summers (ARPA Lombardia, 2020). Floating and emergent species of vegetation prevail over submerged macrophytes due to light limitation in the water column. In particular, *Nelumbo nucifera*, an Asiatic macrophyte commonly known as lotus flower, has become invasive after being imported in the 1920s. Currently, it covers one fourth of the lake's surface with dense vegetation patches. This macrophyte produces a considerable amount of biomass, further worsening the terrestrialization problem, and it also affects the dynamics of dissolved oxygen in the underlying water column, resulting in hypoxia.

This case study gives the opportunity to deal with the complexity of water circulation and related transport processes in a shallow fluvial lake system where all the above-mentioned anthropogenic pressures are present, together with multiple utilisations of the water resource. The management of this environment requires a good understanding of the system from various perspectives, which can be achieved only

through a complete basis of environmental data. With this objective, the present thesis addresses the challenge of including in a monitoring programme all the important drivers of a complex water system. The result is an integrated approach, which also attempts to merge different scientific areas, despite the increasing specialisation of science.

This thesis work tackles the wide topic of transport processes in slow-moving water bodies via the implementation of a detailed field monitoring plan focused on the specific case study of Mantua. In this regard, the main research question that is addressed can be summarised as follows: how to improve water quality in the Mantua lake system and protect its ecosystem from the consequences of land use changes. This has a direct management application in this specific context, but can also be generalised to answer different scientific questions such as:

- What is the best instrument configuration to acquire robust velocity measurements of slow-moving currents using an Acoustic Doppler Current Profiler?
- How fast is the sedimentation trend in a strongly regulated water body with high sediment inputs from the catchment?
- What is the influence of floating and emergent macrophytes on dissolved oxygen fluctuations in a highly eutrophic lake and wetland?
- What are the effects of a dense population of emergent macrophytes on water speed and temperature?

After the description of the study area and the related previous works, this dissertation starts with an introduction about some limnological topics that are considered important for a complete understanding of the following parts. After that, the core of the work is structured in 4 sections: the first one (Section 4) is the most methodological and describes the tests of some current profilers that were conducted before the measurement campaigns to choose the most suitable instrument for this particular environment. Section 5 shows how a bathymetric survey of the lake and wetland area was conducted and compared with historical data to evaluate the system's morphological evolution. Sedimentation rates were estimated and the source of the sediment was characterised with a dedicated monitoring plan. Section 6 presents the results of continuous dissolved oxygen measurements under different conditions. Section 7 deals with the effects of vegetation on water temperature and the resulting density-induced circulations. Lastly, general conclusions are provided, including some management suggestions.

2. Study area

This study focuses on the portion of the Mincio River located in the province of Mantua. The province is located in the south-eastern part of the Lombardy region, Northern Italy (Figure 2.1) and has a predominantly flat morphology with the exception of the northernmost part. The landscape is marked by the valleys of the Po, Oglio, and Mincio Rivers, as well as by the presence of other minor watercourses such as Chiese and Secchia. A substantial irrigation canal network is also present and its importance is clear considering that the predominant land use is arable land, which occupies 79% of the province's area (ERSAF, 2004). The agricultural sector has in fact a strong economic importance throughout the province, with large crops and livestock farms. The climate is continental, as is typical of the Po Valley, characterised by rather harsh winters (average temperature 4.5 °C) and hot and sweltering summers (average temperature 24 °C)(ERSAF, 2004). The context is affected by the presence of the Alps to the north and the Apennines to the south, with a weak wind regime and a typical persistence of stable atmospheric conditions.

The Mincio River starts from the Salionze dam, which regulates the outflow from Lake Garda. After 45 km, near the city of Mantua, the Mulini bridge dam creates an enlargement of the Mincio River, resulting in an artificial lake called "Lake Superiore". The construction of this dam dates back to the XII century and its regulation has remained constant until today, giving the time for the ecosystem to become completely renaturalised. After the dam, the Mincio River forms 3 other water basins, named moving downstream "Di Mezzo", "Inferiore", and "Vallazza", before entering the Po River. Mantua lakes characterise in a particular way the landscape near the city, also constituting a tourist attraction. For example, many boat tours are organised every summer to admire the outstanding blossoming of lotus flower. Upstream of Lake Superiore, the Mincio River forms a transitional wetland with a network of channels, known as "Valli del Mincio" wetland (Figure 2.2). This is a protected area (ZPS IT20B0009 and SIC IT20B0017) with great naturalistic value, also included in Natura 2000 European protected sites. The entire Mincio River is included within the Mincio Park, which participates in the management decisions

Figure 2.1: Location of the Mincio River and the city of Mantua with respect to Mantua Province and Lombardy Region

for this area together with AIPo (Interregional Agency for the Po River), the water management authority. Further upstream on the Mincio River course, 2 artificial channels (Scaricatore and Diversivo) are used to divert the excessive discharge from the river in case of flood, in order to protect the city of Mantua.

The greatest hydraulic threat to Mantua is posed by floods in the Po River: the resulting backwater effect in the Mincio River can easily reach the city and increase the water level up to the urban area. To avoid this problem, 2 floodgates have been installed on the Mincio River, near Formigosa, 5 km downstream from the city of Mantua. In case of flood of the Po River, the gates are closed and the backwater is stopped. However, in this situation all the incoming discharge from the Mincio River cannot be released downstream because of the barrier. To solve this, near Casale di Goito, around 5 km upstream from Valli del Mincio, almost the entire discharge is diverted in the Diversivo channel which by-passes the Mantua lake system and returns the water downstream of the Formigosa floodgate. In this configuration, Mantua and its lakes are disconnected from the Mincio River and are protected from both upstream and downstream effects. This is a very efficient solution for civil protection, but it causes different environmental problems. The lakes and the wetland never experience high discharge events and water level fluctuations. Moreover, when the water is diverted, the remaining discharge in this stretch of the river can be lower than the Minimum Vital Flow (DMV), which was set at $6\,\mathrm{m}^3/\mathrm{s}$ from the Lombardy Regional Water Protection Plan (PTA).

The water from the Mincio River also supports irrigation activities in two main districts, grouped under the “Consorzio del Mincio”, served by two consortiums named “Consorzio Territori del Mincio” and “Consorzio Garda-Chiese”. Given the

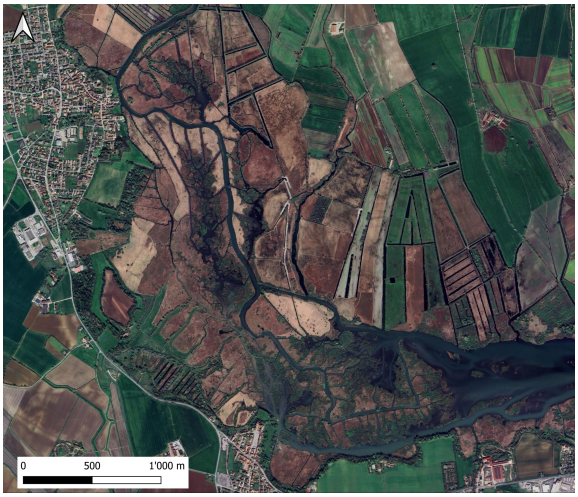

Figure 2.2: Google Satellite image of the Valli del Mincio wetland

high water demand during the irrigation season, these withdrawals often result in difficulties in complying with Minimum Vital Flow regulations. In addition, part of the river network is used for commercial navigation, which implies specific requirements on water level and the presence of several navigation locks.

2.1 Previous works on Mantua lake system

Due to the multiple uses of the water resource in the Mantua hydraulic node, water management is crucial and requires supporting data from scientific studies. This section provides a list of the most important investigations that have been conducted in the last two decades on the Mantua portion of the Mincio River system.

In 2004, the Water and Soil Service of Mantua Province's environmental office published a report on surface water quality in the province of Mantua with measured data and critical considerations on the impact of anthropogenic activities (Provincia di Mantova, 2004).

In 2007, the project "Da agenda 21 ad Azione 21", conducted by Telò et al. (2007), aimed to characterise the environmental state of the Mincio River and proposed an integrated and participated requalification strategy. Data from chemical and microbiological analyses conducted between the late 1980s and 2007, provided by the Mantua Province environmental office and the regional environment protection agency (ARPA), were organised into a database. The database also included discharge data provided by AIPO, Consorzio del Mincio, and ARPA. During this study,

a coarse, yet fundamental bathymetric survey was conducted, producing a map with 209 points on the whole lake system. Sediment samples were also collected from the lake bottom in 38 points. Additionally, the project report contains dissolved oxygen profiles acquired during summer 2006 by Mantua Province. Due to the shading of the water column and the limitation of water-atmosphere gas exchanges, the measured oxygen levels near floating macrophyte stands were much lower compared to those in open water.

As part of the same project, the "STRARIFLU" (River Restoration Strategies) method was applied to evaluate the quality of the Mincio River from many different aspects (Vannuccini et al., 2011). This analysis revealed that some reaches, in particular, showed a good environmental quality index, including the Valli del Mincio wetland and the upstream part of the river. However, the regulated hydrological regime, resulting in low and constant discharges due to irrigation withdrawals and flood protection purposes, appeared to be the main critical issue. The conclusions of the project emphasised the problems of long water renewal times in Mantua lakes and wetland due to low flows, with consequent permanent water stagnation in many marginal parts of the lakes, and of high nutrient load as causes of progressive lowering of water quality. Low discharges were also likely to affect the system's hydrodynamics and thus sediment transport capacity, leading to sediment accumulation and risk of terrestrialization. Some suggested actions were as follows:

- sediment dredging to reduce the internal nutrient load,
- lake flushing operations,
- increasing of the through-flowing discharge to improve the lake hydrodynamics,
- control of nutrient inputs,
- monitoring and management of lotus flower and water chestnut, with the opening of channels inside the vegetation islands to allow water circulation and reduce oxygen depletion caused by macrophytes.

Pinardi (2008) investigated the Mantua lake system from an ecological point of view, focusing on autotrophy and heterotrophy, mass balances of dissolved gases and nutrients, role of submerged and emergent macrophytes, phytoplankton, and hydraulic residence times. Since this work, the aquatic ecology group of the University of Parma has been actively investigating the Mantua case study, performing numerous fieldwork activities. More recently, they were able to combine fieldwork with remote-sensing data thanks to the collaboration with the National Research Council's Institute for Electromagnetic Sensing of the Environment (CNR IREA). They

used satellite data such as Sentinel-2, SPOT5, Landsat 8 and airborne hyper-spectral images to monitor seasonal dynamics in the spread of invasive macrophytes and algal blooms (e.g., Bolpagni et al., 2014; Villa et al., 2017; Pinardi et al., 2018; Villa et al., 2018; Bresciani et al., 2020; Pinardi et al., 2021, Bresciani et al., 2022). They also worked on benthic metabolism and the effect of different macrophyte species on biogeochemical processes (Pinardi et al., 2009) and recently focused on nutrient exchanges between river and groundwater in the Mincio watershed (Pinardi et al., 2020; Severini et al., 2022).

Between 2016 and 2019, the "EcoSUSTAIN" project (Latinopoulos et al., 2018), coordinated by the Mincio Regional Park and co-financed by the Interreg MED programme, involved several European protected areas with the goal of improving environmental monitoring and the sustainable management of aquatic ecosystems. In the Mincio River and the Mantua lake system, multiparameter buoys were installed to measure temperature, pH, dissolved oxygen, and nutrients. The project also studied the role of aquatic vegetation and water residence times in maintaining environmental quality. Best practices were shared among international partners to enhance biodiversity conservation.

ARPA Lombardia monitors water quality in 6 different stations on the Mincio River and at both surface and bottom of Superiore, Di Mezzo and Inferiore lakes. The most recent published dataset refers to 2024, while the most recent aggregated report refers to the period 2014-2019 (ARPA Lombardia, 2020).

The downstream portion of the Mantua lake system, including the Di Mezzo and Inferiore lakes and part of the Vallazza wetland, is a nationally significant contaminated site (SIN) due to the past unregulated activity of a petrochemical plant. For this reason, several studies were commissioned for sediment and water characterisation within this area and also in Lake Superiore.

Between 2003 and 2004 ARPA Lombardia studied sediment and water quality with chemical analysis, phytoplankton samplings, multiparameter probe profiles, sediment cores, and Secchi disc measurement in 9 points between Lake Superiore and Vallazza (Dalmiglio et al., 2005). In 2009 the Italian Ministry for the Environment published the results of a detailed and comprehensive investigation on this area conducted by the Italian Institute for Environmental Protection and Research (ISPRA, 2009). Field measurements included sediment core collection in 77 points from the Valli del Mincio wetland to Vallazza with granulometric curves, chemical, radiochemical and macrozoobenthos analysis, fish and bivalves collections for bioaccumulation analysis of target organisms, water samplings for chemical analysis and multiparameter probe profiles in 32 points (not including Lake Superiore), and a high resolution bathymetric survey (not including Lake Superiore).

From a hydrodynamic point of view, the only study concerning the Mantua lake system is Fenocchi (2015), where a 3D model (STAR-CCM+) was used to simulate the circulation processes that occur under different typical meteorological and hydrological conditions. In this model, lotus flower stands were considered as porous media using a Forchheimer-type formulation. The model was based on the bathymetry map acquired from the University of Parma during the project "Da Agenda 21 ad Azione 21". This map has low spatial resolution (only 107 points for the whole Lake Superiore), but it was the only bathymetry available at that time.

The Garda-Mincio system has also been the subject of several studies developed by the University of Trento in the last decade (Valerio, 2017; Pasinato, 2020, De Vincenzi, 2022; Accordini, 2022). In the Ph.D. work of Hinegk (2022), present and historical daily hydro-meteorological data were collected to assess the influence of climatic and anthropogenic drivers on water availability, the management of changing water demands and the trade-off with existing water ecosystem services over the last two centuries.

In 2024 and 2025 the Lombardy Region, through the Mincio Park authority, commissioned the University of Trento to produce a report on the application of the Environmental Flow in the Mincio River. Each of these works included a 1-year monitoring activity with monthly measurements of discharge, total suspended solids, dissolved oxygen, water temperature, and water quality in 5 different sections of the Mincio River and its 2 main tributaries (Adami et al., 2024; Adami et al., 2025). Some of the results of these works are also used in the present thesis. A similar field investigation had been carried out by the University of Parma in 2022 (Faggioli et al., 2022), although under very different conditions due to a particularly dry year.

3. Theoretical background: ecology of shallow lakes

The following section reports a bibliographic investigation regarding some limnological topics which are relevant for the ecology of low-energy shallow systems and, in particular, for this specific case study.

3.1 Eutrophication

Eutrophication, despite advances in its understanding in the 20th century, remains one of the main problems in the protection of freshwater and coastal marine ecosystems (Schindler, 2006).

Eutrophication is most commonly characterised by the proliferation of dense algal blooms that cause high turbidity and hamper light penetration. As algal biomass settles and decomposes, it contributes to oxygen depletion in the deeper layers of water bodies, leading to hypoxic conditions that can result in fish kills. Algae also interfere with the use of water for recreation, industry, agriculture, drinking, and other ecosystem services. Although eutrophication typically does not pose direct risks to human health (except during toxic cyanobacterial blooms), it significantly affects the availability of water resources. In the context of increasing water scarcity, this decline in water quality increases treatment costs and limits usable water supplies (Carpenter et al., 1998).

A comprehensive overview of eutrophication processes in lakes and rivers was provided by Hilton et al. (2006). Another review of lake's eutrophication dynamics, including recent developments in lake modelling, was presented by Bhagowati and Ahamad (2019).

The scientific understanding of eutrophication has consistently evolved since the 1960s, when Vollenweider (1968) first linked the phenomenon to nutrient loading from watershed sources, particularly phosphorus and nitrogen. Experimental work

by Schindler (1974) in a lake study in Ontario provided compelling evidence: nutrient additions to an oligotrophic lake rapidly induced eutrophic conditions. These findings laid the groundwork for regulatory approaches such as the European Water Framework Directive (Council of European Communities, 2000), which emphasises nutrient control as a central objective for improving water quality.

Nutrient inputs originate from both point sources, such as municipal wastewater treatment plants, and diffuse sources, particularly agriculture. While point sources of pollution can often be monitored and treated at the origin, diffuse sources are more difficult to measure and regulate and are often intermittent because they are related to irrigation or heavy rainfall events (Carpenter et al., 1998). Effective strategies for reducing non-point pollution include the establishment of riparian buffer zones and the restoration of wetlands to enhance natural nitrogen reduction through denitrification.

The Nitrates Directive (Council Directive 91/676/EEC) specifically addresses the risks posed by agricultural nitrate pollution to water bodies and human health. However, from an ecological perspective, the relative importance of nitrogen in driving eutrophication in freshwater systems remains debated (Conley et al., 2009). While phosphorus is widely recognised as the primary limiting nutrient, some researchers argue that the management of nitrogen inputs may be ineffective. For example, Schindler et al. (2008) demonstrated in a whole-lake experiment that reductions in nitrogen input did not prevent algal blooms. In contrast, Lewis and Wurtsbaugh (2008) showed that nitrogen is at least as likely as phosphorus to be limiting to phytoplankton growth.

Today, the focus of restoration strategies is primarily on reducing external nutrient loading. However, even after such reductions, internal loading from sediments (where large amounts of phosphorus accumulate over time) can delay ecosystem recovery, in particular in shallow lakes (Søndergaard et al., 2003). For example, Björk (1972) documented the case of the Swedish Lake Trummen where no improvement was observed even ten years after the external nutrient load was reduced. The persistence of internal loading is influenced by factors such as sediment chemistry, loading history, and hydraulic flushing rates (Marsden, 2006).

Several remediation techniques have been proposed to address internal phosphorus, including dredging, macrophyte harvesting, aeration, and chemical treatments (Cooke et al., 2016). Oglesby and Edmondson (1966) and Welch and Patmont (1980) introduced the idea of lake water dilution by flushing the lake with low-nutrient water. Their efforts were not directed at the control of internal loading, but simply at lowering nutrient concentrations. A successful application of this strategy occurred in Lake Veluwe (Netherlands), where flushing reduced phosphate levels and

phytoplankton biomass, while enhancing macrophyte recovery due to improved light availability (Hosper, 1997).

Water residence time is a crucial factor in determining the severity of eutrophication. Schindler (1978) showed that in lakes with minimal internal loading, halving the outflow (thus doubling residence time) can have similar effects as doubling nutrient inputs. This issue is becoming increasingly important in the context of climate change, which reduces streamflow, lowers lake levels, and lengthens water residence times, thereby exacerbating nutrient retention and the risk of eutrophication (Schindler, 2006).

However, higher discharge rates do not always improve water quality. Rennella and Quirós (2006) observed that in shallow lakes in the Pampa Plain (Argentina), an increase in discharge led to a threefold increase in total phosphorus concentration and a twofold increase in phytoplankton biomass. This was attributed to enhanced nutrient input from agricultural land. Similarly, Haygarth et al. (2005) reported an increase in total phosphorus concentrations during storm events in the River Taw basin (UK) from $26\,\mu gL^{-1}$ to $500\,\mu gL^{-1}$ due to surface runoff from diffuse agricultural sources.

3.2 Aquatic vegetation

Although aquatic vegetation has historically been considered only as a source of flow resistance from a purely hydraulic point of view, it provides a wide range of ecosystem services. The first among them is the improvement of water quality through nutrient uptake and oxygen production.

Macrophytes affect the aquatic ecosystem through physical, chemical, and biological processes. Conversely, environmental conditions determine the development of macrophytes. This raises complex interactions, potentially resulting in feedback effects. For example, vegetation growth and shape are influenced by the flow field existing within and around the vegetated region that is, in turn, influenced by the vegetation structure. Dense canopies reducing near-bed turbulence promote sediment retention and this enhances the supply of nutrient and fine substrate resulting in a further growth of vegetation. On the other hand, when vegetation is sparse, erosion increases because turbulence produced at the stem-scale increases the turbulence near the bed (Nepf, 2012). A review of the wide topic of vegetated flows, including their interactions with channel morphology and ecosystem, has been provided by Folkard (2011).

For a better understanding and management of environmental systems, it is essen-

tial to study the hydrodynamics of vegetation, considering also the interconnections with other disciplines such as biology, geomorphology, ecology, and geochemistry. The main effects of macrophytes on the physical environment are (Carpenter and Lodge, 1986):

- attenuating light under the canopy;
- affecting water temperature, creating thermal gradients with the surrounding areas;
- hampering water flow;
- stabilising substrate and enhancing deposition.

Macrophytes also enhance the retention of phosphorus in the sediment and can alter the release rate of ammonium (NH_4^+) and nitrate (NO_3^-) from the sediment to the overlying water. Due to these factors, it is possible to use some types of aquatic plants for lake restoration projects to improve water quality.

Aquatic vegetation can be divided into three main categories: submerged, emergent and suspended (either rooted or free floating). Emergent and suspended vegetation, in particular, can reduce wind stress at the water surface with possible effects on flow patterns and mixing. In addition, they can also reduce the amount of solar radiation penetrating underwater, with consequences on water temperature, algal growth, and oxygen production. Moreover, the vegetation layer acts as an insulation between water and the atmosphere, reducing oxygen and heat fluxes at the interface (Ribaudo et al., 2012). Some species of aquatic plants that form thick mats of floating leaves can be particularly dangerous to the ecosystem, leading to severe oxygen reduction (Caraco et al., 2006).

Similar effects are produced by floating photovoltaic plants, which have been intensively studied due to their recent diffusion (e.g., Rocha et al., 2024; Woolway et al., 2024; Yang et al., 2022; Trapani and Redón Santafé, 2015). Another boost in the study of suspended vegetation was the need to design artificial floating treatment wetlands to reduce nutrient levels in lakes and ponds (e.g., Ozan and Yilmazer, 2020). This remediation strategy consists in floating mats where macrophytes can grow with roots immersed in the water column without touching the bottom.

Several efforts have been made to model vegetation drag using a modified Manning's equation, but despite being useful for its simplicity, this approach reveals little information about the flow structure within and above the canopy and therefore it is not suitable to represent emergent vegetation (Nepf, 1999). Many laboratory experiments have been carried out on scaled models, where the presence of vegetation

is reproduced mainly by arrays of rigid cylinders (e.g., Kumar and Sharma, 2022). Nevertheless, stem morphology and flexibility can further affect the behaviour of vegetation under water (Stephan and Gutknecht, 2002). For example, a branched or dendritic stem will produce more drag than a cylindrical stem with the same frontal area. In addition, the pronation of flexible stems when the flow speed increases can change the shape of the canopy and consequently its frontal area (Nepf and Vivoni, 2000). Pan et al. (2022) analysed the disturbance effect of different shapes of flexible vegetation patches on the velocity and the water exchange rate in an adapted laboratory flume reproducing slow-flow water bodies.

In many water environments and particularly in Mantua lakes, vegetation is present in the form of patches. Thus, the difference between a fully developed uniform flow across the canopy and a more realistic finite patch of vegetation also has to be considered. For example, the effect of a circular patch of vegetation is not similar to that of a circular solid body; the wake behind a porous obstruction such as vegetation is much longer because the flow passing through the patch delays the onset of the Von Karman vortex behind it (Nepf, 2012). Caroppi et al. (2022) investigated with field-scale experiments the flow and wake characteristic associated with patches of vegetation. The advantage of field-scale experiments, compared to flume studies, is the ability to capture all the hydrodynamic processes that may be relevant for natural systems. On the other hand, field monitoring usually requires a large amount of equipment and manpower. In this context, numerical modelling offers a great opportunity to conduct experiments simulating different scenarios, although field data are needed anyway for validation (e.g., Temmerman et al., 2005).

The extensive topic of hydrodynamical modelling lies beyond the scope of the present thesis. However, it is useful to remember that including the effect of vegetation in hydrodynamical models requires a correct parametrisation depending on the context and type of macrophytes (Al-Asadi and Duan, 2017). O'Donncha et al. (2015), for example, evaluated different types of parametrisation for three-dimensional hydrodynamic modelling in the presence of a suspended canopy. They tested a constant drag term, a constant drag term with an amended turbulence scheme, and three different vertically varying drag terms with amended turbulence schemes, comparing the simulation results with an experiment from a laboratory flume. The most accurate approach was found to be the vertically varying drag coefficient with a two-equation turbulence closure scheme, including additional turbulent production and dissipation terms.

A lake ecosystem experiences large fluctuations in submerged macrophyte biomass and often switches between macrophytes and phytoplankton dominance. In general, shallow lakes could exhibit two different stable states: a clear water condition with

submerged macrophytes dominance, and a turbid water condition dominated by phytoplankton with only floating or emergent macrophytes (Scheffer, 2004). The alternation between these two configurations is mostly controlled by the competition for light. Algae reduce light penetration in the water column, allowing only adapted macrophytes to survive, while heavy crops of macrophytes, once established, inhibit phytoplankton growth through shading and sometimes allelopathy.

3.2.1 Invasive allochthonous species of aquatic vegetation in Mantua lake system: *N. nucifera* and *L. hexapetala*

Mantua lakes are nowadays in a turbid water condition. Due to reduced light penetration, only the most tolerant species of submerged macrophytes such as *Ceratophyllum* can grow, while most of the plant biomass consists of floating and emergent species of vegetation. Among them, *Nelumbo nucifera* (Gaertn. Nelumbonaceae), commonly known as lotus flower or sacred lotus, is the most widespread. It was planted on Lake Superiore in 1921 as an alternative food source, and then it has become so invasive that it has colonised upstream areas up to the Valli del Mincio wetland, forcing the local management authority to invest in major efforts for its control. Today, it forms dense patches of vegetation, the larger of which, located in the central part of the lake, covers an area of 56 hectares, corresponding to about 15% of the lake's surface.

In Mantua, similar to what Kunii and Maeda (1982) observed in a shallow eutrophic pond near Tokyo, *Nelumbo nucifera* germination begins in April and the plant enters its flowering period in July. In the early growing stage, almost all leaves are of floating type. During the subsequent development phases, the emergent type gradually prevails, with leaves reaching up to 1 m above the water surface during the vegetative peak.

Villa et al. (2018) used medium resolution satellite data to assess the seasonal dynamics of lotus flower in Lake Superiore. They found that it has very rapid growth (up to $0.05\,\mathrm{m^2\,m^{-2}\,d^{-1}}$), an extremely high leaf density (LAI up to $1.7\,\mathrm{m^2\,m^{-2}}$) and a very delayed end of the vegetative season (between October and November). After its withering, it remains above the water surface for a few months before sinking to the bottom of the lake.

The decomposition rate (k) of lotus flower was determined by Bai et al. (2020) using the litterbag method in a shallow lake in China. Adopting the following relationship:

$$ln(M_t/M_0) = -kt, \tag{3.1}$$

where M_0 is the initial weight and M_t is the weight at time t (in days), the decom-

position rate k resulted in $0.005\,\mathrm{d}^{-1}$. Zhou et al. (2018) further investigated lotus flower's decomposition rate using the same method but distinguishing between leaves and stems: k for leaves resulted in $0.006\,\mathrm{d}^{-1}$, while the decomposition of the rigid stems was slower, with k =$0.003\,\mathrm{d}^{-1}$. In addition, they reported that after 165 days of experiment, only half of the stem detritus was decomposed.

The maximum reported depth for lotus flower growth is 3 m (Kunii and Maeda, 1982; Nohara and Tsuchiya, 1990), while Alfasane et al. (2009) found the best condition for its growth to be a depth of 1 m, together with full sunshine, high nutrient concentration, and water stagnation. In optimal conditions in Japan, Nohara and Tsuchiya (1990) found that lotus flower reached a maximum LAI of $2.76\,\mathrm{m}^2\mathrm{m}^{-2}$, a maximum petiole elongation rate of $2.9\,\mathrm{cmd}^{-1}$, and an expansion rate of $18\,\mathrm{myear}^{-1}$.

Abd Rasid et al. (2019) evaluated the potential of *N. nucifera* in treating contaminated water from agricultural runoff. They found that it has good characteristics for phytoremediation due to the anatomy of leaves, stems, and rhizomes that provide a good habitat for bacteria. Moreover, it transports oxygen from the surface to its rhizomes through the aerenchyma, locally improving the oxygenation of the sediment, which is otherwise typically anoxic. They also measured a gas flow rate of up to 10 mL/min. In addition, they reported that lotus flower was more effective than *Nymphaea* in reducing turbidity. The resulting removal efficiency was 97% for BOD, 55% for COD, and 88% for turbidity.

The cultural, ecological, and nutraceutical significance of lotus flower is addressed in a multidisciplinary review by Yang et al. (2024). Other scientific works on this particular macrophyte include the contribution of Han et al. (2018), who studied a sequence of lotus flower leaves in a laboratory flume revealing the increased complexity of the flow structure that results from the gap between the leaves.

Ludwigia hexapetala (Hook. & Arn.) Zardini, H. Y. Gu & P. H. Raven (Onagraceae), also known as water primrose, is another non-native species that has spread across the Mantua lakes over the past decade. It initially colonised a calm small bay in Lake Di Mezzo and has more recently extended to the riparian zones of both the Superiore and the Inferiore lakes, and to the Valli del Mincio wetland, where it became especially invasive. In fact, it is native to South America, where it typically grows in wet grasslands and wetlands.

Tóth et al. (2019) compared the morphological traits of *N. nucifera* and *L. hexapetala* to those of native species like *Nuphar lutea*, *Nymphaea alba* and *Trapa natans*. Their results show that these allochthonous macrophytes have specific functional traits such as higher pigment content that make them more efficient than native ones, thus explaining their invasiveness.

Within the Lombardy region, *N. nucifera* and *L. hexapetala* are also present in

Brabbia wetland and Lake Varese, respectively, where they were the object of the LIFE10 NAT/IT/000241 "TIB - TRANS INSUBRIA BIONET" project. In this work, different mechanical removal strategies were tested in colonised pilot areas, with follow-up monitoring activity (Brusa, 2018). In Italy, according to the LIFE14 IPE IT 018GESTIRE2020 project, *N. nucifera* is also reported to be present in Piedmont, Veneto, Emilia-Romagna, Tuscany, and Lazio. Moreover, it is included in the black list of alien plant species subject to monitoring, containment, or eradication (All. E DGR 7736/2008). On the European scale, it is also present in Romania (EPPO Global Database, 2022).

4. Acoustic Doppler Current Profilers measurements in low-energy systems

4.1 Introduction

Acoustic Doppler Current Profiler (ADCP) is a well-established technology, but precise guidelines on how to properly configure these rather complex instruments are sometimes missing. Every brand has its own specific setting options and naming conventions. Published works often focus mainly on the data and do not examine the technical details of the instrument configuration, making it difficult to learn from others' expertise in fieldwork. In this work different instruments were compared in various types of lakes, and different working modes were tested with the aim of collecting good quality data in slow-moving water environments.

Acoustic Doppler Current Profilers are among the most widely used instruments to measure water velocity in environmental applications. The operation of ADCPs is based on the Doppler effect: the instrument sends an acoustic pulse and measures the Doppler shift of the returned signal, which is reflected by suspended particles in water. ADCPs are equipped with two to five transducers that also act as receivers for backscattered signals. Every transducer is able to measure the speed along the direction of the beam it emits. To retrieve a three-dimensional velocity vector, at least 3 beams are needed. The presence of more beams allows for the acquisition of additional information that is used to compute an estimate of the error velocity. Transformation is then applied from beam to orthogonal coordinate system. The oldest models of ADCPs, commonly referred to as narrowband or pulse incoherent ADCPs, employed a single pulse per ping for each velocity measurement. In the early 1990s, broadband ADCP was introduced, which uses multiple short pulses per ping. This results in a higher sample count within a single ping compared to

narrowband ADCPs. As a result, the standard deviation of velocity data obtained with broadband ADCPs is generally much lower than that of narrowband ADCPs.

The instrument measures the water velocity relative to its position; thus, for moving applications a reference is needed to correct the results by removing the instrument velocity. Bottom Tracking is commonly used for this purpose when the bottom is visible from the instrument and in absence of bedload. To obtain this correction, the relative velocity of the bottom is measured again using the Doppler shift principle. If the bottom is not moving, this velocity equals the instrument velocity.

Bottom Tracking cannot work properly if there is sediment transport or if the water depth is greater than the instrument's range. In these cases, it is possible to obtain the instrument position using a GNSS receiver with centimetric accuracy such as a Real Time Kinematic (RTK). Due to the fact that ADCP measures the sound reflected by suspended particles, problems can arise in very clear waters such as oligotrophic lakes because of the low backscatter. Moreover, the presence of submerged vegetation can further hamper the measurement.

One of the main applications of this technology is discharge measurement in rivers; the capability to collect velocity data on the entire river section allows for detailed discharge estimates in a very short time if compared to single point measurements obtained with older technologies. In addition, the instrument can be easily tethered from the shores, offering the great advantage of avoiding the need to wade the river. This allows for increased operation safety, especially in case of flood, and a wider field of application. The accuracy of ADCP instruments has been evaluated by comparing them to other standard stream gauging methods such as current meters, Acoustic Doppler Velocimeters (ADV), and towing basins. Most comparisons show that ADCP's results align with these methods within a 5% margin of error (e.g., Oberg and Mueller, 2007)

ADCPs can also be used to monitor water bodies such as seas, oceans, or lakes, which can experience relatively slow currents. Measurements in lakes or wetlands often imply the presence of water velocities of the order of 1-10 cm/s, resulting in a challenging application of this kind of instrument. The typical accuracy of a 600 kHz or 1200 kHz ADCP is $\pm$ 0.25% of the water velocity relative to ADCP $\pm$ 2 mm/s (Teledyne RD Instruments, 2013), but the standard deviation of the data depends on many factors, such as cell size, working mode, and instrument frequency. For a Teledyne RDI RioGrande 600 kHz in the standard working mode (Mode 1) with a 50 cm cell size, the standard deviation given in the manual is 7 cm/s (Teledyne RD Instruments, 2007).

Muste et al. (2004a) reported velocity fluctuations of 45% in single ADCP data.

This requires post-processing, such as averaging, to filter the data. Gunawan and Neary (2011) showed that the streamwise velocity becomes stable after averaging the data over 180 s.

The instrument accuracy and standard deviation reported in the technical documentation refer to optimal conditions, without strong movements of the ADCP. A common solution to achieve these conditions is to deploy the ADCP in a fixed frame mounted on the lakebed. Another solution is to moor the instrument at a fixed depth on a line with a buoy. This adds the advantage of enabling measurements in a specific area of interest even if the instrument depth range is limited. The main limitation of these solutions is that they allow for the monitoring of only one point. To have a spatially-distributed information, it is possible to mount the instrument on a boat and acquire data from the surface both in a stationary configuration or from a moving boat. However, in both cases the instrument motion (pitch, roll, and heading) increases the noise in the measurement. Additionally, with a moving boat there is the necessity to subtract the boat speed, resulting in further source of errors, and it is not possible to average multiple data referring to the same position.

Muste et al. (2004b) compared ADCP measurements from a moving boat and from a stationary one in a river. They proved that despite the scattering of the data acquired with a moving boat, it is possible to compute a good estimate of the discharge, while to obtain a good representation of the velocity profile on the water column it is suggested to keep the boat fixed in a point for a minimum amount of time. In fact, the discharge computation includes an averaging process along the transect section that allows smoothing of anomalies in the velocity measurements (Muste et al., 2004a).

Various technical papers are available on discharge measurement with ADCP instruments. Several application cases of single-point ADCP velocity measurements in oceanographic fields have been documented in many published works (e.g., Van Haren, 2009). Despite the analogies, the applications of this technology in lakes are very limited. This can be explained by the fact that in lakes velocities are usually lower than in seas and can be close to the instruments' working limits. This requires a lot of attention in the deployment setup and a precise parameter configuration. A good example of ADCP measurements in a lake is the work of Doda et al. (2022) on the monitoring of density currents in Lake Rotsee (Switzerland).

Recently, ADCP technology has evolved significantly. For example, Teledyne RDI instruments are now equipped with a high resolution water profiling mode called Mode 12, which, according to the manual, can reduce by one order of magnitude the standard deviation of measurements compared to the original Mode 1 (Teledyne RD Instruments, 2013). ADCP manufacturing brands are constantly launching new

instruments with improved performances. For example, Teledyne RDI invested in the development of StreamPro: a 2000 kHz ADCP designed for discharge measurements in shallow streams and rivers up to 6 m deep. It is managed by Teledyne RDI WinRiver II software, which also allows it to connect to an external GNSS receiver. Its transducer head is much smaller (3.5 cm diameter) compared to other ADCP instruments, making it portable and easy to deploy. Moreover, it can provide high spatial resolution, with cells up to 2 cm and only 3 cm of blanking distance near the transducer head. Additionally, a special low noise high resolution working mode (Mode 13) is available with a minimum cell size of 1 cm, for speed lower than 0.25 m/s and a maximum depth range of 1 m. The accuracy of the velocity measurement is 1% of the water velocity relative to ADCP $\pm$ 2 mm/s (Teledyne RD Instruments, 2021). All these features make the StreamPro very attractive for monitoring slow currents.

Although StreamPro ADCPs are able to acquire data only down to a depth of 6 m, these data can still be of interest for studying deeper lakes, when focusing on water circulation in the surface layers. Possible applications are, for example, the validation of surface velocities derived from remote sensing techniques (e.g., SAR, LSPIV) or from hydrodynamic models and the comparison with measurements from drifters.

Despite this, no applications of this ADCP model could be found in the literature for fixed-boat velocity measurements and slow-moving water. In the following paragraph, different tests are provided in slow-moving water conditions of Teledyne RDI StreamPro and Monitor, two among the most widely used ADCPs. After testing, these instruments were used to collect data in Lake Superiore of Mantua, to characterise the hydrodynamical processes described in Section 7.

4.2 Materials and methods

On 14 September 2024, a StreamPro ADCP was tested on Lake Superiore (Mantua) in a moored-boat configuration: two ropes with anchors were used to moor the ADCP float in order to avoid it from drifting. As an alternative to Bottom Tracking, a Stonex S850+ GNSS receiver was mounted on the float and connected to the regional RTK positioning service (SPIN3) to achieve centimetric accuracy. Using Teledyne WinRiver II two measurements (called "transects" in the software) were acquired in working mode 12 with a duration of 10 minutes and a cell size of 17 cm. The maximum water depth was 4 m, the transducer depth was 7 cm, the first cell depth was 31 cm. In all the following tests, the sampling rate was always set to the

default 1 Hz, while other instrument configuration parameters varied depending on the deployment conditions and are reported in Appendix.

A Teledyne Monitor Workhorse 600 kHz ADCP was tested in the same place and under similar conditions on 8 November 2024. The instrument was controlled using Teledyne VMDas software and it was mounted on a self-made version of the Teledyne High-Speed Riverboat, kept in place with 3 anchors. Also in this case, the S850+ GNSS receiver was mounted on the instrument and used as an alternative to Bottom Tracking. The cell size was set to 10 cm and the instrument was left collecting data for 1 hour.

On 29 November 2024, a simultaneous comparison between StreamPro and Monitor was conducted with adjacent concurrent measurements in Lake Superiore. The two floats were tied together and fixed with anchors. The different operation frequencies of the two instruments (600 and 2000 kHz) prevent interferences despite the small distance.

In addition, the Monitor ADCP was tested in deeper waters with two measurement campaigns in Lake Garda. In this case, given the depths reaching more than 100 m, it was impossible to use anchors to fix the instrument, which was therefore left loose and free to drift together with the boat. In this context, two different ADCP operating modes were tested: Mode 1 and Mode 11. Mode 1 is the general-purpose profiling mode, the most robust mode of operation, which allows data collection in all environments. Mode 11 is a high resolution "Pulse to Pulse coherent" option that allows for higher precision, but requires low turbulence and relative water velocities lower than 1 m/s. Its main limitation is the maximum measurement range of 8 m in depth, but even in deeper contexts it can be useful for studies that focus on surface layer dynamics.

A test in deeper water was also performed with the StreamPro ADCP. Caldonazzo Lake (Trento Province) was chosen for its maximum water depth greater than StreamPro Bottom Tracking range (7 m), combined with a smooth depth gradient near the shores allowing for transition between operation and non-operation of Bottom Tracking.

After each test, the data were exported from binary files to .mat tables using WinADCP, a Teledyne software for data visualisation. Then, a simple post-processing was performed in Matlab to plot and average the data.

4.3 Results and discussion

4.3.1 Tests on Lake Superiore of Mantua

The data resulting from the StreamPro measurement in Mantua Lake Superiore are very scattered (Figure 4.1), with a standard deviation of the order of 5 cm/s on the horizontal velocity components. Coherently with Gunawan et al. (2009), averaging over 180 s was sufficient to stabilise the data (Figure 4.2). Moreover, the resulting water velocity in the surface layer has a direction of 120° (Figure 4.3), which is aligned with the direction of the light wind (3.6 m/s) blowing from 310° during measurements (data from ARPA Lombardia, Lunetta weather station). The time-averaged speed of this water layer was 8.5 cm/s, proving that it is possible to use the StreamPro ADCP to collect data, albeit noisy, even in slow-moving water bodies, provided that the instrument remains stationary in a certain point for a sufficient amount of time. Interestingly, the ADCP trajectory obtained with the Bottom Tracking is very different from the one obtained using the GPS as a reference. In general, bottom tracking should be more precise than a centimetric-accurate RTK GNSS receiver: according to the StreamPro manual, the accuracy of the Bottom Tracking is 1% of the bottom velocity relative to ADCP ± 2 mm/s (Teledyne RD Instruments, 2021). In this particular case, however, the GPS trajectory seems more reasonable considering the fact that the instrument was tightly moored with two anchors and it was able to move only in one direction, perpendicular to the ropes, due to a possible small slack of the fastening. Given the low velocity, the hypothesis of sediment transport near the lakebed can be excluded, but there may have been vegetation altering the bottom velocity reading.

The data from Monitor ADCP in high resolution working mode (Mode 11) in Lake Superiore (Mantua) are much better than the one from StreamPro ADCP, although the water was slower during this test (the maximum velocity after averaging was 3 cm/s). As reported in Figure 4.4, noise is lower and some trends in the data are visible even without averaging. The standard deviation of the horizontal velocity components is on the order of 2 cm/s, allowing for considerations about the lake's currents even in this extremely slow environment.

In the simultaneous test between the two instruments, unexpectedly, the StreamPro ADCP was able to acquire continuous data only to a depth of 2 m, despite the nominal range of 6 m (the bottom was at 3 m). The Monitor ADCP instead correctly acquired data on the whole water column down to 2.5 m (a blanking area of approximately 10% of the depth is always present above the bottom for signal sidelobe interference). This is probably due to the Monitor signal's lower frequency

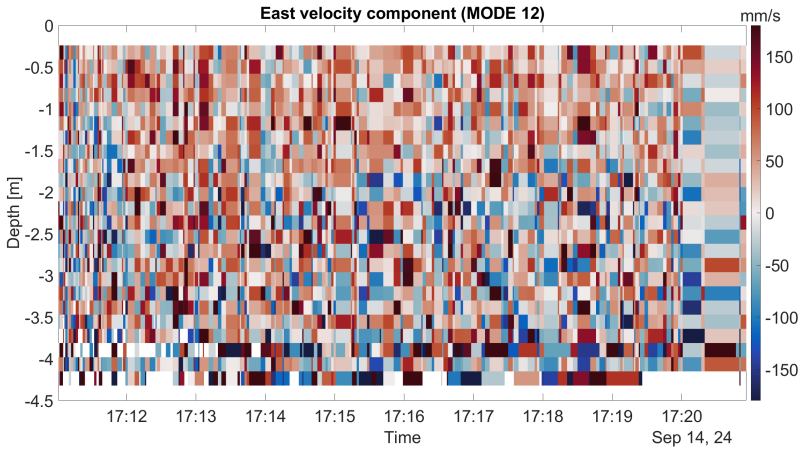

Figure 4.1: East velocity component of a StreamPro ADCP measurement in Lake Superiore (Mantua)

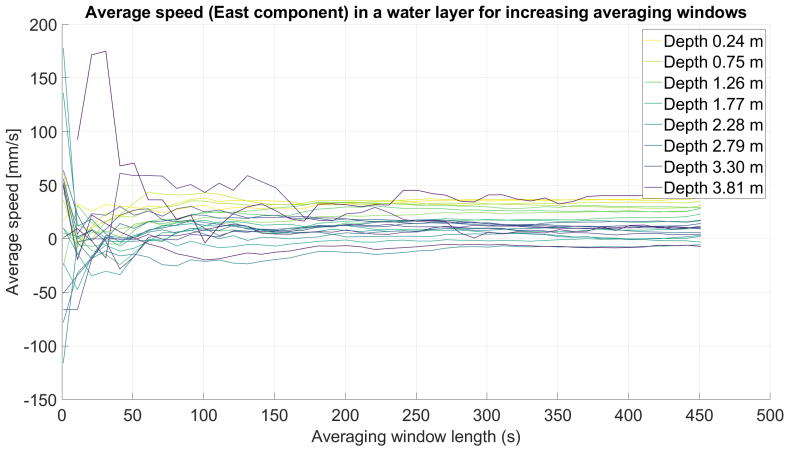

Figure 4.2: Trend of the time-averaged East velocity component in a layer as the averaging window length varies (StreamPro ADCP measurement in Lake Superiore)

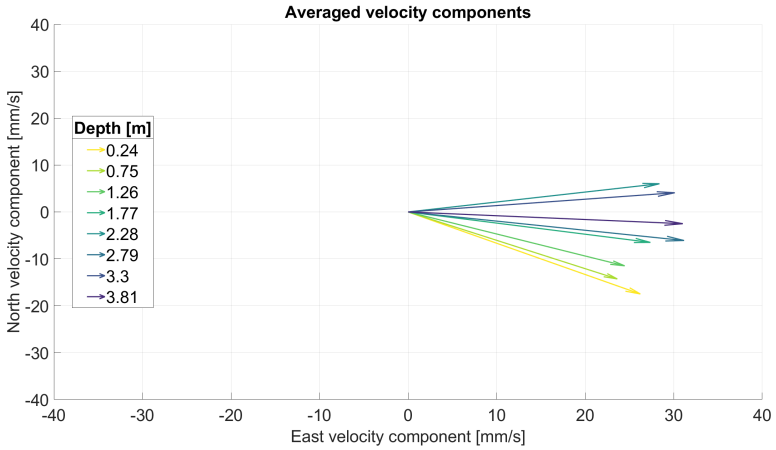

Figure 4.3: Averaged velocity components in different layers of a StreamPro ADCP measurement in Lake Superiore

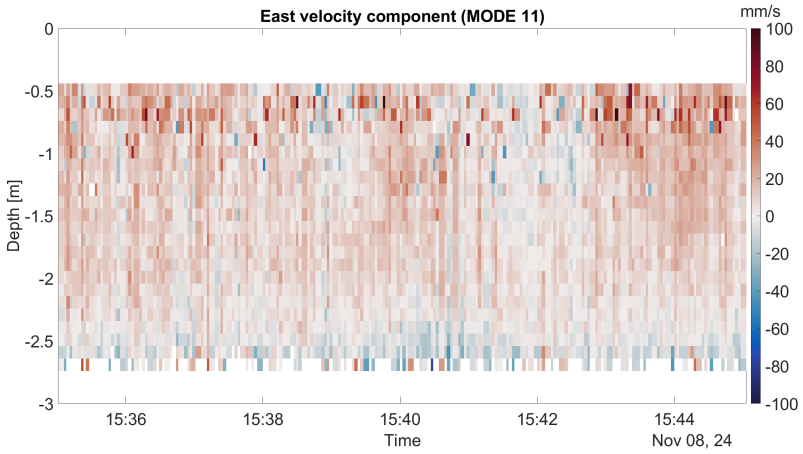

Figure 4.4: East velocity component of a Monitor ADCP measurement in Lake Superiore

(600 kHz), resulting in more energy in the water, allowing the instrument to receive a pulse even in the low presence of suspended backscatterers in the water column. Figure 4.5 compares the velocity components of the two instruments after averaging on the same time window of 10 minutes. This result confirms the better suitability of Monitor ADCP for this environment, as it was evident from the previous tests. In this case, the standard deviation of the StreamPro measurement is larger than the velocity itself, compromising its robustness.

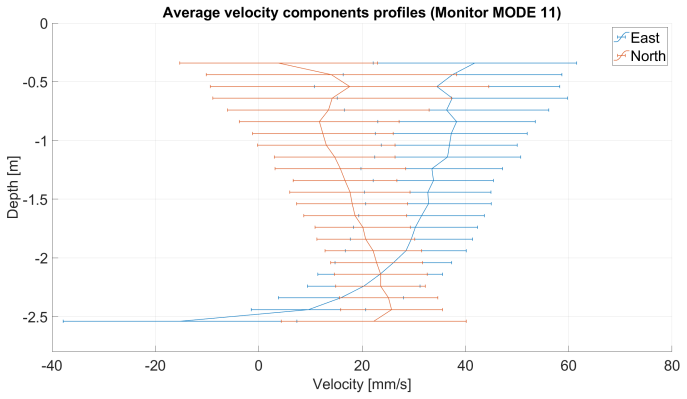

(a)

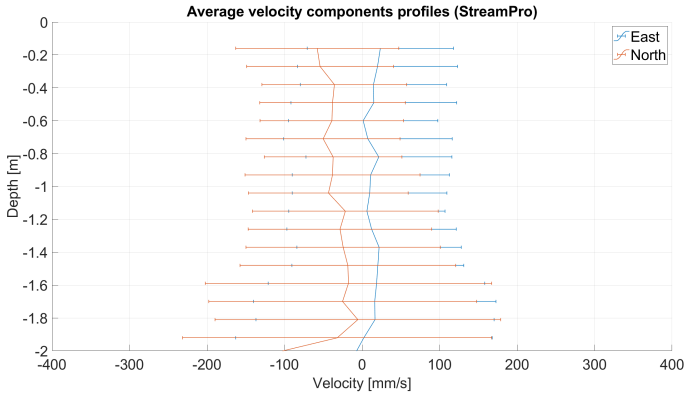

(b)

Figure 4.5: Comparison between the averaged velocity components of Monitor ADCP Mode 11 (a) and StreamPro (b) measurements in the same point in Lake Superiore. Error bars represent standard deviation (note the different axis scales)

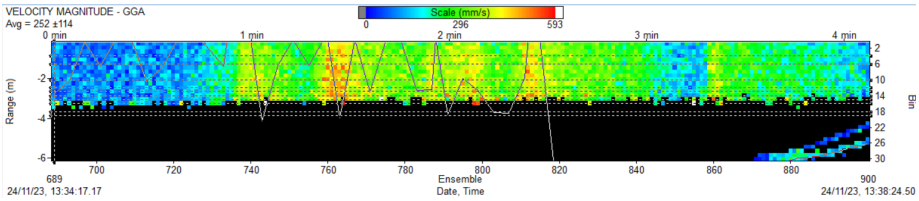

(a)

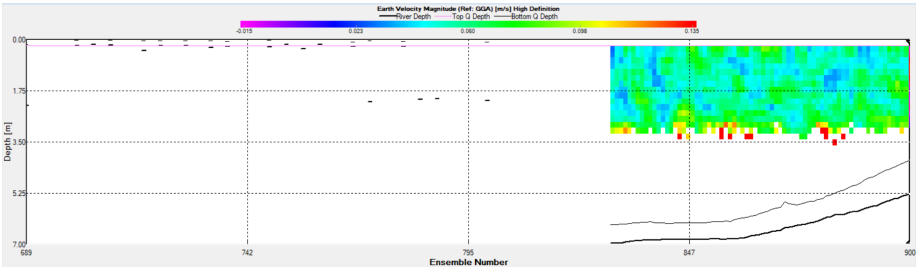

(b)

Figure 4.6: Comparison between the same StreamPro ADCP measurement opened with WinADCP (a) and WinRiver II (b)

4.3.2 StreamPro ADCP test on Lake Caldonazzo

The SteamPro test in deep water apparently demonstrated that this instrument is not working (no data were shown in the acquisition software) when it is not able to detect the bottom (i.e., with a depth greater than 7 m, maximum range for Bottom Tracking), even if GNSS positioning was set as a reference instead of Bottom Tracking. However, a more detailed data analysis contradicted this observation. After measurement, the raw data files (.PD0) were opened with WinADCP, where it was possible to see the missing data. In addition, a false bottom line was present at random depths when the instrument was not able to see the real bottom. Figure 4.6 shows the comparison between the same measurement opened with WinRiver II and with WinADCP. This measurement was made slowly moving through the shore with the boat, from a depth greater than 7 m to a shallower one. The same visualisation can be obtained in WinRiver II by unflagging the "Mark below bottom Bad" and "Mark below sidelobe Bad" filters in the postprocessing (Teledyne Field Service, personal communication). Removing filters may lead to sidelobe errors when the bottom is visible, but this can be easily solved by manually removing the data in the 6% portion of the water column above the bottom, as described in Teledyne RD Instruments (2011).

4.3.3 Monitor ADCP tests on Lake Garda

Figure 4.7 shows the vertical profiles of every velocity component after averaging over 8 minutes, with error bars representing the standard deviation of the data for each depth. Mode 1 has a standard deviation on the order of 10 cm/s on the horizontal velocity components, which are less than 5 cm/s except for some spikes. This makes the data very difficult to use. Mode 11 instead allows for a reduced standard deviation of 2 cm/s. This can also be seen by looking at the plots in Figure 4.8 where the raw data of a velocity component are shown along time and depth. Thanks to the redundancy of information collected by the ADCP (data from 4 beams are used to retrieve 3 velocity components), the instrument itself gives an estimate of the error in the velocity measurement. Figure 4.9 compares the Error Velocity for the two different working modes. With Mode 11 the error is more than one order of magnitude lower than with Mode 1. From Figure 4.8 it is possible to notice a potential sign of a malfunction encountered during Mode 11 measurement: the velocity profile that is acquired for each ping is almost uniform along the depth. This phenomenon is probably not physical and seems to be caused by an error in the correction of the boat motion. However, another Mode 11 test in a different part of Lake Garda showed a clear velocity variation along the water column, with a distinct current that also changed its depth during the measurement (Figure 4.10). The only difference in this case is that Bottom Tracking was intentionally turned off, only relying on GPS positioning as a reference. One possible explanation for this behaviour is that GPS may provide greater accuracy than Bottom Tracking when the depth approaches the instrument's operational limit. Another advantage of turning off Bottom Tracking is the capability to use the instrument in deeper water than its maximum bottom detection range (100 m), when high accuracy is needed in the top layers. Otherwise, in fact, Monitor ADCP stops working with Mode 11 when the bottom is out of range, similarly to what happened with StreamPro ADCP in Lake Caldonazzo.

4.4 Conclusions

Teledyne RDI Workhorse Monitor 600 kHz and StreamPro 2000 kHz, two among the most widely used acoustic Doppler profilers, were tested and compared under different conditions. The test sessions can be summarised as follows.

- StreamPro in low depth (Lake Superiore);
- Monitor in high resolution mode (Mode 11), in low depth (Lake Superiore);

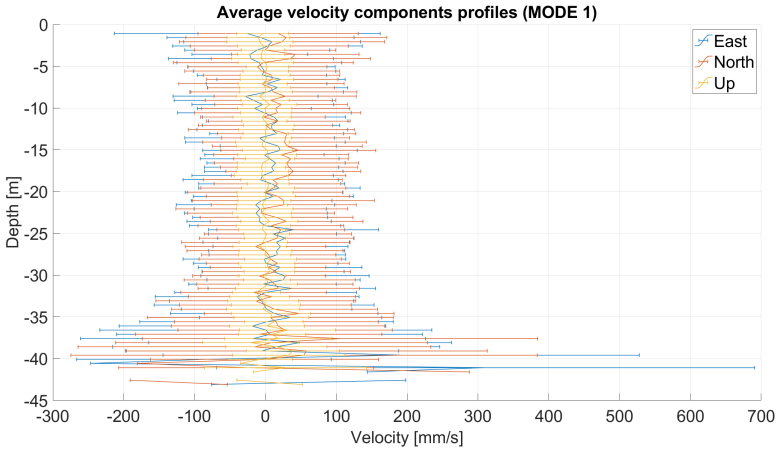

(a)

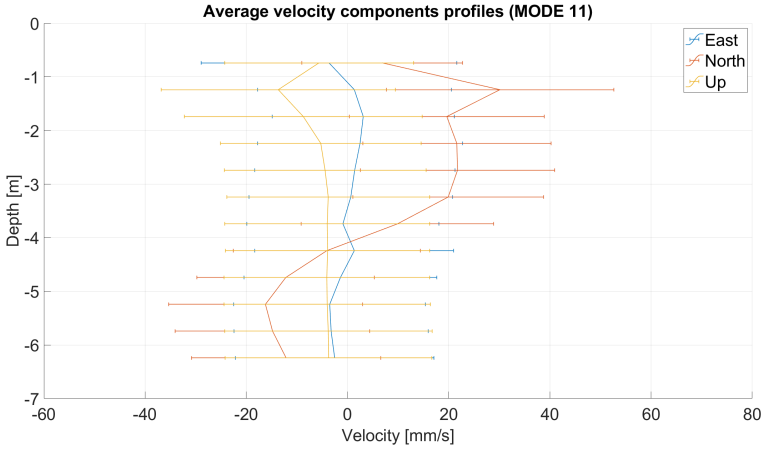

(b)

Figure 4.7: Comparison between the averaged velocity components of Monitor ADCP Mode 1 (a) and Mode 11 (b) measurements in the same point in Lake Garda. Error bars represent standard deviation (note the different axis scales)

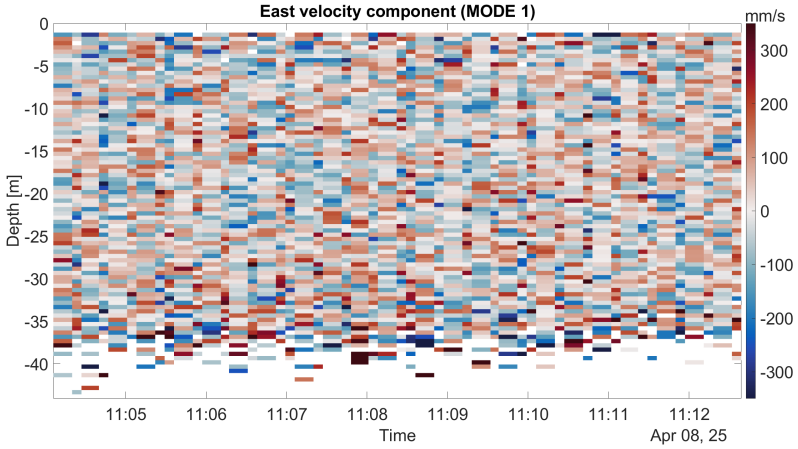

(a)

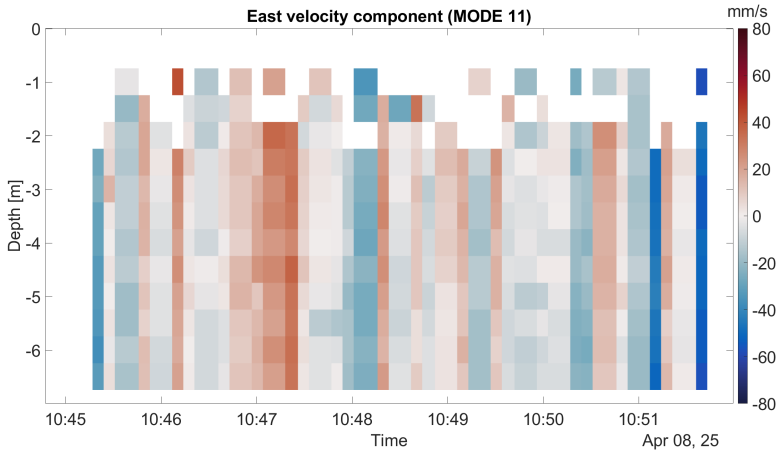

(b)

Figure 4.8: Comparison between the East velocity component of Monitor ADCP Mode 1 (a) and Mode 11 (b) measurements in the same point in Lake Garda

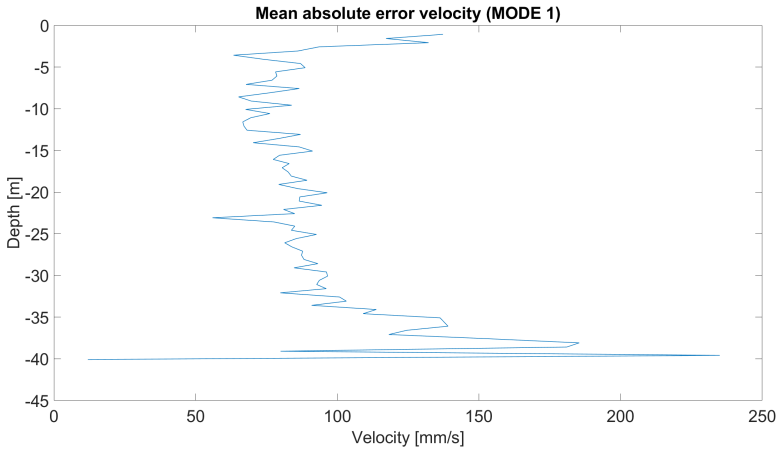

(a)

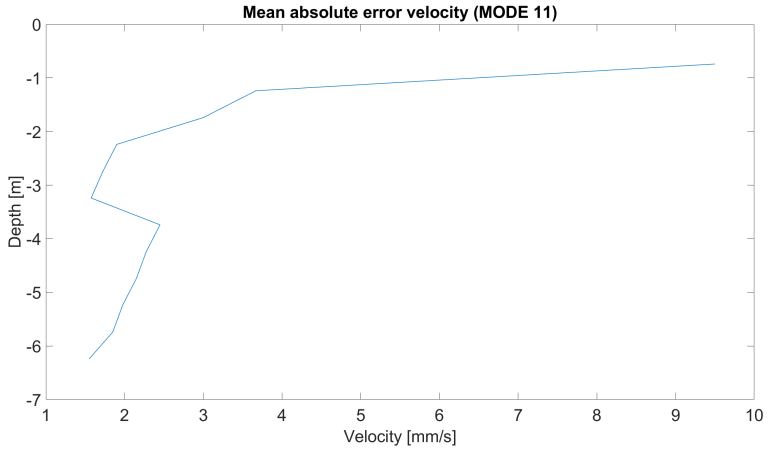

(b)

Figure 4.9: Comparison between the averaged Error Velocity of Monitor ADCP Mode 1 (a) and Mode 11 (b) measurements in the same point in Lake Garda

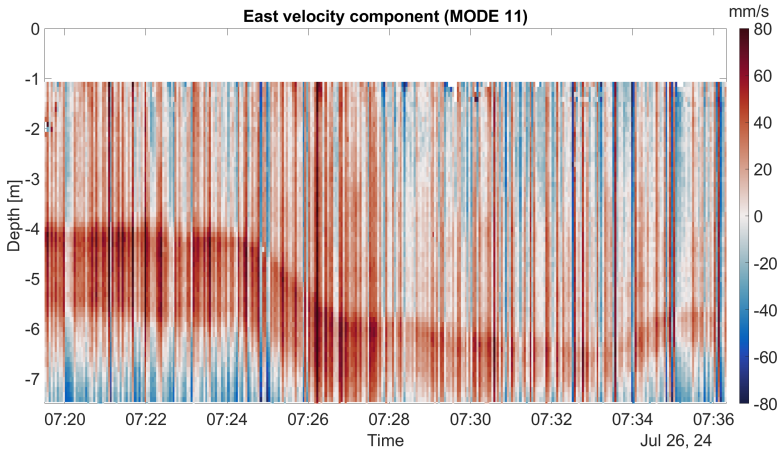

Figure 4.10: East component of a Mode 11 Monitor ADCP measurement in Lake Garda without bottom tracking

- simultaneous deployment of StreamPro and Monitor in high resolution mode (Mode 11) in low depth (Lake Superiore);
- StreamPro in high depth (Lake Caldonazzo);
- Monitor in multi-purpose mode (Mode 1) in high depth (Lake Garda);
- Monitor in high resolution mode (Mode 11) in high depth (Lake Garda);

Although StreamPro ADCP was not conceived for fixed-point velocity measurements in low-energy systems, it showed reasonable data in a test in Mantua Superiore Lake with speeds as low as 8.5 cm/s. In case of lower speeds, a detrimental increase in the standard deviation of the data was observed, and the instrument's accuracy was not sufficient to retrieve reliable measurements. The Monitor ADCP instead offered better accuracy; with a proper configuration and averaging window, it was able to measure extremely slow currents of the order of a few centimetres per second without excessive noise, thanks to its high resolution working mode (Mode 11). The main limitation of this working mode is the capability of collecting data only for the first 8 m below the surface. On the other hand, the measurements with Monitor in multi-purpose mode allowed for an increased depth range, but with a deterioration of one order of magnitude in the data quality.

With both StreamPro and Monitor, the GNSS receiver used as a reference to correct for boat motion provided better results than Bottom Tracking in difficult conditions (vegetation, deep water). In these cases, according to the test results, it

may be better to turn off Bottom Tracking to prevent some possible malfunctions of this feature. With this arrangement, it is possible to exploit the high accuracy of Mode 11 also in deep waters when the focus of the study is the top portion of the water column. Similarly, the suggested solution for StreamPro ADCP (disabling the filtering in WinRiver II software and manually post-processing the data if needed) allows one to use this ADCP in every water body, regardless of the water depth, if interested only in the first 6 m. Thanks to this it is possible to take advantage of the StreamPro's light weight and ease of deployment when the velocity is not extremely low (i.e., above 10 cm/s).

In this section, the performance of different ADCP models and configurations was evaluated through the analysis of data obtained from test deployments. Future tests are needed to compare the ADCP results with references from other instruments such as drogues, Acoustic Doppler Velocimeters, or Particle Image Velocimetry techniques.

5. Morphological evolution of Lake Superiore and Valli del Mincio wetland

5.1 Introduction

This section aims to estimate the morphological evolution trends in a reservoir (Lake Superiore) and a transitional wetland (Valli del Mincio), which are located in the Mincio River system upstream the city of Mantua and are heavily impacted by agricultural runoff. This was accomplished through an extensive bathymetric-mapping effort, which also included the development and testing of a custom-built instrument based on a sport fishing sonar. In addition, sediment loads transported by the different watercourses in the system were investigated through a comprehensive monitoring programme.

Lake Superiore is regulated by a dam and is affected by important sedimentation problems. Reservoir embankments retain sediments in a way similar to fluvial check dams (e.g., Verstraeten and Poesen, 2002). For this reason, most reservoirs are threatened by loss of storage capacity due to sediment deposition. Perera et al. (2023) conducted a global assessment finding that many regions in the world have already lost between 13 and 19% of their water storage availability.

The Mantua basin is heavily exploited for intensive agriculture with a high water demand during the irrigation season, resulting in high sediment input from the tributaries and low discharge flowing into the Mincio River. According to Borrelli et al. (2018) the annual soil loss in the Mincio River basin is 1.28 tonnes per hectare. Water-driven soil erosion represents a significant threat to soils, adversely affecting ecosystem services, agricultural productivity, drinking water quality, and carbon storage. Among European countries, Italy exhibits the highest mean annual soil loss rate (8.46 t/ha) (Panagos et al., 2015). After soil erosion within a catchment, most

of the sediments are delivered to aquatic systems with huge environmental and economic impacts. The European Union Soil Observatory (EUSO) estimated a volume of the order of 1 billion m^3 of sediments to be removed from European reservoirs every year at a cost ranging between 5 and 8 billion euros (Panagos et al., 2024).

Terrestrialization can be defined as the succession process from a lake or wetland to a terrestrial ecosystem due to the deposition of sediment and detritus on the bottom (Tallis, 1973). For Lake Superiore, the infilling problem is particularly critical because of the following aspects:

- it is a fluvial lake: the through-flowing discharge is relatively large compared to the lake volume, which suggests that the incoming sediment input may play a major role;
- it is a shallow lake: a few metres of deposition can lead to terrestrialization of large portions of the lake;
- it is strongly regulated: the water level is allowed to fluctuate only for a few centimetres;
- the Mincio River flood management plan does not allow the lake to be flushed: the excess discharge is diverted into an artificial channel bypassing the lake system to protect the city of Mantua.

In addition, the presence of the invasive macrophyte *Nelumbo nucifera* (lotus flower, Section 3.2.1), which covers almost 25% of the lake's surface, results in a huge amount of biomass that is deposited every year after the vegetative season on the lake bed. Aquatic vegetation can also affect sedimentation rates by capturing suspended particles.

The accumulation of plant detritus resulting from the vegetative cycle of different aquatic macrophytes, including lotus flower, was investigated by Bai et al., 2020. Many similarities with Lake Superiore can be identified in the work of Papastergiadou et al. (2007), who studied the environmental impacts of land use changes on a Mediterranean shallow lake in Greece.

The same problems also affect the Valli del Mincio wetland, immediately upstream of the lake. In this case the situation is further worsened because:

- wetlands are among the most productive ecosystems in the world;
- the mean depth is even lower than in the lake, making it easier to transition from wetland to dry land;

- the wetland has a braided morphology: the incoming discharge tends to choose a preferential path and abandon the remaining part of the channel network, similarly to what happens in a tidal flat (e.g., Toffolon and Todeschini, 2006).

In another shallow wetland in the Mantua province (Paludi di Ostiglia), a sedimentation rate of 10 cm/year was measured by Longhi et al. (2008). Progressive landfilling can be part of the natural evolution of a wetland over long timescales. Nevertheless, given the uniqueness of the Valli del Mincio wetland and its great naturalistic value, it is important to manage this area to preserve as much as possible the functionality of its aquatic ecosystems.

In fact, wetlands are particularly susceptible to land conversion and sediment accumulation driven by upland agricultural activities, which can turn them into sediment sinks, threatening their ecosystem services. Zarrinabadi et al. (2023a) and (2023b) assessed the contribution of tillage, water and wind erosion to sediment infilling in a Canadian wetland. According to these works, tillage-induced erosion is the dominant factor, while wind and water have a minor impact on total soil erosion.

Bathymetric mapping repeated over time allows for the estimation of the system's morphological evolution. Professional sonar instruments are available for this purpose, with prices ranging from a few thousand euros for single beam solutions to tens or even hundreds of thousands of euros for advanced multi-beam systems. Instead, a cheaper solution was developed for this work, with the aim of making depth data collection accessible to a wider range of users. The adopted solution was based on a sonar device widely used for recreational fishing (Deepersonar CHIRP+) that was tested and adapted for the purpose.

Many previous scientific works already used a Deepersonar low-cost instrument such as the CHIRP+ or the similar PRO+ model in different applications. For example Bandini et al. (2018) developed a novel approach to retrieve accurate and high-resolution bathymetry maps using a PRO+ sonar attached to an unmanned aerial vehicle (UAV). They tested it on a lake and two Danish rivers, obtaining an accuracy of ~2.1% of the actual depth for observations up to 35 m. A similar UAV solution with a Deeper PRO+ was also adopted by Alvarez et al. (2018) in a small reservoir in Oklahoma (USA), by Ruffell et al. (2021) in Northern Ireland, by Koutalakis and Zaimes (2022) on the Aggitis River (Greece) and by Sanjou et al. (2022) on the Yodo River (Osaka, Japan). Bogoyavlensky et al. (2020) used a Deeper PRO+ in an Arctic expedition to study the Seyakha Crater in the north of Western Siberia. Kellerer-Pirklbauer et al. (2021) investigated the evolution of an ice-contact lake on the Pasterze Glacier (Austria) using a Deeper CHIRP+. Walker et al. (2022) tested a Deeper Fishfinder in shallow waters comparing it with manual depth measurements and obtaining a mean absolute difference of 1.8 cm. Subsequently,

they used it for the quantification of water storage within Lake Naivasha (Kenya). Similarly, Giambastiani et al. (2020) used the PRO+ sonar for the volume estimation of different lakes and reservoirs in Tuscany, Italy.

Other applications of Deeper sonars include macroplastic monitoring: Broere et al. (2021) demonstrated that CHIRP+ is a promising tool for underwater plastic monitoring even if at the time of that work it was not possible to access the raw sonar data. Recently, Deepersonar added the possibility to download the echo strength for each depth in the whole water column, further expanding the field of application. Moreover, Deepersonar included the possibility to send NMEA0183 messages containing information on time, position from the internal GPS and depth to an external device via UDP connection. Bandini et al. (2023) took advantage of this feature while comparing a Deeper CHIRP+ to a Ground Penetrating Radar.

5.2 Bathymetric survey

5.2.1 Materials and methods

For the bathymetric mapping a Deepersonar CHIRP+ sonar was used. This sonar was conceived for fishing, but, as already mentioned, it was also proved to be suitable for scientific application. According to the manual, the CHIRP+ is capable of measuring depths of up to 100 m and acquiring up to 15 data per second. It allows for 3 different working frequencies: 100 kHz, 290 kHz, and 675 kHz, resulting in beam angles of 47°, 16°, and 7°, respectively. The narrower beams are capable to map also small details of the bottom, but higher frequencies have less power than the lower ones, so they can be affected by ambient noise or too turbid water. This instrument is extremely portable, thanks to a diameter of 6.5 cm and a weight of 90 g, and it is very easy to use: the sonar turns on automatically once it comes into contact with water, and using the FishDeeper app it connects to the user's smartphone via Wi-Fi technology. After the measurement, data can be uploaded on a cloud from which it is possible to download a .csv file containing depth, coordinates, water temperature and time. Its intuitive functioning and affordable price (~300 €) compared to professional devices make it also suitable for citizen science campaigns. It can be fixed to a boat or a kayak using a flexible mounting arm provided by Deepersonar or cast from the shore. For the "fishing from shore" mode, an internal GPS receiver allows the SONAR to record its location, while in the boat mode the phone positioning system is used.

Preliminary surveys were conducted on Lake Superiore to test the instrument. First, a CHIRP+ sonar was fixed on a pier and left to acquire data for 12 minutes.

The resulting 10000 data showed a very good precision in static conditions, with a standard deviation of 7 mm. The instrument was then mounted on a Teledyne RDI StreamPro ADCP and the depth readings were compared over a track of approximately 1 km. The resulting root mean square error was 13 cm, probably due to the different orientations of the 4 ADCP transducers (StreamPro does not have a vertical beam). The same issue was reported by Bandini et al. (2018) for the Deeper PRO+ sonar. In addition, during the survey, a manual depth measurement was performed in 7 different points on the lake. The maximum difference between echosounder and manual sounder measurements for the same point was 0.1 m, with an average error of 0.05 m. The manual sounder tended to slightly overestimate the depth compared to the sonar, probably because the sounder ballast was sinking inside the extremely soft bottom sediment. Finally, the phone GPS was tested with repeated coordinates measurements in the same position acquired through the FishDeeper app. The standard deviation obtained over 600 points was 1 m, with a maximum error of 4 m.

According to the technical specification for the standardisation of hydrographic surveys defined by the Italian Navy Hydrographic Institute (Istituto Idrografico della Marina, 2023), the following limits are prescribed for depths lower than 100 m:

- maximum Total Vertical Uncertainty $TVU_{max} = \sqrt{0.25 + (0.013 \cdot D)^2}$,
- maximum Total Horizontal Uncertainty $THU_{max} = 0.05 \cdot D + 5$,

where D is the water depth in metres.

Considering a reference depth for the shallow lake system of Mantua, $D = 4$ m, the maximum allowed vertical and horizontal uncertainties result in 0.5 m and 5.2 m, respectively. Thus, the Deeper CHIRP+ sonar complies with the official requirements for bathymetric surveys.

Given the satisfactory test results, the instrument was used to map the whole Lake Superiore between 2022 and 2023, using the "fishing from boat" working mode. The instrument was fixed to a small boat that was steered along lake transects with a spacing of approximately 25 m. The speed of the boat was always kept lower than 5 km/h, as suggested by Deepersonar (Deepersonar, 2023) to avoid problems in the measurements. The sonar frequency was set to 675 kHz to obtain the narrowest beam, resulting in more detailed scans: for a depth of 4 m, the 7° cone produces a circle with radius 0.5 m on the bottom. Given the shallow depths measured, no issues related to the attenuation of the high-frequency signal were encountered.

The survey revealed two potential sources of errors:

- the sonar was fixed to the boat using the Deepersonar flexible arm; this connection is flexible, so the instrument can tilt after contact with obstacles such

Figure 5.1: Float for bathymetric surveys with Deeper sonar and Stonex GNSS receiver

as emergent vegetation or due to its drag with water; when the instrument is tilted, the depth reading is biased and may result in completely wrong (overestimated) measurements;

- the phone positioning system has an accuracy of the order of 3-5 m and is located on the boat, close to the sonar but not exactly in the same place; this may lead to an error in the positioning of the acquired depth data, which is not negligible for the bathymetric survey of small rivers or other contexts requiring high precision. Using the sonar's internal GPS receiver removes the offset with the phone but does not improve the quality of positioning; in fact, the built-in system uses a single point L1 receiver that has an accuracy of up to 3 m. (Bogoyavlensky et al., 2020).

These problems were solved by building a tetherable hand-made catamaran that is capable of keeping the sonar always vertical (Figure 5.1). On this float, a Stonex S850+ RTK GNSS receiver was mounted, keeping the alignment between the antenna and the sonar in order to achieve centimetric accuracy in positioning. The Stonex receiver is managed with an Android tablet. The FishDeeper application was downloaded on this tablet and was used in the"Fishing from boat" mode after forcing it to use the position provided by the external GNSS receiver. This was possible because the receiver was connected via Bluetooth, while the sonar works via Wi-Fi connection.

This approach closely follows that of Vozza et al. (2023), which differs primarily in the use of a custom configuration in place of a commercially available GNSS system, and in the less advanced design of the float.

With the above-described instrument setup, between 2024 and 2025, most of the wetland (where the depth was sufficient for the transit of the boat) was mapped. The instrument was towed with a small motorboat, using a boom to keep it laterally to avoid disturbance of the propeller. Longitudinal sections were acquired in 1 or 2 lines for the secondary channel network and 3 or more for the main Mincio River branch. Subsequently, river transects were added at every bifurcation and section of interest. The distance between consecutive points inside a measurement path was about 1-2 m depending on the boat velocity. The maximum spacing between different longitudinal sections was approximately 13 m.

Using the QGIS Inverse Distance Weighting (IDW) algorithm, the depth data resulting from the wetland's survey were interpolated to obtain a raster map with 1 m resolution. The interpolation method was chosen on the basis of Diaconu et al. (2019), and a cross-validation procedure was applied using a randomly-selected 10% subset of the data. The resulting map was then compared with a previous bathymetric survey conducted in 2016 with a Lowrance Chirp 7 sonar by Telò and Menna (2016) (Davide Menna, personal communication). This map, similarly to the new one, was mainly composed of single point depth measurements along longitudinal sections.

The analysis was performed in QGIS with a point sampling tool (Jurgiel, 2022) comparing the depth in each point in the 2016 dataset with the corresponding value in the new interpolated bathymetry. Using this procedure, the interpolation of the 2016 dataset was avoided to remove another potential source of error. Given the interpolation's weakness in the representation of the irregular bathymetry of the wetland's study area, all the points in the interpolated reference map with a distance greater than 1 m from any new measurement points were excluded from this analysis. The depth difference was computed for every point as (depth2025 - depth2016) and then changed in sign to obtain the (more convenient) difference in bed elevation, which shows erosion with negative values and deposition with positive values.

A similar approach was used also for the post-processing of the lake's data with the difference that, considering the larger number of points, the CloudCompare rasterize tool was used instead of QGIS for the interpolation. A Kriging algorithm was used, setting the output resolution to 10 m. The interpolated map was compared with a bathymetric dataset acquired in 2006 from the University of Parma (Telò et al., 2007) consisting of 107 points. As was done for the wetland, this part of the analysis was made with QGIS point sampling tool. Again, the bed elevation difference was computed for every point as: (depth2006 - depth2023). This method works because Lake Superiore is regulated at a constant level of 17.50 m a.s.l. with fluctuations within $\pm$ 5 cm.

To detect whether bed elevation differences could be affected by potential errors in the interpolation of the new survey's data, field validation was conducted on a subset of 15 points belonging to the 2006 bathymetry. The selected points were located in the most critical areas for interpolation: around the lotus flower patch and inside the main channel in the northern part of the lake, where abrupt changes in the bathymetry may be smoothed by interpolation, leading to errors. The points were reached using a Stonex S850+ GNSS receiver, and the depth was measured using the Deepersonar CHIRP+ as was done for the survey. The maximum difference between the interpolated and measured depth was 0.6 m with an average error of 0.2 m. For this reason, differences in bed elevation between 2023 and 2006 smaller than 0.2 m were not considered a true morphological evolution.

5.2.2 Results and discussion

Lake Superiore

The bathymetric survey of the lake resulted in a map containing approximately 1 million measured depth points. From the results of the interpolation (Figure 5.2), it is possible to notice the presence of a bifurcated morphology, with two main channels and a shallower area in the middle, where lotus flower grows, with a minimum depth of 0.5 m. The northern channel, in the hydraulic left, is the deepest one with a maximum depth of 6 m, while the lake's mean depth is 3.2 m. In the north-west part of the lake, a disused quarry is present, with an irregular bottom and a maximum depth of 8 m. The volume of the lake (without considering the quarry) is equal to 8.85 million cubic metres.

Figure 5.3 shows a map of the estimated morphological evolution between 2006 and 2023. The maximum difference refers to a point inside the former quarry with 4.8 m of deposition. This extreme value can be considered as the result of an interpolation error; inside the quarry the bottom is irregular, thus the interpolation of the available bathymetric data may be too coarse to represent it in an accurate way and can be affected by local bedforms. A new survey with higher resolution should improve the representation of this area, but in the following analysis it was excluded from the study domain. This choice is supported by the fact that the quarry is rather separate from the lake and exchanges water and sediment with it only through a small aperture in the embankment. Satellite images acquired during high sediment transport events confirm the low interactions between the lake and the quarry (Figure 5.4), while an impressive turbidity pulse coming from the wetland was visible in the lake.

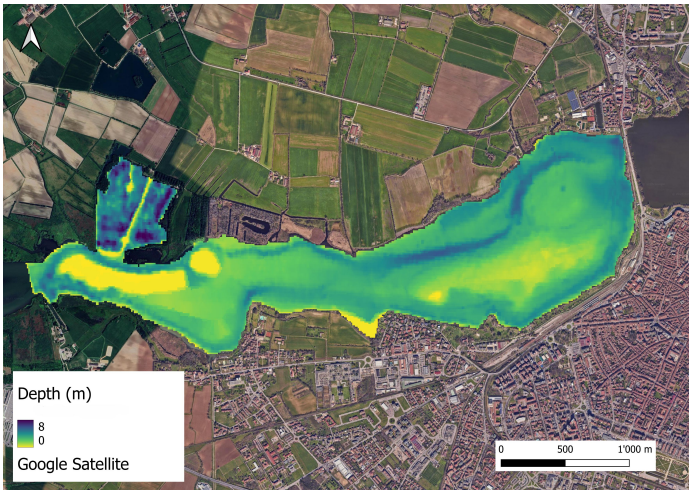

Figure 5.2: Bathymetric map of Lake Superiore obtained after the measurements interpolation

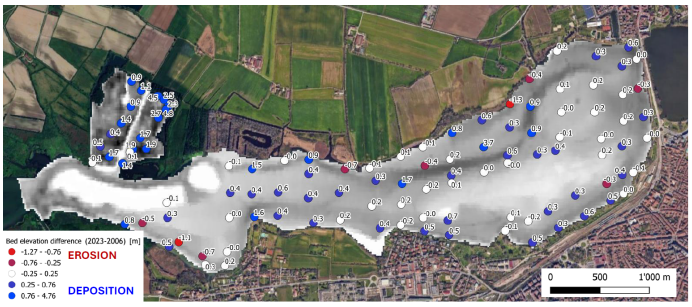

Figure 5.3: Difference in bed elevation between 2006 and 2023 in Lake Superiore

Figure 5.4: Planet satellite image of a sediment transport event (16 March 2025) showing high turbidity coming from upstream, with low interactions with the former quarry area

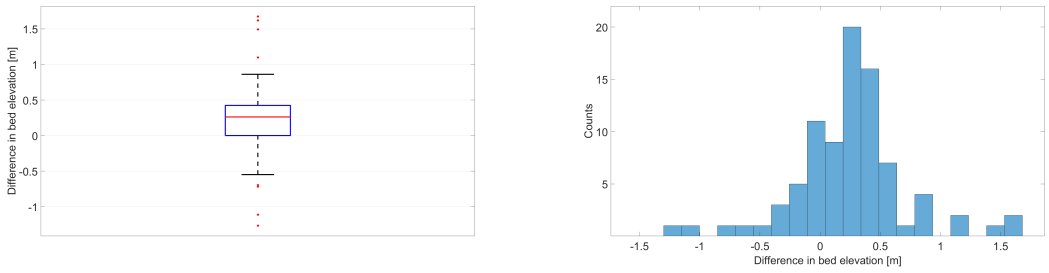

(a) (b)

Figure 5.5: Boxplot (a) and histogram (b) of the difference in bed elevation between 2006 and 2023 in Lake Superiore

Another source of error is the low accuracy in the positioning of the points that was achieved in 2006 using an old GPS receiver. In case of a steep slope in the lakebed, a few metres of horizontal error can lead to significant discrepancies in the corresponding depth. This problem probably applies to the 6.5 m deep point measured in 2006 north of the lotus flower patch, near the main channel in the lake's hydraulic left. The depth measured in 2023 in this area is around 3 m, while the measured point was likely located inside the main channel, 100 m apart. For this reason, the resulting 3.6 m value of deposition, which is clearly out of scale, was removed.

The difference in bed elevation between the two surveys, averaged over the remaining points after filtering, results in 0.26 m of deposition, with a maximum value of 1.67 m of deposition (Figure 5.5). The maximum deposition of the order of 1 m can be considered reasonable and was also found in the Vallazza wetland (downstream of Mantua) where a deposition level of 1.41 m in 22.5 years was measured with radiochemical analysis on sediment cores (ISPRA, 2009). The maximum value of 1.67 m divided by 17 years leads to a sedimentation rate of approximately 10 cm/year. However, if the average deposition trend (0.26 m) is considered, the resulting rate becomes approximately 1.5 cm/year. According to these rates, 1 m of deposition in Lake Superiore can take place in 10 or 66 years, respectively.

Interestingly, Figure 5.6 shows a statistically significant slight correlation ($R^2 = 0.25$, p-value $= 7 \cdot 10^{-7}$) between the depth values measured in 2006 and the morphological evolution between 2006 and 2023, indicating a gradual smoothing process of the lake's bedforms. The same trend can also be observed from the map in Figure 5.3, where it is possible to notice that the deepest parts of the lake have been progressively filled with sediment, while the shallow areas near the coastline have been subject to erosion.

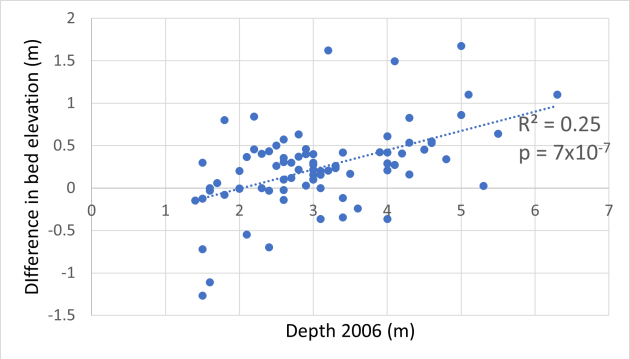

Figure 5.6: Correlation between 2006 depth and bed elevation difference (between 2006 and 2023) in Lake Superiore

In Lake Superiore, an area of 1.9 km^2, corresponding to 53% of the lake's surface, has a depth of less than 3 m (Figure 5.7), which is the maximum depth for lotus flower growth (Nohara and Tsuchiya, 1990). This means that this area could become completely covered by emergent vegetation if the local authority stops its effort to control invasive macrophytes spread. This could lead to a feedback effect: vegetation increases the lakebed aggradation rate due to sediment trapping and dead biomass accumulation, thus creating better conditions (shallower depths) for new growth of emergent vegetation (see, for example, Papastergiadou et al., 2007). Within the already vegetated area, a surface of 0.1 km^2 has a depth less than 1 m. This can potentially switch to dry land within a timeframe of the order of decades if the measured trend remains constant, or even less, if the above-mentioned feedback effect develops.

Using the QGIS IDW algorithm, the point data of differences in bed elevation were interpolated with a 10 m resolution to obtain a map of the morphological evolution and then an estimate of the deposited volume. The net deposited volume according to this calculation is 888 960 m^3, which corresponds to 10% of the total volume of the lake, and divided by 17 years gives a value of 52 291 m^3/year. Using the dry-bulk density, defined as the mass of the dry solids divided by the total volume of the wet sample, it is possible to compute the mass accumulation rate (e.g, Kathleen A. et al., 1992). The dry-bulk density of sediments in the Mantua lake system was measured in 2008 (Langone, 2009) with 4 sediment cores. Data from a sample on Lake Di Mezzo (the closest available to Lake Superiore) were used for this computation after averaging the values of the whole core down to 109 cm. The resulting dry-bulk density is 0.4 g/cm^3, which multiplied by 52 291 m^3/year gives the accumulation rate of 20 916 t/year, or 57 t/day.

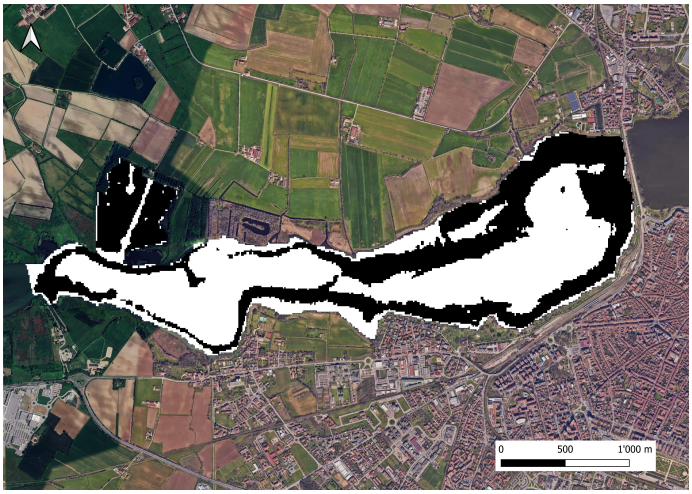

Figure 5.7: Extension (shown in white) of the Superiore Lake's area with depth lower than 3 m

Valli del Mincio wetland

The bathymetric map of the wetland shows a clear difference between the main course of the Mincio River and the secondary channel network (Figure 5.8). The mean depth in the secondary channel network is 1.1 m, while inside the main branch of the Mincio River it is 2.4 m with a maximum depth of 4.4 m.

The main Mincio River course proved to be the most morphologically-active portion of the system, with classical deposition on the internal side of the bends and erosion on the external side (Figure 5.9). The shallowest and narrowest portion of the channel network has not shown important changes in depth during the past 9 years. This is probably due to the low depth and the presence of aquatic vegetation resulting in an extremely low water and sediment discharge that is flowing inside this area. As a consequence, from a morphological point of view, this portion can be considered almost disconnected from the river.

Only a limited subset of the channel network was available for the depth comparison between 2016 and 2025, because many dredging operations were carried out by the Mincio Park authority to prevent channel infilling. Among these untouched channels, only a very small portion was mapped in both 2016 and 2025 bathymetric surveys, because many of them have been filled with sediments or obstructed by vegetation and were therefore no longer accessible by boat. This observation is already a sign of the rapid evolution that is going on in the wetland's morphology. Figure 5.10 shows the only complete channel for which depth data are available for both 2016 and 2025, and where no dredging operations were carried out between the

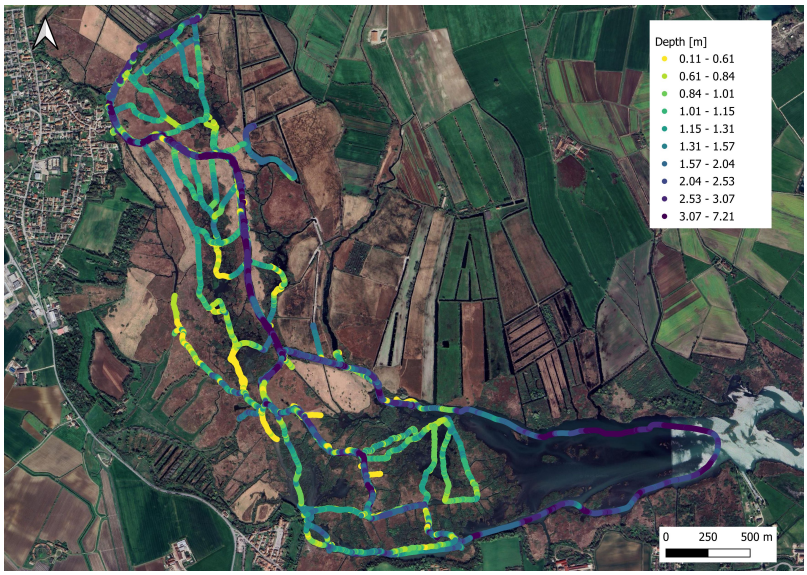

Figure 5.8: Bathymetric map of the Valli del Mincio wetland acquired in 2024/2025

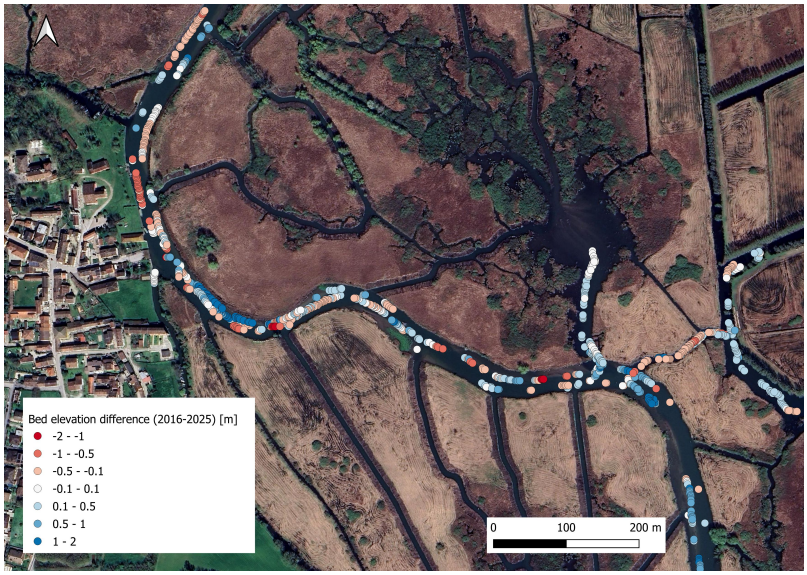

Figure 5.9: Bed elevation difference between 2016 and 2025 in the main Mincio River course near the village of Rivalta

Figure 5.10: Bed elevation difference between 2016 and 2025 in a channel inside the wetland

two surveys. Almost the entire channel was affected by sediment deposition, with differences of approximately 0.5 m and locally up to 1 m occurring in 9 years. This results in a rate of up to 11 cm/year, consistent with what was measured by Longhi et al. (2008) in the Paludi di Ostiglia wetland.

These analyses were conducted on the hypothesis of a constant and uniform water level in the entire wetland. However, the use of an RTK GPS with centimetric precision mounted on the float for the bathymetric survey also made it possible to map the water surface elevation of the entire channel network. From these measurements (Figure 5.11), a gradient is present along the Mincio River, with an elevation difference of 30 cm over a distance of approximately 5 km. Using these data, it is possible to estimate the slope of the river, 6×10^{-5}, which gives an idea of the low energy of this riverine system. Water surface elevation in the wetland is influenced by the discharge and the level of Lake Superiore, therefore it was not possible to use the same measurements also for the 2016 depth survey to compare the real bed elevation data. However, future surveys with the same technique will be able to take advantage of this useful additional information for a more precise bathymetric comparison.

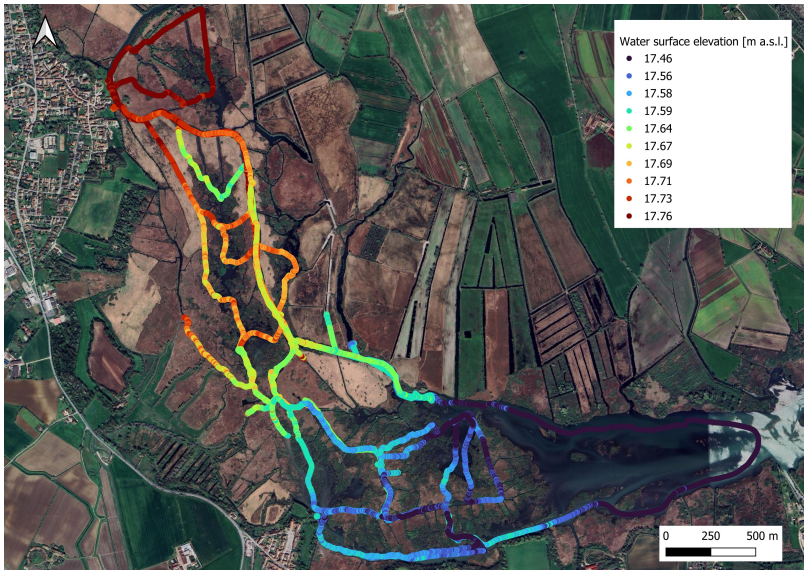

Figure 5.11: Measured water surface elevation in the wetland's channel network

5.3 Water and sediment discharge characterisation

5.3.1 Materials and methods

From February 2024 to December 2025, 23 field campaigns have been carried out on a monthly basis to study the physical and chemical parameters of the Mincio River reach between Pozzolo (municipality of Marmirolo, 30 km upstream from Mantova) and Grazie (municipality of Curtatone, inside the Valli del Mincio wetland), and also its main tributaries. Each field campaign consisted of discharge measurements, multiparameter probe measurements, and water sampling for laboratory analyses in 6 different sites: 4 of them located on the Mincio River (Pozzolo, Goito, Rivalta, Grazie) and 2 on the main tributaries (Goldone and Osone channels). The discharge was measured using a Teledyne RDI StreamPro ADCP tethered between the river's banks from a bridge or using a tagline. Each measurement was repeated until at least 4 transects were acquired with standard deviation lower than 5%. The water samples were collected with plastic bottles, kept refrigerated, and analysed by Fondazione Edmund Mach hydrobiology laboratory the day after the sampling. A Total Suspended Solids (TSS) measurement was carried out by filtering the samples through Whatman GF/C glass fibre filters with a porosity of 1.1–1.2 microns. The

TSS concentration (mg/L) was determined by drying the filters in an oven at 110°C. The mineral content was obtained by further combusting the filters in a muffle furnace at 550°C, and the organic matter was calculated by subtracting the two values. Moreover, for a complete characterisation (not discussed in this thesis), a detailed chemical analysis was performed on the samples, including pH, different nitrogen forms, phosphorus, and silica. The availability of both discharge and concentration measurements acquired at the same time made it possible to compute the nutrient and sediment loads entering the Mincio River and being transported to the wetland and the lake.

The grain size distribution of the suspended sediment was measured using laser scatter technology with a Malvern Panalytical Mastersizer 3000. Two water samples from the Goldone channel and two from the Osone channel were analysed in this way. To reach a sufficient laser obscuration degree, part of the water was removed from the samples after proper settling of the suspended particles. The granulometric curves of the bottom material were available for 6 different points between the wetland and the lake thanks to a survey conducted by ISPRA in 2008 (ISPRA, 2009).

Supplementary rainfall data were obtained from the ARPA Lombardia weather station in Goito, located roughly in the centre of the study area.

5.3.2 Results and discussion

Figure 5.12 shows the sediment loads calculated from the discharge and concentration measurements collected during the monthly field campaigns. According to these estimates, the maximum daily loads would be 44 t/day for the Goldone channel, 143 t/day for the Osone channel and 47 t/day for the upstream portion of the Mincio River. It is important to emphasize that, in the absence of continuous measurements, these data represent only approximate estimates, because sediment concentration may be subject to rapid fluctuations during the day, especially during flood events. For comparison, Telò et al. (2007) in March 2006 estimated TSS loads of 2 t/day and 14 t/day in Goldone and Osone, respectively, using the same method. Especially for the Goldone and Osone channels, it is possible to observe a strong influence of the rainfall events that occurred in the days before the samplings. In fact, maximum values were measured the day after a heavy rainfall event in December 2024. Conversely, during 2025, which was in general a less rainy year, no extreme values were observed. Due to this variability, individual measurements are not representative of the phenomenon, although they are repeated monthly. For this reason, the average load over the entire 2-year monitoring period is reported in Table 5.1. From the table it is possible to see that, despite their low discharge, Goldone and Osone have

a higher sediment yield than the Mincio River. The same table also shows the percentage of organic matter, which is lower in the tributaries than in Mincio. The fact that this sediment is composed mainly of mineral material supports the hypothesis of its provenance from surface runoff.

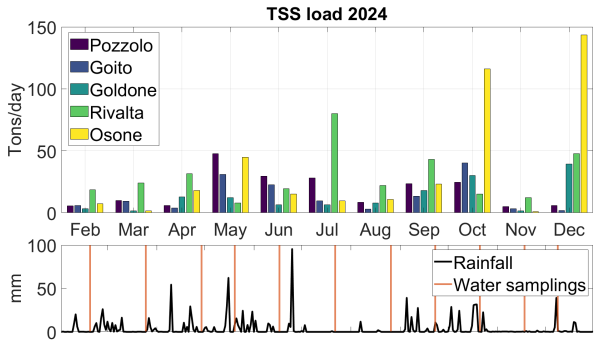

(a)

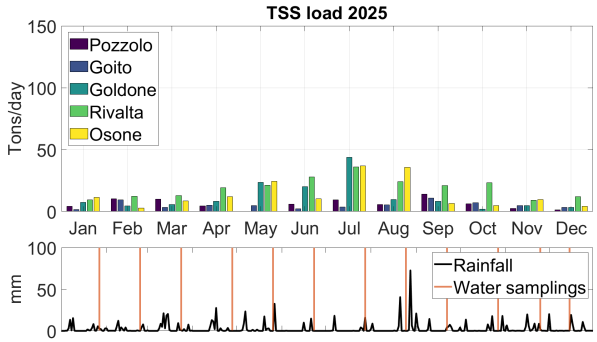

(b)

Figure 5.12: Histogram of 2024 (a) and 2025 (b) TSS loads with the indication of the sampling day over a rainfall time series

Laser granulometric analysis of two water samples for each of the tributaries resulted in an average median particle size (D50) of 14 µm for Goldone and 12 µm for Osone. These diameters correspond to silt, which has a strong tendency to be transported in suspension. This explains why it settles mainly in the secondary channel network of the wetland, where the water velocity is slower, and can easily reach Lake Superiore during flood events. This also explains the low efficiency of a recent sediment retention basin created by the Mincio Park authority on the Osone channel before its confluence with the Mincio River.

Figure 5.13 shows the relationship between discharge and TSS in all monitored

Table 5.1: Comparison between average sediment load transported by the Mincio River and its main tributaries in the study area

Station	TSS concentration (mg/L)	% organic matter	Discharge (m^3/s)	TSS load (t/day)
Upstream (Goito)	5.0	33	18.5	9.2
Goldone	44.2	15	2.8	12.6
Osone	51.6	15	4.1	25.2

stations. A clear difference is visible between the river tributaries (Goldone and Osone) and all the other stations on the Mincio River. The tributaries show low variations in discharge, while they cover a wide range of suspended solid concentrations. On the other hand, in the Mincio River the behaviour is the opposite. In the tributaries, there is a correlation between discharge and TSS, suggesting that they are linked to the same physical process. This further confirms the fact that the suspended sediments in these channels originate from surface runoff, which increases after rainfall events together with discharge. In contrast, the river is regulated and has limited sediment input from agriculture. As expected, the Rivalta sampling station shows a trend between the two, because it is located on the Mincio River downstream of the Goldone channel inflow.

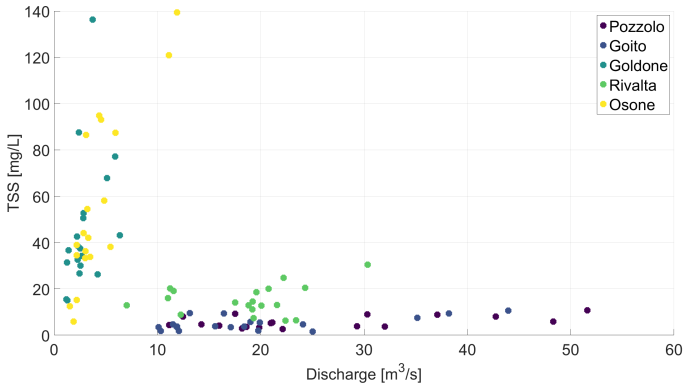

Figure 5.13: Relationship between discharge and TSS in all the monitored stations

The sum of the average TSS loads of Mincio, Goldone, and Osone expressed in Table 5.1 results in a total load of 47 t/day entering Lake Superiore. This value is consistent with the sediment deposition estimate provided by the bathymetric analysis described in the previous chapter.

The quantification of sediment transport is often characterised by substantial uncertainties. To compare the results with a reference value, the soil loss map for the Mincio River basin was downloaded from the JRC European Soil Data Centre (ESDAC) (Panagos et al., 2024). The estimated soil loss in this region is on the order of $1\,\mathrm{t\,ha^{-1}\,yr^{-1}}$, which, multiplied by the Mincio catchment area of $600\,\mathrm{km^2}$, yields a total soil loss of approximately 60 000 t/yr or 164 t/day. This figure represents an overestimation of the sediment load in the Mincio River reaching Lake Superiore, because Mantua is 20 km upstream of the catchment's outlet. In addition, not all incoming sediment is transported to the lake. Thus, 57 t/day of deposition resulting from the estimate of Lake Superiore morphological evolution can be considered a reasonable value, at least as an order of magnitude.

5.4 Conclusions

A bathymetric map of Lake Superiore and Valli del Mincio wetland was produced using a low-cost sonar instrument after having tested and specifically adapted it for this purpose. The comparison of this map with previously acquired data allowed for an analysis of the system's morphological evolution. This comparison was complicated by the low resolution of the available historical data. Despite this, a clear deposition trend is visible both in the lake and in the wetland, with maximum deposition of the order of 1 m, although with different mechanisms; in the lake it is quite uniform, while in the wetland it takes place mostly at the inner part of bends and in secondary channels. This difference is a consequence of the strong dependence of fine sediment transport on flow velocity, which plays a crucial role in shaping these types of environment.

The analysis of the lake's morphological evolution allowed for the estimation of the total amount of sediment that deposited in the lake in the last 17 years. The impressive result of a mean accumulation rate of the order of tens of tonnes per day was confirmed by the estimates of sediment load inputs based on both field samplings and literature soil loss data.

The sedimentation trend is producing negative impacts, such as the reduction of 10% of the lake's available water storage capacity in 17 years, the loss of aquatic ecosystems, and the rapid spread of invasive macrophytes. The sediment source was detected through a 2-year monitoring campaign with monthly discharge and TSS measurements. The Goldone and Osone channels were shown to transport considerable amounts of sediment coming from the agricultural lands they drain, especially after rainfall events. Based on this observation, a suggested solution to

mitigate the ongoing terrestrialization could be the reduction of sediment inputs from agricultural runoff creating buffers of riparian vegetation along the ditches network.

Important future developments of the monitoring activity have already been planned. In October 2025 a Solitax t-line sc turbidimeter was installed on the Osone channel and calibrated with concurrent TSS measurements. A more detailed calibration of this instrument from turbidity (FNU) to sediment concentration (mg/L) will allow a continuous measurement of the sediment concentration. This will result in a more precise estimate of the incoming load in the wetland. In addition, a numerical sediment transport model for the Valli del Mincio wetland is currently being developed. This is made possible thanks to the acquired knowledge of the morphology of the system, together with the water and sediment discharges, the slope, and also the diameter of the transported and bottom sediments. This model will help the management agency understand the evolution trends of the system, plan future dredging operations, and predict the effects of different river regulation strategies.

6. Dissolved oxygen exchanges

6.1 Introduction

This section gives insight into the dynamics of dissolved oxygen in Mantua Superiore Lake and wetland, with a particular focus on hypoxia and hyperoxia conditions. The analysis is based on continuous measurements at different depths and under different vegetation coverages and also includes the effect of discharge.

Dissolved oxygen (DO) is present in the water column as a result of diffusion from the atmosphere or photosynthesis from aquatic plants. Different biotic and abiotic factors can influence its concentration, such as atmospheric pressure, water temperature, salinity, ice cover, respiration, and photosynthesis. Moreover, mixing plays a crucial role, since dissolved oxygen sources and sinks may be located in different parts of the water column or in different portions of a water body. In this regard, the Lake number, a quantitative indicator of lake mixing, has been used successfully to estimate changes in dissolved oxygen by Robertson and Imberger (1994).

The decline in dissolved oxygen is widespread in temperate lakes due to reduced oxygen solubility in warmer water temperatures, stronger thermal stratification, and lower water clarity (Jane et al., 2021). By contrast, a subset of highly productive lakes is showing an increase in surface water's dissolved oxygen, probably owing to increased phytoplankton production. During anoxic conditions, nutrients such as phosphorus can be released from bottom sediments (internal load), further exacerbating lake's eutrophication (Frodge et al., 1991). This process can also favour harmful algal blooms with potentially detrimental consequences for water supplies and human health.

Dissolved oxygen is one of the most important factors for aquatic animals, which therefore affects the biodiversity of a water ecosystem: many aquatic species require well-oxygenated habitats to survive, but also hyperoxia (oxygen oversaturation) can be dangerous, for example, for fish (McArley et al., 2021). For a review of the effects

of dissolved oxygen concentration on freshwater fish, the reader can refer to Ali et al. (2022).

Supersaturation is usually a consequence of oxygen production from photosynthesis, especially in highly-stratified conditions. On the other hand, Craig et al. (1992) reported a dissolved oxygen saturation of 240% in an ice-covered Antarctic lake resulting from oxygen-rich meltwater inflow (only 11% of oxygen was produced by biological activity) and limited exchange with the atmosphere due to the ice coverage. While anoxia has been well-documented in many scientific works, supersaturation remains less explored.

Photosynthesis from algae and submerged aquatic vegetation plays a crucial role in maintaining good dissolved oxygen levels, especially in the deeper part of the water column. This is particularly true during stratification periods, where respiration from the sediment cannot be compensated for by diffusion from the atmosphere. The submerged parts of aquatic plants also act as substrates for epiphytic photosynthetic organisms resulting in additional oxygen production. In contrast, floating and emergent species of vegetation can alter dissolved oxygen dynamics due to various physical and biological factors:

- oxygen produced by plants with photosynthesis is released directly into the atmosphere and not in water (Pokorný and Rejmánková, 1983);
- the shading of the underlying water column reduces light penetration, hampering the oxygen production by photosynthetic organisms such as phytoplankton and in particular periphyton (Cattaneo et al., 1998);
- the canopy reduces the exchanges at the water-atmosphere interface (Moore et al., 1994);
- the stems and other submerged parts reduce the water speed, increasing the local residence time of the water (Moki et al., 2020);
- the dead biomass accumulating at the bottom at the end of the vegetative season is decomposed, resulting in oxygen consumption for bacteria respiration (Longhi et al., 2008).

Caraco and Cole (2002) measured frequent dissolved oxygen values below 2.5 mg/L in the Hudson River inside large floating macrophyte beds of *Trapa natans* during the summer growing season. In contrast, during the same period, DO inside a submerged macrophyte bed (*Vallisneria americana*) never declined below 5 mg/L.

Anthropogenic activities can promote hypoxia events in aquatic systems due to the direct organic load that can consume dissolved oxygen in the water column. For example, Clark et al. (1995) measured an increase in the minimum dissolved oxygen concentration in the Hudson River after improved wastewater treatment. Additionally, discharge reduction can lead to reduced mixing and an increased retention time in a water body.

Individual dissolved oxygen profiles can lead to incomplete or misleading results because, in highly eutrophic environments such as the present case study, oxygen concentration exhibits large fluctuations between day and night (Xu and Xu, 2015). Given its low solubility in water, high daytime oxygen values above saturation (sign of dystrophic conditions) often conceal nighttime hypoxia issues, which are not recorded by normal spot monitoring activities (usually conducted during the day).

Previous investigations in Mantua lakes and wetland highlighted high hypoxia concerns related to low summer discharges and the expansion of floating invasive macrophytes. Despite this, a continuous measurement of dissolved oxygen was missing. The Mantua Province conducted a monitoring campaign with diurnal dissolved oxygen profiles in different parts of the lake system, under different macrophyte coverages. For Lake Superiore, the minimum measured value was 4 mg/L below the main lotus flower patch, while in open water it was always close to saturation or even far above, with a maximum value of 12 mg/L (Telò et al., 2007). Pinardi (2008) conducted 9 intensive monitoring activities with high frequency samplings over 24 hours to compute the dissolved gas balance of Lake Di Mezzo. They noticed a deficit in dissolved oxygen between April and August, corresponding to the period of maximum expansion of the floating macrophyte water chestnut (*Trapa natans*). They also measured the respiration rate of the lake sediment through laboratory incubation of sediment cores. In the *T. natans* meadow it resulted in $0.71\,\mathrm{mmolO_2\,m^2d^{-1}}$ during winter and $2.54\,\mathrm{mmolO_2\,m^2d^{-1}}$ during summer, showing a possible cause of hypoxia because the oxygen consumed at the bottom could not be replaced due to the effect of the vegetation cover.

6.2 Materials and methods

During 2024 and 2025 4 PME MiniDOT dissolved oxygen sensors were deployed for a total period of 12 months inside the Valli del Mincio wetland and Lake Superiore. The measurements took place mostly during summers, when hypoxia events are more likely to occur, but additional deployments were conducted also in spring, autumn

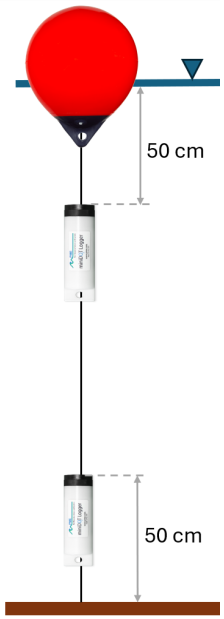

Figure 6.1: Schematic representation of the DO sensors' configuration

and winter 2024, and autumn 2025 for a better understanding of the oxygen dynamics in different seasons. For most of the time, the sensors were fixed to 2 buoys, each of them mounted one sensor at 50 cm from the surface and one at 50 cm from the bottom. A schematic of the sensors' configuration is visible in Figure 6.1. To avoid biofouling, a PME MiniWiper automatic cleaner was mounted on every sensor near the surface. The sensors near the bottom were not affected by biofouling because they were below the euphotic zone due to the low light penetration for high turbidity. The sensors' sampling rate was set to 5 minutes and the wiping interval to 4 hours. In Lake Superiore one buoy was located 40 m inside the main lotus flower patch, under the vegetation coverage, and one outside, at a distance of roughly 10 m from the patch's edge, 50 m from the other buoy (Figure 6.2). Within the wetland the sensors were located under a *Ludwigia hexapetala* cover, under a lotus flower patch, and in open water.

MiniDOT sensors also acquired water temperature. Other useful additional information such as air temperature, wind speed, and solar radiation was downloaded from ARPA Lombardia Lunetta weather station, located about 3 km east of the lake (https://www.arpalombardia.it/temi-ambientali/meteo-e-clima/form-richiesta-dati/).

The Lake Analyzer software (Read et al., 2011) was used to compute different stratification indexes based on measured temperature time series (Section 7) and

Figure 6.2: Position of the buoys near the edge of the main lotus flower patch in Lake Superiore

additional weather data such as wind speed from the ARPA Lombardia weather station.

For the analysis of the influence of discharge on dissolved oxygen, the discharge data of the Mincio River downstream of the Casale di Goito sluice-gate were obtained from a rating curve. Continuous water level data were provided by AIPo, while discharge measurements for the rating curve were conducted with an ADCP during the monthly field campaigns described in Section 5.3.

6.3 Results and discussion

6.3.1 Lake Superiore

During April 2024 a 1-week deployment inside the area where lotus flower grows showed concerning dissolved oxygen values. The lotus flower begins to wither in autumn, thus during spring all the plants are usually completely decomposed or lying on the lake bottom in the process of decomposition. This was the scenario during April 2024, without any floating or emergent plant portion altering light penetration, and with water temperature ranging between 15 and 22 °C during the monitoring week. Despite this, a minimum dissolved oxygen value of 20% was measured near the bottom and a maximum value of 170% at the surface (Figure 6.3).

An abrupt dissolved oxygen decline began on April 10, a rainy day with low solar radiation and strong water mixing. The oxygen trend showed evidence of two processes that were taking place in the water column: destratification and strong respiration near the lakebed for biomass degradation. As soon as solar radiation was back, on April 11, surface oxygen saturation started to increase, while at the bottom

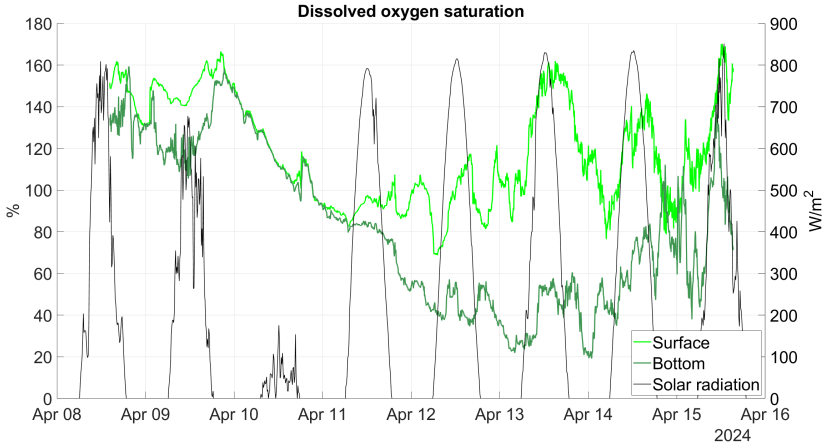

Figure 6.3: Overlay of solar radiation and dissolved oxygen saturation in Lake Superiore before the lotus flower growth (April 2024)

it continued its decline for 2 more days even if the sky was clear, probably because stratification was restored. This compromised situation even before the beginning of the summer season was a warning sign that was confirmed by subsequent monitoring activities. During June 2024, in fact, frequent DO saturation values around 0% were measured near the bottom, both inside and outside the lotus flower patch, which was at the beginning of its growing season. Near the surface, an extremely high dissolved oxygen saturation was present, with frequent exceedances of 300% (corresponding to 25 mg/L) and a maximum value of 380% (Figure 6.4).

Such elevated levels of oxygen saturation have never been documented in any previous published work on natural waters. Being the sensor upward looking, this cannot be a consequence of a gas bubble trapped below it. Additionally, both upper sensors measured similar values, making it less likely that the measure was the result of instrument malfunction. Although such high DO values are outside the instrument's calibration range, they can be considered valid, at least as orders of magnitude (PME, personal communication). As a reference, ARPA Lombardia measured dissolved oxygen saturation in the surface layer around 300% 4 times in the period 2009-2019 in Lake Superiore (ARPA Lombardia, 2020). This finding indicates a strong eutrophication of the lake, resulting in very high algae biomass. Considering that the Secchi disc depth of the lake is always less than 1 m during summer, all photosynthetic organisms are probably concentrated in the very upper part of the water column, creating a dense algae layer floating around 50 cm below the surface. This layer producing a high amount of oxygen right at the sensors' depth can be the

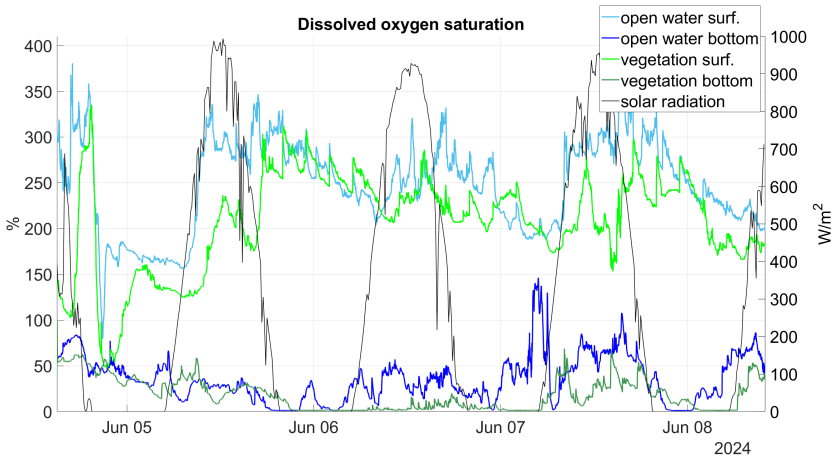

Figure 6.4: Overlay of solar radiation and dissolved oxygen saturation inside and outside vegetation in Lake Superiore at the beginning of the lotus flower growing season (June 2024)

cause for the extreme oxygen readings.

As expected, dissolved oxygen under the vegetation cover was lower than outside, both at the surface and at the bottom. The difference between the surface and the bottom DO values is quite impressive considering that the total depth was less than 3 m and the vertical distance between the sensors was only 180 cm. This difference is well described by the Schmidt stability parameter (Figure 6.5), which represents the amount of work per unit surface area (J m^{-2}) required to completely mix a stratified water column to uniform density. This index was computed from the temperature data with the following equation:

$$S = \frac{g}{A_0} \int_0^{z_{\max}} (z - \bar{z})\ \rho(z)\, A(z)\, dz\,, \tag{6.1}$$

where g is the gravitational acceleration, A_0 is the surface area of the water body, z is depth, $\rho(z)$ is the water density at depth z, $\bar{z}$ is the depth of the centre of volume, and $A(z)$ is the horizontal area at depth z.

When the water column is stably stratified, it is more difficult for the oxygen available in the surface layers to reach the lake bed and compensate for the one that is consumed at the sediment level. The same consideration is valid also for the data acquired during the end of summer (August-September), but with the difference that the DO saturation at the bottom of the vegetation remained close to 0% for the entire measurement period of 3 weeks (Figure 6.6). This may be explained by the fact that the lotus flower was at its maximum expansion level, sheltering the water column from the mixing effect of the wind. In contrast, extreme hyperoxia conditions were

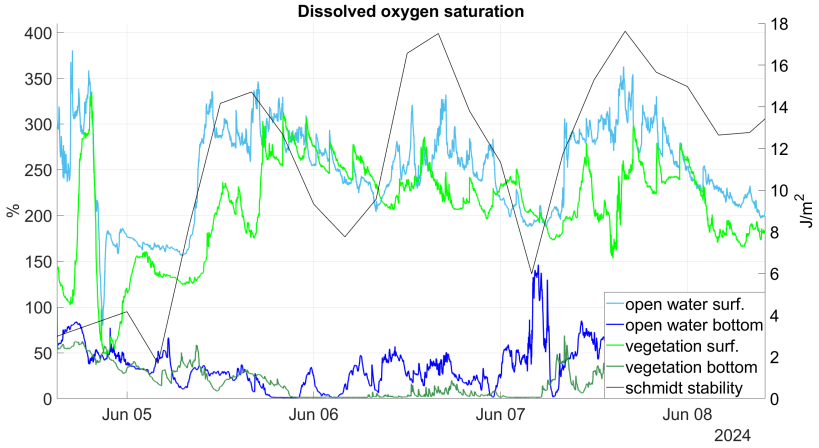

Figure 6.5: Comparison between dissolved oxygen saturation inside and outside vegetation in Lake Superiore and the Schmidt stability index

measured near the surface with a peak of 400% (30 mg/L), probably due to a strong algal bloom enhanced by the high water temperatures (reaching 30 °C at the sensor's depth of 50 cm).

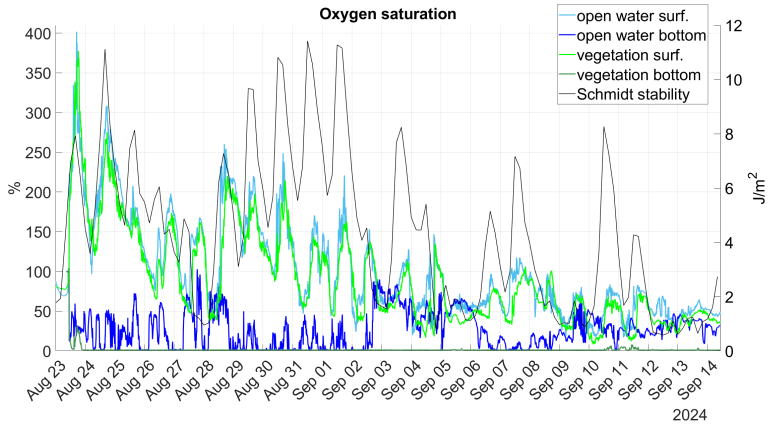

Figure 6.6: Comparison between dissolved oxygen saturation inside and outside vegetation in Lake Superiore and the Schmidt stability index at the peak of the lotus flower growing season

Although Robertson and Imberger (1994) found the Lake number to be a good indicator of oxygen flux across the thermocline, here it was not correlated with the observed oxygen fluctuations. A possible explanation for this mismatching is the fact that the Lake number, differently from the Schmidt stability parameter, includes the

Figure 6.7: Position and picture of the buoy for dissolved oxygen monitoring inside the lotus flower near Grazie in the Valli del Mincio wetland

effect of wind in the computation, and the only available wind data were measured from a station 3 km away from the lake in an urban context, which might have altered the wind field.

A set of dissolved oxygen measurements was acquired during the closure of the Casale gate, resulting in water diversion into the Diversivo channel and reduced discharge in the Mincio River. These data do not show a correlation between Casale gate closures and dissolved oxygen values. In fact, the through-flowing discharge in Lake Superiore is the sum of the Mincio River discharge and many other contributions that must be taken into account, especially after heavy rainfall events, which is often the case when the Casale gate is closed. To date, continuous monitoring of the total discharge in Lake Superiore is still missing. For this reason, there are not enough available data for a precise analysis of the influence of discharge on dissolved oxygen in the lake.

6.3.2 Valli del Mincio wetland

The lotus flower also grows in the shallowest parts of the Valli del Mincio wetland. DO was monitored inside a lotus flower patch near Grazie (Figure 6.7) during June 2024 and from July to October 2025. The water depth in this area was 70 cm; therefore, a sensor was deployed 20 cm from the surface and another 20 cm above the bottom, that is, at a depth of 50 cm. Despite the proximity of the two sensors, only 30 cm apart, great differences in dissolved oxygen saturation were recorded (Figure 6.8). This provides evidence of the extremely low mixing that occurs due to the effect of emergent vegetation inside an already slow-moving environment.

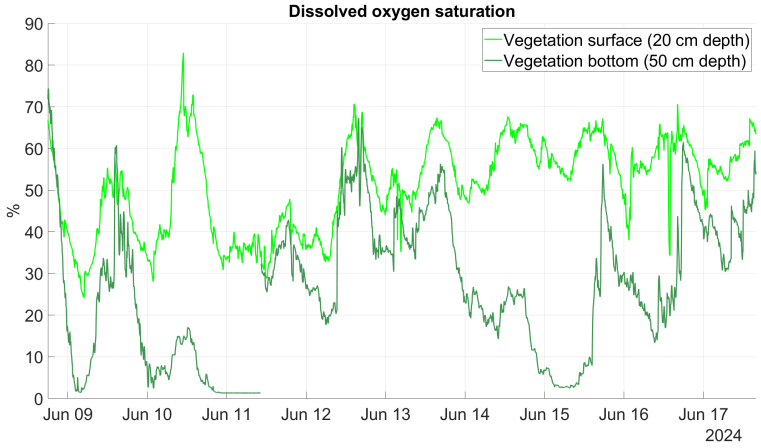

Figure 6.8: Comparison between dissolved oxygen saturation near the surface and near the bottom inside a lotus flower patch in a shallow portion of the Valli del Mincio wetland

In Figure 6.9 a comparison is shown between dissolved oxygen saturation inside and outside a *Ludwigia* mat on the main branch of the Mincio River (Figure 6.10). The buoy in open water mounted an oxygen sensor near the surface at a depth of 45 cm and one near the bottom at 90 cm, while it was not possible to deploy a sensor near the surface inside the *Ludwigia* mat because of the thickness of the vegetation layer, so this buoy mounted only a bottom sensor at a depth of 85 cm. Looking at the differences between the data measured at the bottom inside and outside the vegetation, it is possible to see the effect of *Ludwigia* on dissolved oxygen saturation. Most of the time, under the vegetation coverage, oxygen is lower than in open water at the same depth and often approaches 0% saturation. This result is particularly interesting because the vegetation patch was located on the main branch of the Mincio River, where the water current can potentially be strong enough to mix the water column and prevent oxygen depletion at the bottom. In this case, instead, the effect of vegetation was prevailing.

Continuous oxygen data acquired under different discharge conditions in the Mincio River made it possible to infer the effect of discharge on dissolved oxygen levels in the wetland. This analysis is made more complex by the fact that dissolved oxygen is influenced by many other factors such as solar radiation, wind, temperature, vegetation, algal blooms, which may change during the monitoring period, altering the results.

Nevertheless, a clear reduction in oxygen levels can be observed in conjunction with the closure of the Casale sluice gate, which occurred between 29 and 31 August

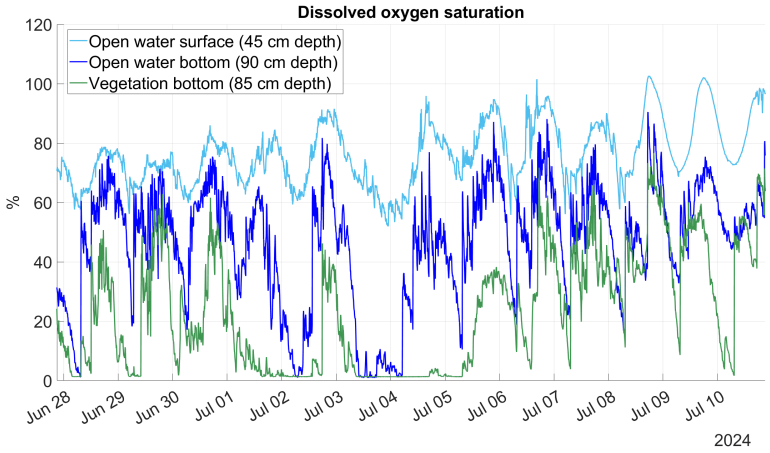

Figure 6.9: Comparison between dissolved oxygen saturation inside and outside a *Ludwigia* mat in the main branch of the Mincio River

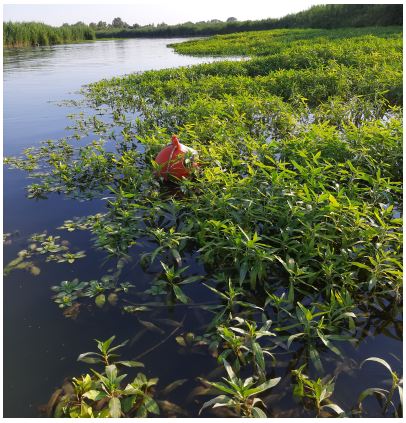

Figure 6.10: Picture of the buoy measuring dissolved oxygen inside the *Ludwigia* mat

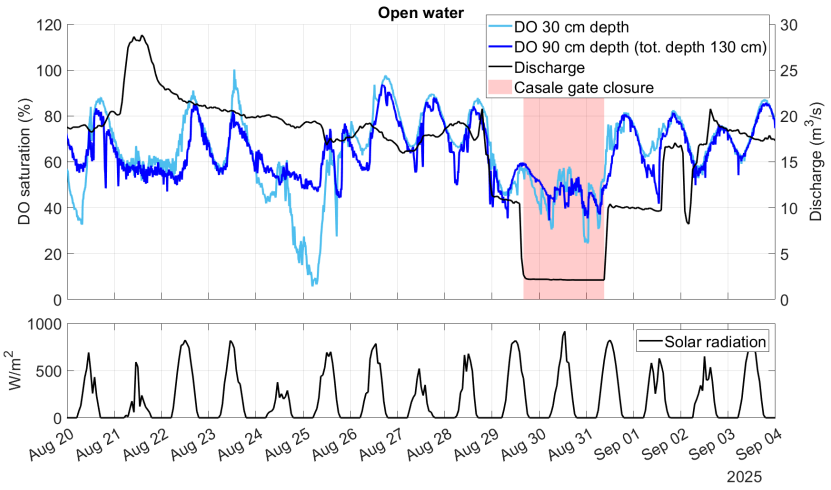

Figure 6.11: Effects of solar radiation and discharge reduction on dissolved oxygen saturation in open water on the main branch of the Mincio River

2025. From the graph in Figure 6.11, which refers to measurements in open water on the main course of the Mincio River, it can be noted that the reduction resulting from gate closure is less pronounced than that observed on 24 August during a day with low solar radiation. This effect is more marked within areas colonised by floating or emergent aquatic vegetation (*Ludwigia* and *Nelumbo*), as shown in Figures 6.12 and 6.13, respectively. The effect of reduced flow velocity on dissolved oxygen dynamics is likely to be particularly exacerbated in these areas, where mixing is already hampered by the presence of vegetation. In both cases, the closure of the sluice gate caused anoxic conditions, with saturation values close to zero, which were resolved as soon as the discharge was restored.

During 2024 long and frequent flow reductions were implemented for hydraulic safety reasons. The Casale gate remained closed for 89 days, compared to 9 days in 2025. The daily minimum values of dissolved oxygen for summer 2024 were correlated with discharge, especially near the bottom ($R^2 = 0.62$, p-value $= 1 \cdot 10^{-9}$), except for some outliers (Figures 6.14 and 6.15).

By comparing the dissolved oxygen data recorded during 2024 and 2025 at sites with similar characteristics, it is clear that 2025 was a less critical year for anoxia-related issues. In fact, in 2024 near-bottom conditions with saturation levels close to zero were measured, persisting for several consecutive days. At the same time, super-saturation values were sometimes observed at the surface due to oxygen production from algal blooms, further indicating a dystrophic condition. Figure 6.16 compares

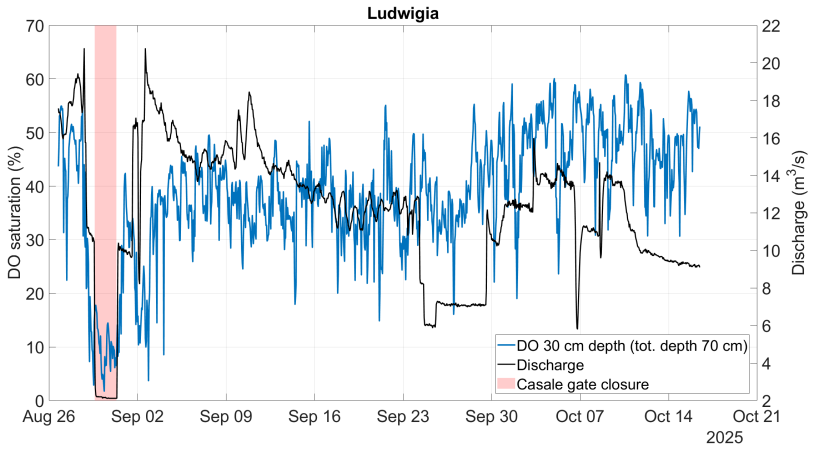

Figure 6.12: Effect of the discharge reduction on dissolved oxygen saturation under a *Ludwigia* mat in the wetland during a closure of the Casale gate

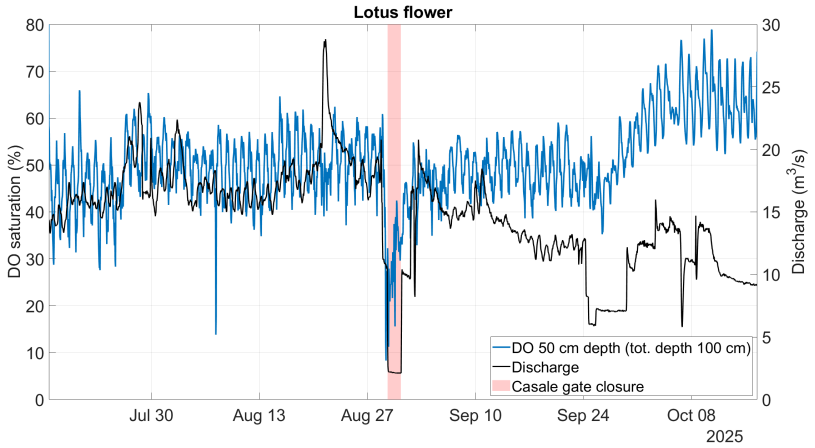

Figure 6.13: Effect of the discharge reduction on dissolved oxygen saturation under a lotus flower meadow in the wetland during a closure of the Casale gate

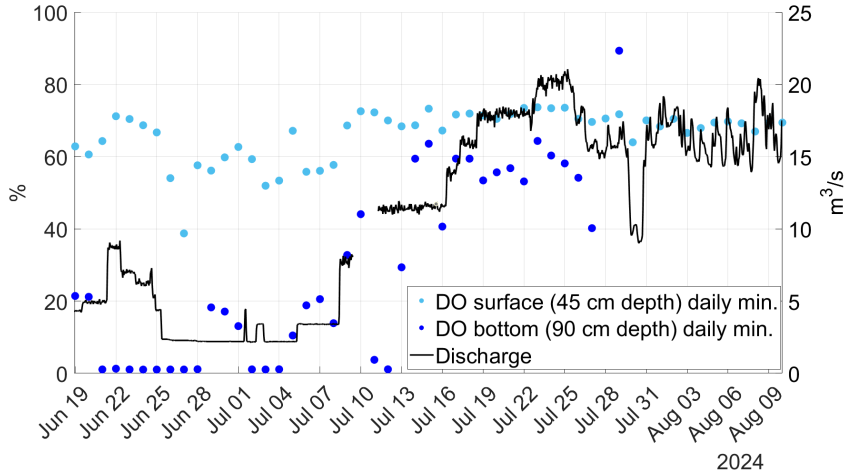

Figure 6.14: Surface and bottom daily minimum DO values in open water during summer 2024, with different through-flowing discharges

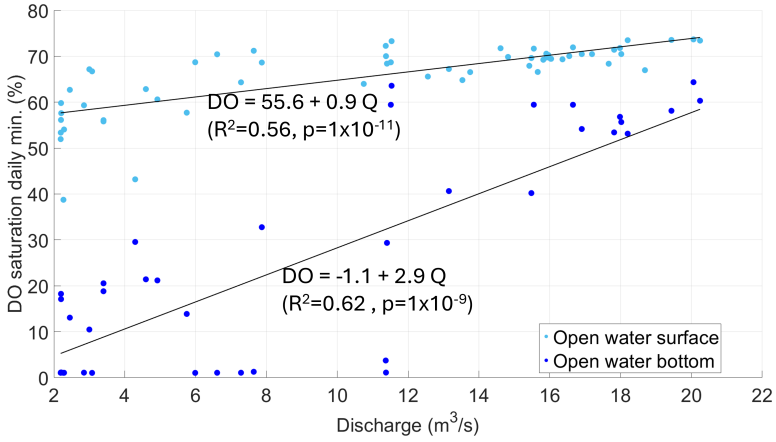

Figure 6.15: Correlation between daily minimum dissolved oxygen and daily mean discharge values during summer 2024

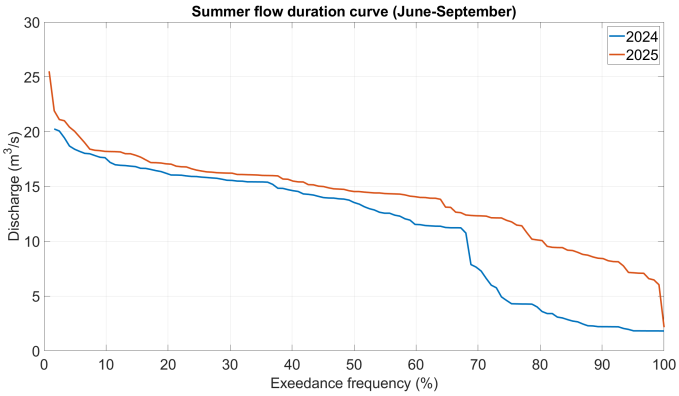

Figure 6.16: Flow duration curves during summer 2024 and 2025

the summer flow duration curves for 2024 and 2025, highlighting the lower discharge observed in 2024 as a result of the continuous regulation of the Mincio River. Figure 6.17 shows the duration curves of the dissolved oxygen values at several monitoring sites in 2024 and 2025. It can be noted that all the 2024 curves lie below those of 2025, with the exception of the graph referring to the surface in open waters, where the 2024 values are higher, probably due to proximity to a supersaturated layer.

Based on these considerations, a deterioration in water quality can be hypothesised due to the repeated flow reductions implemented in 2024. Therefore, it is possible to distinguish between anoxia events caused by brief and sporadic closures of the Casale gate and chronic phenomena resulting from the repetition of these events over a long period. The former are reversible and attributable to hydrodynamic factors that affect the mixing of the water column (and thus a simple oxygen transport from the surface to the bottom), whereas the latter are linked to more complex dynamics occurring over a longer time scale, such as the accumulation of organic matter and nutrients in the sediment, or the development of algal blooms.

6.4 Conclusions

High-frequency dissolved oxygen data were collected in different seasons for a total deployment of 12 months at different depths and in different parts of the Mantua Lake system, which is characterised by distinct vegetational and hydraulic conditions. The greatest variability was found to be related to the depth at which the data were recorded. Hypoxia or anoxia was often measured near the bottom, while in some cases hyperoxia was present close to the surface, sometimes even with extreme values

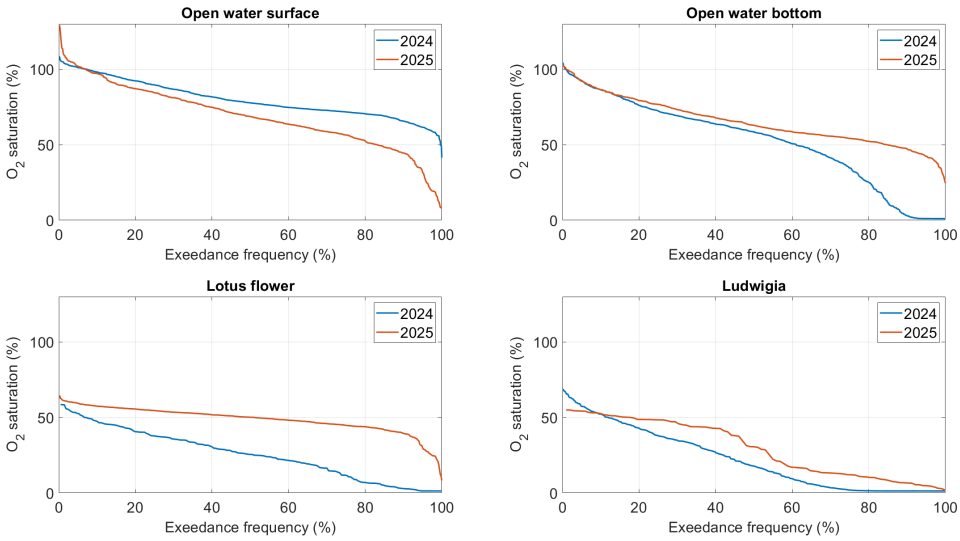

Figure 6.17: Comparison of dissolved oxygen saturation duration curves during summer 2024 and 2025 in different measurement points

due to strong eutrophication and low mixing. Both *Nelumbo nucifera* and *Ludwigia hexapetala* led to a reduction in dissolved oxygen in the underlying water column. However, it is particularly concerning the total anoxia that persisted for several weeks in the bottom waters under vegetation in Lake Superiore.

The influence on dissolved oxygen of the through-flowing discharge in the system was inferred from measurements corresponding to different discharges in the Mincio River. Although it is difficult to distinguish the effect of the flow from that of many other controlling variables, it seems that a strong reduction in discharge can immediately result in lower dissolved oxygen values in the Valli del Mincio wetland, especially in vegetated areas.

If the reduction lasts only a few days, as occurred during the summer of 2025, the effect is transient and is completely resolved once the discharge is restored. This phenomenon is likely a consequence of reduced mixing as a result of a decrease in flow. If, on the other hand, the flow reduction persists over time, more complex mechanisms could be superimposed on this hydrodynamic effect, linked to bio-geochemical processes such as the accumulation of organic matter or the proliferation of phytoplankton due to reduced flushing.

The same analysis cannot be repeated for Lake Superiore due to a lack of flow data. In addition, the complexity of the system does not allow, based on available

data, the definition of a minimum flow threshold in the Mincio River to ensure adequate dissolved oxygen levels. Conducting a multi-factor statistical analysis could help in the assessment of the relative importance of the different variables involved.

7. Effect of lotus flower on the lake's thermal regime

7.1 Introduction

This section aims at the characterisation of Lake Superiore's thermal behaviour with a particular focus on the effects of vegetation throughout the year and the potentially resulting density-driven currents. A process-based interpretation of these dynamics is attempted, while a more detailed investigation, including the fluid mechanics behind this circulation, is beyond the scope of this thesis.

The presence of aquatic vegetation can alter the temperature regime of a lake in different ways. Submerged vegetation generally absorbs more solar radiation than an unvegetated lake bed and also hampers water circulation, leading to higher water temperatures (Dale and Gillespie, 1977). Floating vegetation can create the same effect on the water surface: due to solar radiation, plant surfaces can become much warmer than air temperature, transferring this heat by conduction to the first centimetres of the water column. Dale and Gillespie (1976) measured on the water surface inside a floating Lemnaceae (duckweed) mat a temperature of 4 to 11 °C warmer than adjacent uncovered waters on clear days. For *Nuphar lutea* leaves, which are more similar to lotus flower ones, the temperature difference at the surface was 9 °C. In this case, the gradient decreased to less than 1 °C at 2 cm depth and became negligible at 10 cm depth, due to reduced wind mixing under the canopy.

Vegetation density also has an influence on the thermal regime: Sharip et al. (2012) measured a surface water temperature 1.3 °C warmer under a sparse *N. nucifera* cover (13%) than in adjacent open water in a tropical wetland. On the other hand, dense macrophytes meadows of floating and emergent species create a barrier for solar radiation to penetrate in the water column, resulting in colder water in the shaded area than in the open one. Lövstedt and Bengtsson (2008) measured temperature differences up to 1 °C between a shallow reed belt and adjacent open water

with a similar depth on Lake Krankesjon (Sweden). In this case, the net radiation reaching the water surface in the reeds was on average 15% of the net radiation in open water.

In the absence of strong background currents, temperature differences between adjacent water masses can trigger density-driven circulations, also known as thermal siphons (Monismith et al., 1990). Colder water intrudes under warmer water creating a bottom current, while warmer water replaces it at the surface creating an opposite current. In lentic environments, these currents can have an important effect on water circulation and play a crucial role in transport processes. As already mentioned in chapter 3.2, the water chemistry within the vegetation coverage is often different from that of open water, and the flushing provided by thermal siphons can be the main driver for the exchange of dissolved constituents such as oxygen and nutrients (James and Barko, 1991, James et al., 1994), significantly influencing the large-scale chemistry and ecology of lakes.

Lövstedt and Bengtsson (2008) used a simple lock-exchange equation based on density differences to estimate a velocity scale for the thermal siphon on Lake Krankesjon. The obtained estimate of 1.9 cm/s was verified with field measurement finding the existence of surface currents of up to 1.3 cm/s. They also noticed that these velocities are larger than the swimming velocities available in the literature of most freshwater zooplankton (1 cm/s or less), adding emphasis to the ecological importance of thermal siphons. In fact, aquatic vegetation serves as a refuge for different phytoplankton, zooplankton, and fish communities that may be affected by these currents and the resulting transport processes.

Many studies (Michael and John, 1994; Zhang and Nepf, 2009; Zhang and Nepf, 2011) analysed the flow between an illuminated and a shaded portion of a lake. All the cited works performed a detailed scaling analysis, confirmed by a laboratory experiment, considering a flat bottom configuration with floating or emerging vegetation adjacent to open water. They assumed that the incoming solar radiation was completely blocked by vegetation, resulting in colder water within vegetation during the daytime. In the analysis, they also took into account the drag resulting from the submerged portion of the plants.

However, the temperature gradient can also be an effect of bathymetry (e.g., Sturman et al., 1999; Ulloa et al., 2022): during the day, uniform solar radiation causes the temperature in shallow regions to rise more quickly than in adjacent deeper areas, as the same heat flux is distributed over a smaller volume of water. In contrast, at night, as heat is lost, the shallow region cools more rapidly than the deeper region. Recently, Doda et al. (2022) studied thermal siphons in Lake Rotsee (Switzerland) with a series of field measurements lasting more than a year.

They used a moored ADCP and different thermistor chains between the littoral and pelagic parts of the lake. Doda et al. (2022) analysed the seasonality of density currents, finding that they are more common from late summer to early winter, with a peak frequency in November. Bouffard et al. (2025) offer a comprehensive and updated review on the thermal siphon dynamics over sloping boundaries. Since the littoral part of a lake often hosts aquatic vegetation, different works examined the effect of vegetation drag on slope-induced density currents. For example Oldham and Sturman (2001) modelled it using the Forchheimer equation for porous-media flow and tested the resulting scaling in both a laboratory and a mesocosm experiment.

Although many authors were able to directly measure slope-generated bottom currents, including measurements with old rotor and electromagnetic current meters (e.g., Adams et al., 1984), direct measurements of vegetation-induced thermal siphons are extremely rare. Lövstedt and Bengtsson (2008) used a very rudimentary Particle Image Velocimetry technique to measure the flow moving towards the reed belt: they released floating objects (oranges) and manually recorded their position in a coordinate system made of cords attached to poles a few centimetres above the lake surface.

In Lake Superiore, both the bottom slope and the shadowing effect of vegetation are present. The lake bathymetry is characterised by a shallow area in the centre of the lake, where lotus flower grows, surrounded by a sloping bottom to deeper areas. This aquatic plant can form multiple layers of overlapping leaves, creating a strong blockage of solar radiation. In addition, cutting operations to control the expansion of this invasive species lead to a trimmed vegetation patch with a sharp transition between covered and open water. Thus, the management activity unintentionally created a perfect field laboratory for the study of vegetation-induced thermal siphons. Lake Superiore's configuration is of particular interest because the two effects of vegetation shading and bathymetry may be in competition. In fact, during daytime the shallow lake portion tends to heat up faster, potentially suppressing the cooling effect provided by the vegetation and preventing the onset of a temperature gradient (Lin and Wu, 2014). Moreover, the absence of lotus flower from late winter to the beginning of summer allows investigation of the phenomenon without the effect of vegetation.

In this context, characterising the occurrence of thermal siphons has significant practical implications, given that the dissolved oxygen monitoring campaign discussed in section 6 has revealed serious anoxia issues in the vegetation patch. This problem is particularly intensified by water stagnation during summers, while the mixing promoted by thermal siphons may attenuate it. Thus, the lake management authority can take advantage of this effect by cutting the vegetation patch in a shape

that favours the occurrence of temperature-induced circulation.

7.2 Materials and methods

From November 2023, two temperature logger chains were deployed near the north-west side of the main vegetation patch in Lake Superiore to continuously monitor water temperature. One buoy was 10 m inside and the other 10 m outside the edge of the patch. Each chain was equipped with 5 Onset HOBO Pendant MX2202 sensors, at a spacing of 50 cm in depth, acquiring temperature and light at a sampling rate of 5 minutes. The shallowest sensor was placed at a depth of 20 cm, while the deepest one at a depth of 2.2 m, approximately 50 cm above the lake bed, since the water depth in the observation points was similar (about 2.8 m). The sensors have the following specifications: accuracy of $\pm 0.5\,^{\circ}\mathrm{C}$, resolution of $0.04\,^{\circ}\mathrm{C}$, response time of 7 minutes. A calibration test with the Hart Scientific calibration bath model 7025 was conducted on a subset of 20 out of the 32 sensors deployed. All the tested sensors showed an inter-calibration error within $\pm 0.1\,^{\circ}\mathrm{C}$. The MX2202 sensors could also acquire light intensity (in Lux), but due to the high level of eutrophication of the lake, biofouling started to interfere with measurements just one week after the deployment (Figure 7.1). For this reason, every sensor was manually cleaned approximately every month and only the light measurements of the following 5 days were considered.

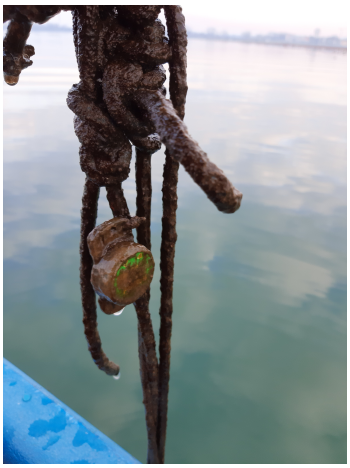

Figure 7.1: HOBO temperature and light sensor after one month from the deployment

Subsequently, during the first year of deployment, other chains were added further inside and outside the vegetation patch, and then other sensors were added on

Buoy n.	Description	Tot. depth [cm]	Progr. distance [m]
1	Center of the vegetation patch	145	0
2	Vegetation patch, 25 m from border	265	110
3	Vegetation patch's border	280	135
4	Open water, 25 m from border	290	160
5	"Undisturbed" open water	310	340

Table 7.1: Temperature logger buoys position details

previously-developed chains to refine the spatial resolution of the data in some specific points of interest. The first year monitoring can be considered as an exploratory survey that was necessary to adjust the sensors configuration, in preparation for the second year during which the deployment remained more stable (Figures 7.2 and 7.3), except for sensors' failures. Sensor malfunctions occurred four times during the monitoring period, with the recording being stopped without any clear reason, and a loss in the data as a consequence until the subsequent maintenance visit. In addition, sometimes it was not possible to communicate with the sensors for data download. Most of the time, this issue was solved simply by removing and reinserting the batteries. The battery duration allowed approximately one year of deployment with data downloads every month. The logger memory was sufficient to record 6 months of temperature and light measurements, or one year of only temperature. Monthly downloads were conducted during the first year to verify the data and plan future deployments.

Figure 7.2: Map of the temperature logger chains positions. (See Figure 7.3 for details.)

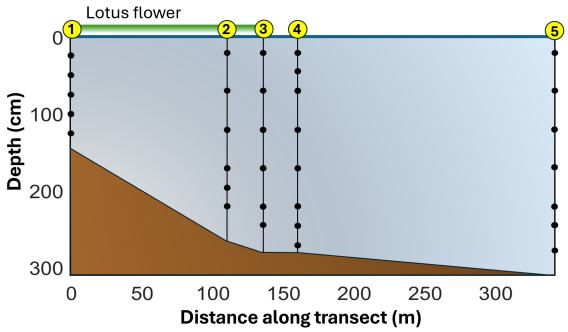

Figure 7.3: Schematic representation of the complete setup of temperature logger chains. (See table 7.1 for description.)

After testing different ADCP instruments and configurations as described in section 4, two velocity measurement campaigns were conducted during November 2024 to achieve a direct measurement of the bottom current that was visible from the temperature data. The most precise instrument setup resulting from the test, Monitor ADCP in Mode 11, was used. The measurements were conducted from the surface with the same method as during the tests, but with a longer acquisition duration of 1 hour. The resulting data were averaged on the whole measurement period, resulting in a single velocity vector for each depth cell. The instrument was placed near the main lotus flower patch in Lake Superiore (position shown in Figure 7.16), at a distance of 30 m from its boundary. As visible in the image, lotus flower was starting to wither, but was still present during the November field campaigns.

7.3 Results and discussion

The maximum temperature recorded during the whole monitoring period is 33.6 °C. This was measured in the surface layer in open water (buoy 4) on 12 August 2024 at 14:00. The lake's temperature increased above 30 °C for 31 days in summer 2024 and 23 days in 2025. Such high temperatures are among the reasons for algal blooms and hypoxia problems as described in chapter 6. The minimum temperature measurement is 3.3 °C, which was recorded in the surface layer in the shallow part of the lake (buoy 1) on 27 December 2024 at 23:00, due to the fact that shallow regions of a lake generally experience faster cooling. This is the only point where temperatures lower than 4 °C were observed, and only for 7 days during winter 2024. For this reason, inverse thermal stratification in Lake Superiore is very rare.

The effect of lotus flower on the temperature difference between open water and

vegetation was analysed considering data from buoy 4 and buoy 2, which were deployed in places with similar depths, in order to minimise the influence of water depth on the results. The temperature difference between these two areas was computed for every sensor layer as $T_{diff} = T_{buoy4} - T_{buoy2}$. The maximum value was measured in the surface layer during a sunny day in summer (10 June 2025 13:00) and reached 1.7 °C (warmer water outside vegetation) due to the shade of lotus flower. On average, during summer, the daily (10:00 - 17:00) mean temperature difference resulted in 0.5 °C. This difference is similar to the value of 0.4 °C found by Lövstedt and Bengtsson (2008) between open water and a reed belt in a shallow Swedish lake, while the maximum difference reported (also in this case in the surface layer) was 1 °C, therefore lower than the one measured in Lake Superiore. This is probably due to the stronger solar radiation peaks in Mantua compared to Sweden. In fact, the temperature difference between open water and vegetation shows a daily trend that is well in accordance with solar radiation (Figure 7.4). During daylight hours, the exposed portion of the lake experiences a more rapid thermal gain due to direct solar radiation, whereas at night the vegetative cover functions as an insulating layer, reducing radiative and convective heat loss and thereby maintaining a comparatively warmer water column.

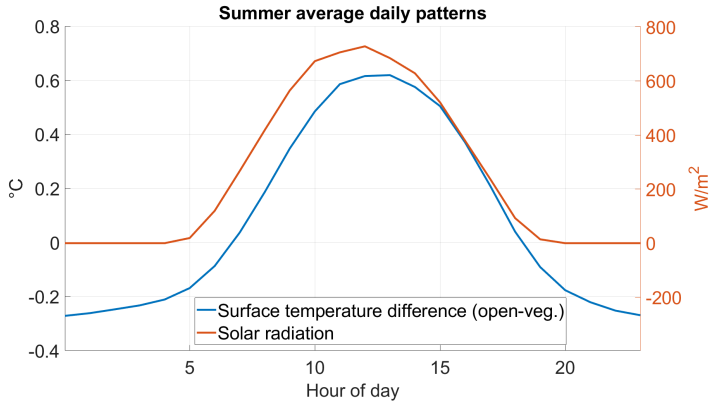

Figure 7.4: Average diurnal cycle of solar radiation and temperature difference (in the surface layer) between open water and vegetation for summer 2025

Figure 7.5 shows an example of the diurnal evolution of the temperature profiles inside and outside the vegetation during summer. During daylight hours, the top layers of the unshaded area become warmer than the covered ones, while during night faster cooling from the surface occurs in open water.

Thanks to light measurements, it was possible to quantify the blockage of solar radiation acted by lotus flower. Figure 7.6 shows an example of light measurements

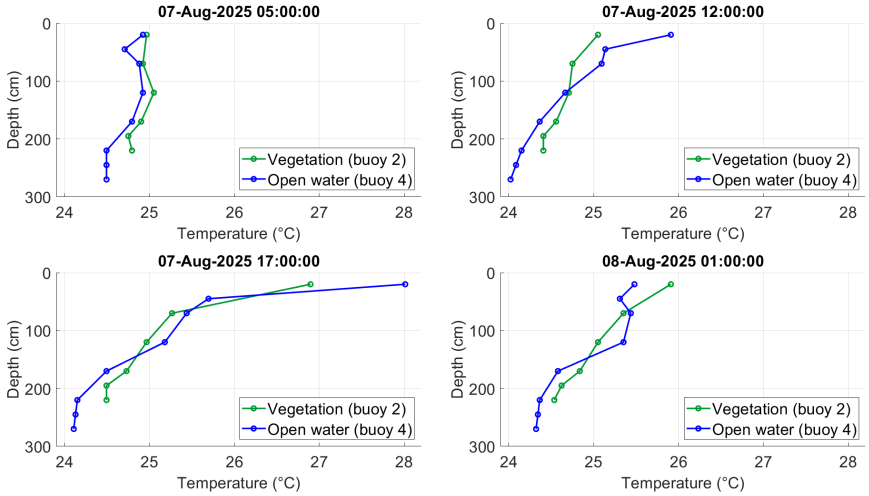

Figure 7.5: Diurnal evolution of the temperature profiles inside and outside vegetation (August 2025)

right after sensor cleanings in autumn and summer. It is important to point out that conventionally light sensors are mounted either upward- or downward-facing, while the HOBO sensors were mounted on a rope, facing horizontally and free to rotate together with the buoy. This explains unexpected values in the time series due to solar reflections or different sensor orientations with respect to the sun. A precise characterisation of light penetration in Lake Superiore was beyond the scope of this study; nevertheless, these data provide an estimate of the effect of lotus flower on the underwater light climate. The daily mean light intensity at the shallowest sensor was computed and compared between open water and vegetation chains. The results were expressed as a percentage of light under the canopy with respect to uncovered water and then averaged over a period of 5 days after the sensors were cleaned. During July, light penetration under lotus flower at its vegetative peak was on average 15% of the one in open water, exactly as Lövstedt and Bengtsson (2008) reported for reeds. On the other hand, at the beginning of November, during the withering season of lotus flower, the amount of light passing through the canopy increased to 20%.

Strong stratification was measured, with differences between surface and bottom temperatures of up to 4.4 °C over a depth of 1 m in the shallow part of the lake during spring (before lotus flower's growing season), or 8.2 °C over a depth of 2 m in open water during summer. Stratification in this context is enhanced by high water turbidity due to algal blooms and washload transport of fine sediments. Occasional

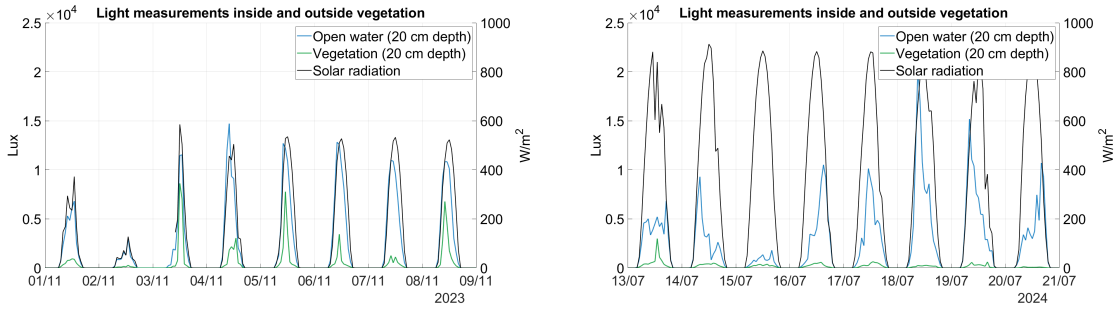

(a) (b)

Figure 7.6: Comparison between light measurement in the surface layer inside and outside vegetation in autumn (a) and in summer (b)

Secchi disc depth measurements were carried out during sensor maintenance campaigns, resulting in a depth of approximately 0.8 m in summer and 1.3 m in winter, in agreement with previous observations from ARPA Lombardia (ARPA Lombardia, 2020).

As a consequence, strong daytime heating for solar radiation is mainly confined in the top of the water column. Due to stratification, the difference between depth-averaged temperatures inside and outside the vegetation was much lower than the difference in the surface layer only, reaching a maximum value of 1.2 °C and a daily (10:00 - 17:00) mean temperature difference of 0.2 °C. Figure 7.7 shows this difference for buoy 4 - buoy 2 and for buoy 4 - buoy 1, where it is possible to notice the influence of depth: during the cooling season, the temperature is lower in the shallow part of the lake, while starting from spring it is the opposite. This behaviour is not related to the presence of lotus flower, since its growing season starts in June.

The classic lock-exchange (or sluice gate) equation (Benjamin, 1968) offers a way to estimate density-driven exchange flow between two adjacent fluid portions:

$$u = \frac{1}{2}(g'H)^{0.5}, \tag{7.1}$$

where u is the flow velocity, $g' = g\frac{\Delta\rho}{\rho}$ is the reduced gravity and H in the case of open regions is equal to the water depth. Equation (7.1) works under the hypothesis of vertically uniform fluid density. Thus, the depth-averaged temperature difference was used for the computation, which has to be considered only as an estimate given the significant stratification that actually exists. The water density was calculated using the UNESCO formula for 28 °C and 28.2 °C. Considering a depth $H = 2.7$ m, equation (7.1) results in a velocity of 1.9 cm/s. This estimate matches the one

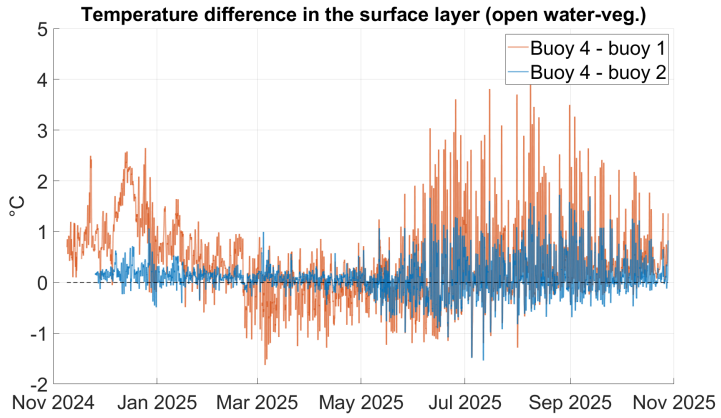

(a)

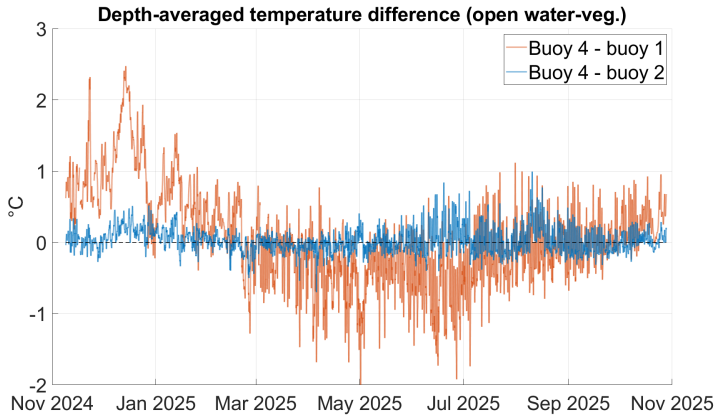

(b)

Figure 7.7: Surface (a) and depth-averaged (b) temperature difference between open water and vegetation during 1 year

obtained by Lövstedt and Bengtsson (2008) for Lake Krankesjon using the same method.

ADCP velocity measurements were conducted close to the vegetation patch border during a sunny day in summer (29 July 2023), but without obtaining clear evidence of thermal siphons. For logistical reasons, it was not possible to plan other ADCP campaigns during the summer. In addition, the temperature data did not show signs of deep water cooling outside the vegetation or surface water warming inside the vegetation, which could prove the onset of thermal siphons. Thus, this phenomenon has not been confirmed.

However, during spring and summer, occasional peaks in bottom temperature signals were observed, especially in open water. Rather than due to thermal siphons, this behaviour can be caused by the onset of a strong stratification with the formation of internal waves, resulting in periodic oscillations of the thermocline. To confirm this hypothesis, the internal wave frequency was calculated using Merian's formula:

$$T = \frac{2L}{c^2}, \tag{7.2}$$

with

$$c = g\frac{\rho_2 - \rho_1}{\rho_2}\frac{h_1 h_2}{h_1 + h_2},$$

where T is the wave period, L is a representative length of the lake along the main wind direction, h_1 and h_2 are the average thicknesses of the epilimnion and hypolimnion, respectively, and ρ_1 and ρ_2 the water densities in these two layers.

The water density was computed using the buoy 4 data during diurnal stratification as a reference (see Figure 7.5), assuming a temperature of 28 °C in the epilimnion and 24 °C in the hypolimnion. The thermocline depth was assumed to be 0.8 m and the total depth 3.5 m (the lake's average depth). L was considered 2 km. The resulting internal wave period was approximately 15 hours. Continuous Wavelet Transform (CWT) was applied on buoy 4 bottom temperature timeseries to look for evidence of seiches. CWT was selected because it provides a joint time–frequency representation, thus overcoming Fourier's limitation in the analysis of a trend with occasional fluctuations in both amplitude and frequency, as observed in this case. Traditional Fourier-based techniques, in fact, assume stationarity, providing only a global frequency spectrum and are therefore not suitable for capturing local or time-varying characteristics. The CWT plot in figure 7.8 shows a well expected peak corresponding to a period of 24 hours, and some less intense peaks corresponding to shorter periods, which may be explained by the presence of internal waves.

Sometimes, these deep-water cooling events were particularly abrupt, with temperature fluctuations of almost 2 °C in 1 hour. All events of this kind exhibited a

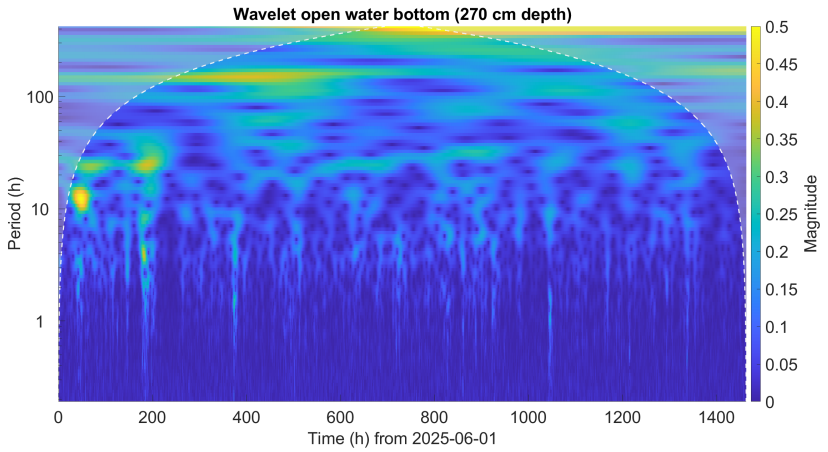

Figure 7.8: Continuous Wavelet Transform plot for open water's deepest sensor from 1 June to 1 August 2025

similar pattern: strong stratification was present before the event, the wind produced mixing, removing the stratification, and after a certain amount of time of up to 30 hours a rapid decline in near-bottom temperature was recorded, approaching the pre-mixing values (Figure 7.9). The cooling of the bottom waters appeared without concurrent cooling of the upper part of the water column, indicating a bottom current (e.g., Oldham and Sturman, 2001). The temperature loggers in the shallow area (buoy 1) did not detect the cold currents. Moreover, most of these events occurred in spring, when lotus flower was still absent. Thus, the source of this cold water can be supposed to be the deepest part of the lake (where no temperature sensors were deployed), which is probably not fully reached by wind-induced destratification.

The time shift between the cold peaks sensed by different temperature logger chains confirmed this hypothesis: most of the times the signals were first observed by the open water buoy, and then sequentially by the others, moving towards the shallow lake portion. However, it should be noted that the delays are small (5 to 15 minutes) and may be affected by the sensors' height above the bottom, which is not equal for every chain.

During autumn and winter, a different dynamic was observed. Between November and January, a slow cooling of the deeper part of the water column was measured frequently, often during daytime, when the upper layers were warming. Compared to spring and summer cooling events, these events were slower and less intense, with temperature fluctuations at the deepest sensor generally lower than 1 °C and lasting from 2 to 8 hours. During this period of the year, lotus flower is progressively

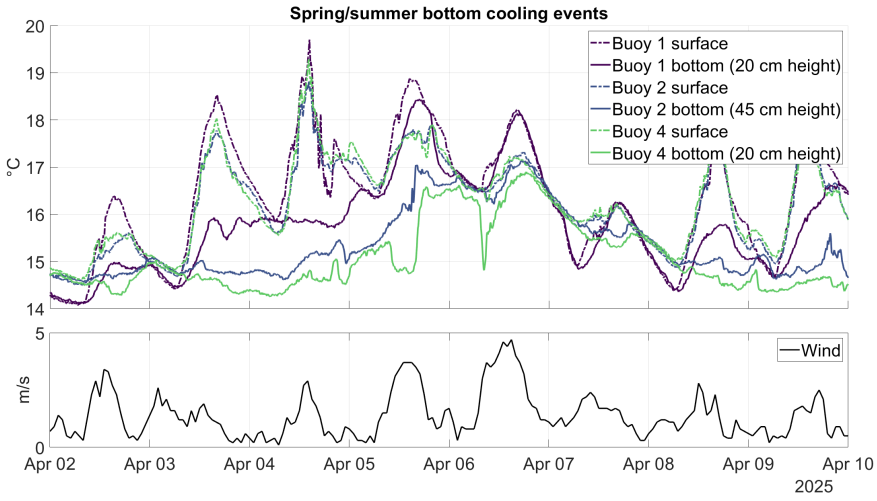

Figure 7.9: Water temperature and wind time series of a rapid bottom cooling event during spring 2025

withering but still present. Under the lotus flower in the shallow part of the lake (buoy 1), the water was significantly colder than outside, with a temperature difference of up to 2.5 °C. It can be assumed that this area is the source of the cold water mass that creates a convective current moving towards the deeper part of the lake. Interestingly, most of the cooling events were detected by the deepest sensor (220 cm depth) in buoy 2, but not by the sensor at the same depth in buoy 3 (Figure 7.10). This is probably due to the sloping lake bed resulting in a greater distance from the bottom of the buoy 3 sensor (60 cm instead of 45 cm). This observation indicates a convective current that flows close to the bottom, following the lake's bathymetry, with a thickness of approximately 50 cm. Figure 7.11 shows an interpolation of temperature data along a lake transect (from buoy 1 to buoy 5) where this dynamic is visible. Figure 7.12 shows the temperature time series of the same event (2 December 2024). Additionally, The overlap of time series in Figure 7.13 shows the time shift of the temperature signal's propagation through different points. This analysis confirmed the direction of the current and allowed for an estimation of the order of magnitude of the velocity (0.5 cm/s).

An algorithm for the automatic detection of bottom currents based on temperature data was developed in Matlab. For this purpose, an event was identified when the discrete derivative of the temperature near the bottom was negative, indicating cooling, whereas it was positive at the surface. This analysis was conducted on the hourly-averaged temperatures to avoid excessive noise in the data due to small fluc-

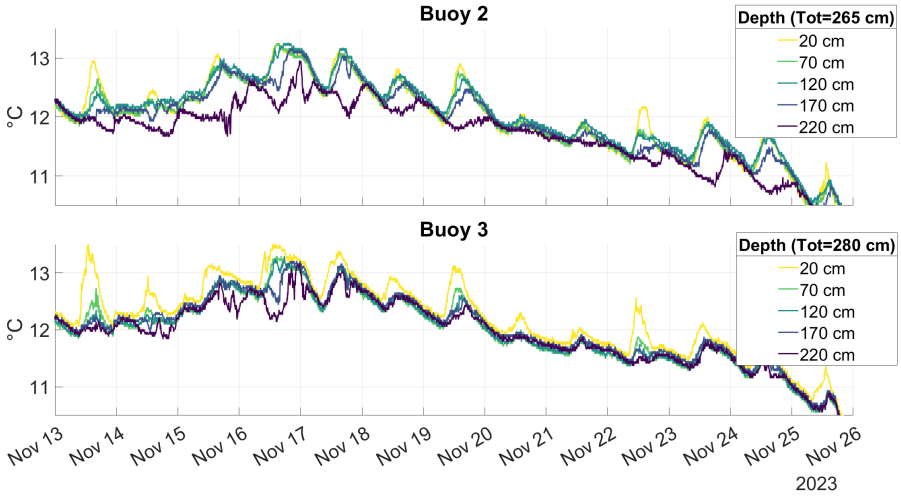

Figure 7.10: Temperature time series at different depths showing multiple evidence of bottom convective currents in November 2023

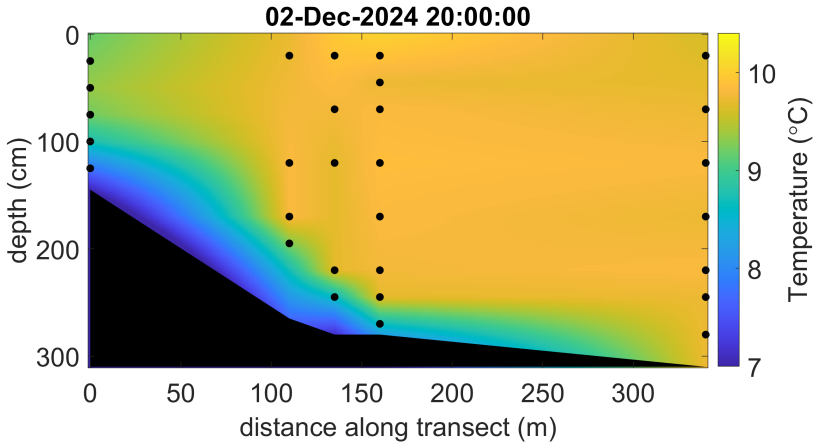

Figure 7.11: Interpolation along a lake transect of the temperature data measured during the cooling event of 2 December 2024

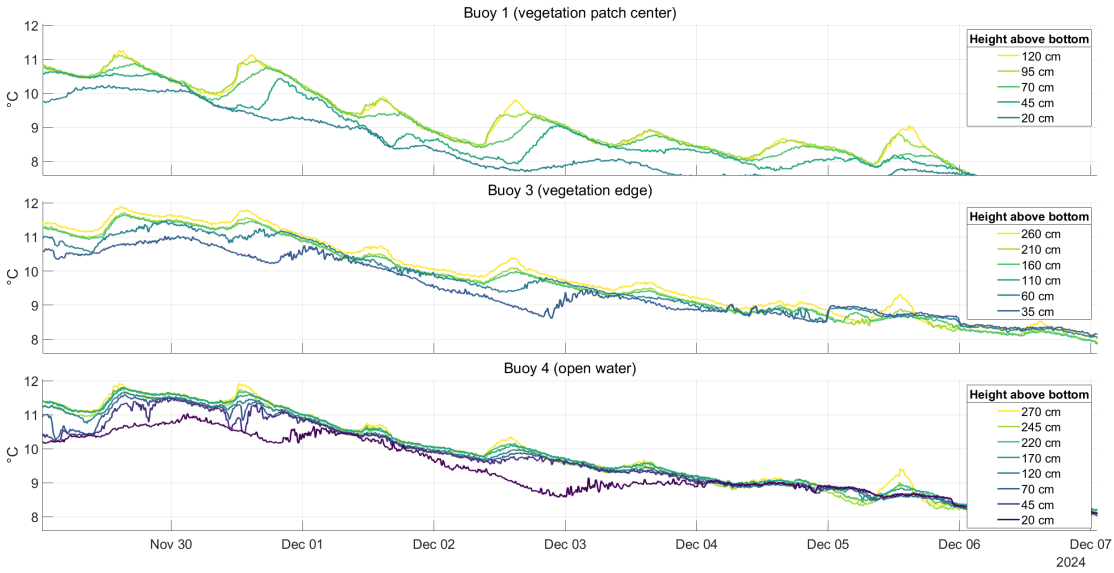

Figure 7.12: Temperature time series measured at different depths and positions showing evidence of a bottom convective current (2 December 2024)

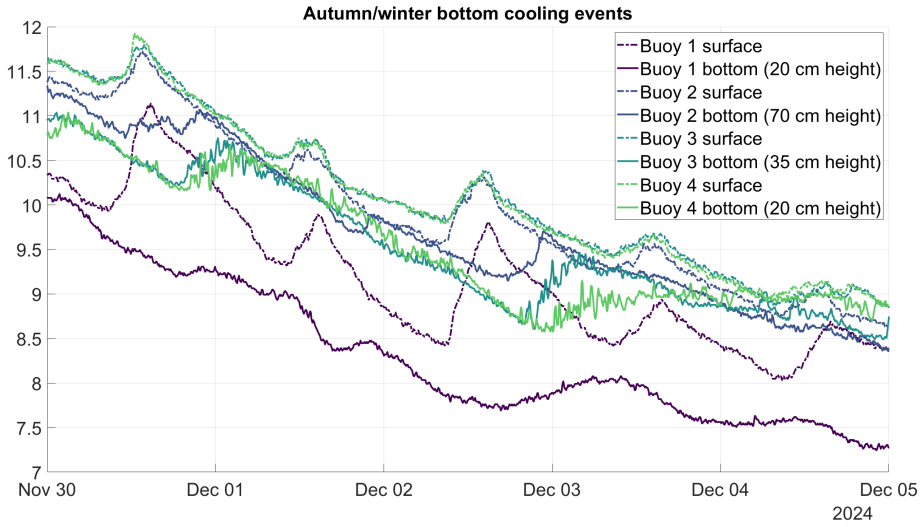

Figure 7.13: Overlap of temperature time series measured from bottom and surface sensors in different positions

tuations. A minimum duration of the event was set to 3 hours and a threshold on the intensity of the cooling (defined as the temperature difference between the beginning of the event and its peak) was arbitrarily set to 0.3 °C. The data from buoy number 2 were used for this analysis. With this method, 13 events were detected between November 2023 and January 2024 and 11 between November 2024 and January 2025. Interestingly, the application of this algorithm does not work with the same thresholds from April to September, when it gives false results with almost daily frequency due to the fast temperature fluctuations occurring in spring and summer.

Figure 7.14 shows a portion of the identified events plotted in the air temperature time series after removing the seasonal trend. Differential cooling events were observed mainly during periods of net daily heat loss in the water column. As also reported by James et al. (1994), pronounced differential cooling at night followed by strong daytime differential heating was never observed. Overall, these findings indicate that convective exchange patterns may be partially controlled by broader weather-driven warming and cooling trends. Additionally, the wind plot in Figure 7.14 suggests that the wind does not influence the occurrence of differential cooling events in Lake Superiore, as these events were observed under both strong and calm wind conditions.

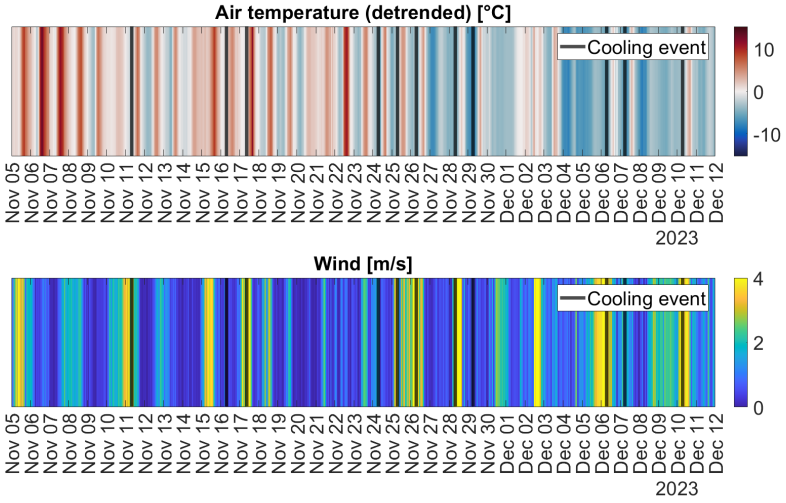

Figure 7.14: Air temperature and wind time series with indication of bottom water cooling events

Another factor that has to be considered is the presence of lotus flower; its shading effect can last even long after the end of the growing season, with some stems still in place until January or later. This effect can contribute to the creation of a cold

water reservoir in the shallow portion in the centre of the lake, which tends to disappear after the complete senescence of lotus flower around mid-January (Figure 7.15). Looking at the cooling events distribution reported in the figure, the presence of lotus flower seems to have an influence on the development of bottom currents because of its shading effect.

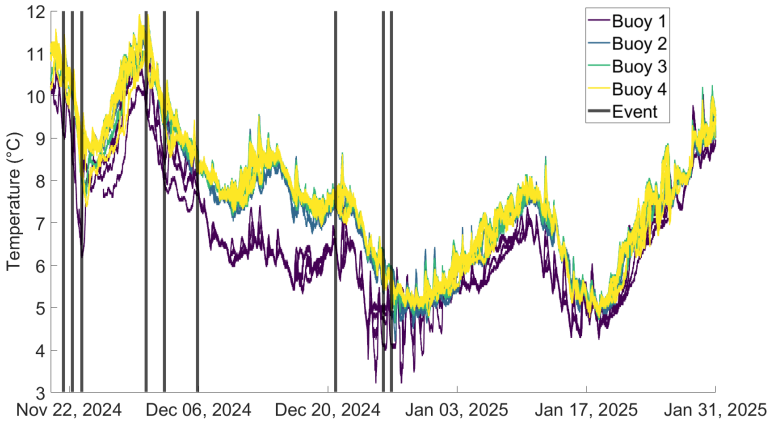

Figure 7.15: Evidence of colder water in the shallow portion of the lake during lotus flower presence

The ADCP measurements acquired on 8 November 2024 show evidence of a bottom current moving away from the lotus flower patch, in a direction perpendicular to its edge (Figure 7.16). The bottom current, directed towards the north-west, has a magnitude of the order of 1 cm/s, while the rest of the water column moves eastward with a greater speed of up to 2 cm/s, probably due to the through-flowing discharge in the lake (Figure 7.17). Evidence of a bottom cooling during ADCP acquisition is also present in the temperature time series (Figure 7.18). The temperature data show a general cooling trend in the week before the ADCP campaign. Deep-water cooling events during daylight hours occurred often during that period, with intensities comparable to the one for which a direct measurement of the bottom current is available. This suggests that the measured current is not a rare event; on the contrary, it may occur with an almost daily frequency during specific periods.

The ADCP measurement allowed for a better estimation of the current's thickness. The water depth in the measurement point was 2.95 m and the current was detected up to the bin centred at 2.44 m, resulting in a height above the bed of 50 cm, consistent with the estimation derived from the temperature data. Note that the blanking distance above the bottom for side-lobe interference, approximately 10% of the water depth (i.e., 30 cm in this case), has been filtered out from the data shown,

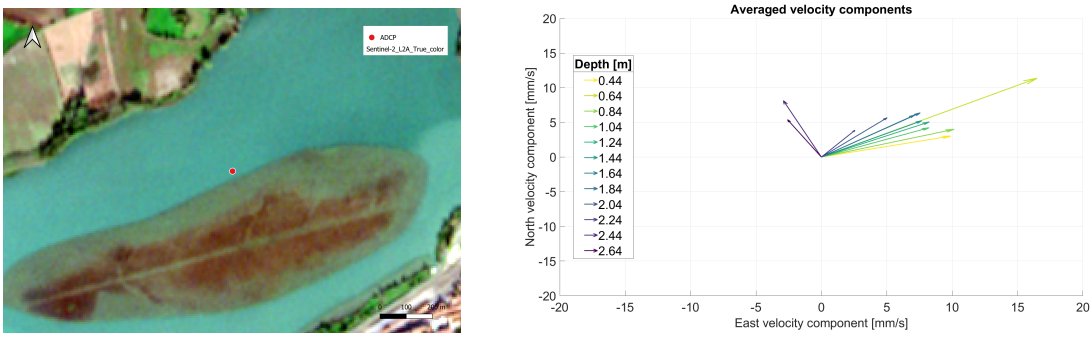

(a) (b)

Figure 7.16: (a) Position of the November 2024 ADCP measurements relative to the lotus flower patch (Sentinel-2 image) and (b) Vector plot of the ADCP measurement results (8 November 2024)

so as not to alter the results.

The ADCP measurements acquired on 29 November exhibit a similar pattern, but with a slightly weaker bottom current of 0.7 cm/s and a stronger background current of about 4 cm/s (Figures 7.19 and 7.20).

7.4 Conclusions

A 2-year dataset of continuous temperature measurements has been collected at different depths and locations on Lake Superiore (Mantua), together with light under water measurements. This allowed for the quantification of the effect of lotus flower on water temperature and light climate, resulting in colder water during daytime, with a daily (10:00 - 17:00) mean temperature difference during summer of 0.5 °C between the surface layers or 0.2 °C averaged over the water column. These values are compatible with those reported in previous studies available in the literature on the development of thermal siphons under similar differential-heating conditions. This dynamic is created by cold water under vegetation that intrudes the bottom in open water and is replaced with warmer water near the surface.

The order of magnitude of these currents was computed with a simple lock-exchange equation based on temperature data, resulting in 1.9 cm/s. Nevertheless, it was not possible to confirm this hypothesis despite a dedicated ADCP field campaign. Strong stratification was established in the lake starting from March, before the beginning of the growing season of lotus flower. These vertical temperature gradients are likely to be among the reasons for the rapid temperature fluctuations measured in the deep layers during spring and summer, probably due to internal waves.

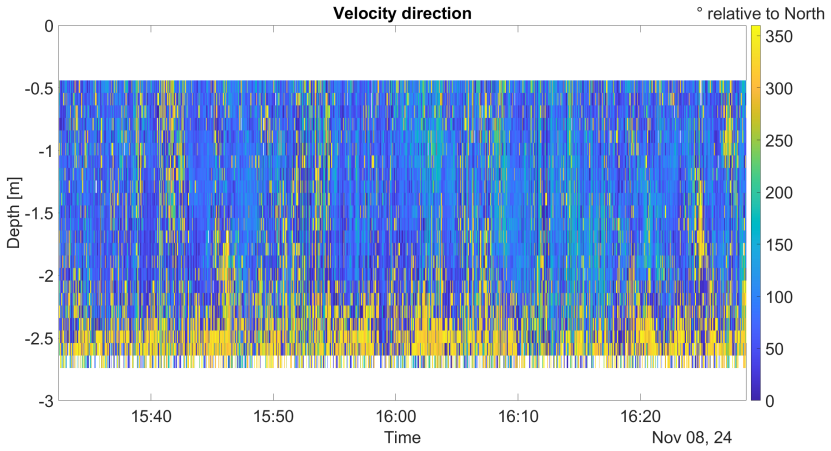

Figure 7.17: Velocity direction on the water column for the ADCP measurement of 8 November 2024

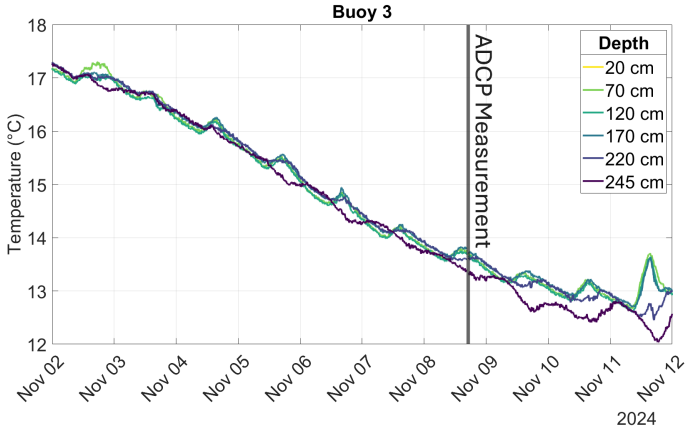

Figure 7.18: Detail of the temperature measurements from buoy 3 during 10 days including the 8 November ADCP campaign (shown in black)

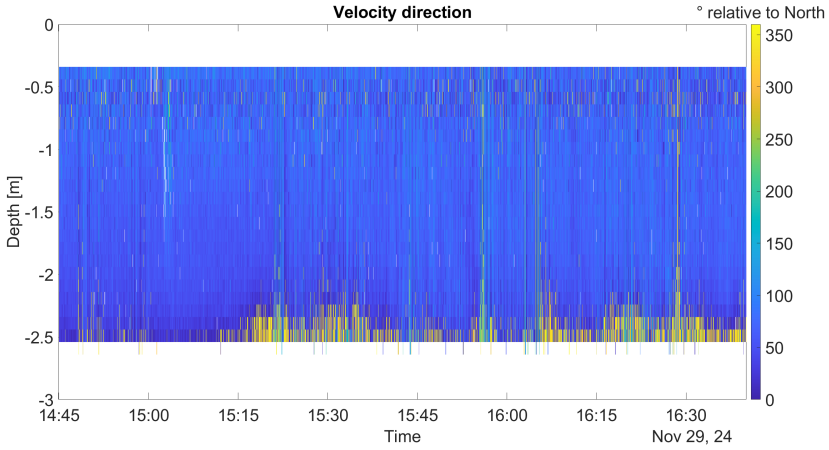

Figure 7.19: Velocity direction on the water column for the ADCP measurement of 29 November 2024

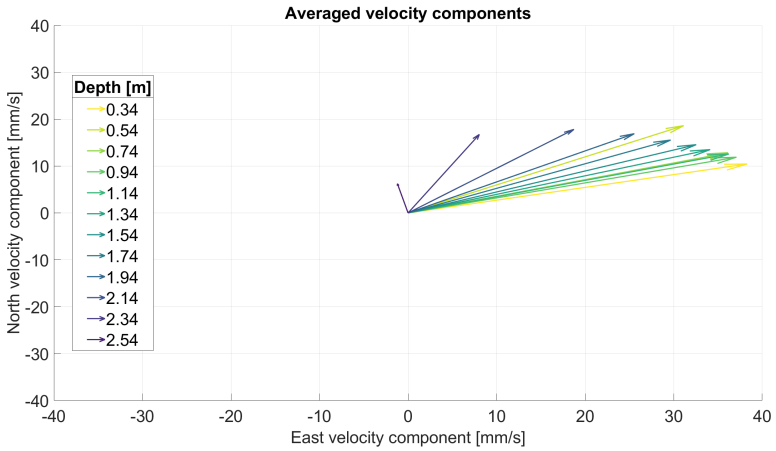

Figure 7.20: Vector plot of 29 November 2024 ADCP measurement near the lotus flower patch

During autumn and winter, the onset of a bottom current directed away from the lotus flower patch was inferred from the temperature time series and confirmed with two distinct ADCP measurement campaigns. This current had a thickness of 0.5 m, a speed of the order of 1 cm/s, and occurred approximately 11-13 times per year between November and January. This phenomenon was apparently related to periods of general cooling of the lake and was enhanced by the presence of lotus flower, further creating a cold water storage in the shallow part of the lake. For this reason, it can be considered as a differential-cooling convective exchange dynamic. Nevertheless, it was not possible to define a precise set of conditions in the weather forcing that provide an explanation for the occurrence of the cold currents only in some specific days. Functional Principal Component Analysis (FPCA) is suggested as a future development to answer this question. FPCA works similarly to traditional Principal Component Analysis, but instead of analysing isolated data points, it considers entire functions, such as curves or time series, and identifies the main patterns of variation across them. In addition, another summer ADCP field campaign could confirm the onset of thermal siphon circulation resulting from vegetation-induced differential heating and provide a more precise quantification of its intensity.

In summary, three different water circulation processes were detected:

- thermal siphons induced by differential heating during summer, resulting from vegetation shading (estimated by means of equations and comparison with analogous cases);
- wind-induced internal waves with thermocline oscillations during the stratification period (visible from temperature data);
- thermal siphons induced by differential cooling during autumn and winter, resulting from a bathymetric effect with a possible influence of vegetation (visible from temperature data and confirmed with ADCP measurements).

All observed temperature-induced water circulations are of great ecological importance because they result in a water exchange between lake portions with different water qualities: the area colonised by lotus flower and the surrounding open waters. These currents can transport hypoxic water away from vegetation, mitigating the anoxic condition especially during summer (Brothers et al., 2017), and supply vegetation with nutrient-rich water, improving its growth (Michael and John, 1994). Additionally, since the swimming speed of zooplankton is typically lower than 1 cm/s, these organisms, which often use aquatic plants as a refuge, are also probably transported from the currents.

8. General conclusions

This work aimed to investigate various physical processes that characterise the Mincio fluvial system near the city of Mantua, through the acquisition and analysis of an extensive dataset of field measurements.

A detailed bathymetric survey of Lake Superiore and Valli del Mincio wetland and a comparison with historical data allowed the estimation of a rapid sedimentation trend of up to 0.1 m/year occurring in the area, threatening its aquatic habitats, its accessibility by water, and its water storage capacity. The main cause of this problem was identified through a comprehensive monitoring programme and was found to be the high load of fine sediments that is transported by the Mincio River tributaries. This sediment, originating from agricultural sources, deposits within the system as a result of the progressive lowering of the current's velocity, and thus the transport capacity of the river, moving downstream. In addition, the presence of invasive vegetation affects sedimentation rates and adds substantial amounts of biomass deposited in the form of plant detritus after each vegetative season.

The monitoring of dissolved oxygen showed a dystrophic situation that was further worsened by the low mixing resulting from the presence of dense vegetation patches and from discharge reductions. As a consequence and also due to interactions with biological processes, frequent anoxic conditions were measured in the deepest part of the water column, while hyperoxia, sometimes with extreme saturation levels, was observed near the surface.

A focus on the effects of lotus flower on the lake's thermal regime completed the characterisation of the main transport processes in the system; two years of continuous temperature data acquisition showed evidence of density-driven currents created by temperature gradients resulting from both the shading effect of the canopy and the sloping bottom of the lake. ADCP velocity profiles, acquired after a testing phase on different instruments, confirmed the occurrence of bottom currents of the order of centimetres per second.

The study shows the importance of dealing with a scientific problem from different points of view, integrating various components to understand the whole system.

Peters (1990) observed that limnology has become fragmented into very specialised fields that lack dialogue. Ecosystems like those analysed in this work, due to feedback effects and interactions, are complex systems, the properties of which may be different from a simple sum of their components. Therefore, their properties cannot be completely understood by considering only single constituent parts (Harris, 1999).

The Mantua lake and wetland system is an example of the complexity of lentic environments, where multiple variables are intertwined, and where apparently negligible forcings can be important controllers:

- sediment deposition from high sediment load tributaries increases the spread of invasive macrophytes, which further aggravates the deposition trend;
- invasive vegetation in Lake Superiore is shaping the bathymetry, creating the conditions for the onset of density-driven currents;
- high temperatures and low discharges during summer, together with high nutrient loads, favour algal blooms;
- algae and macrophytes completely alter oxygen dynamics, resulting in both anoxia and hyperoxia problems.

All these issues must be addressed in a "holistic" way to reach an effective solution. For example, it is not possible to solve the anoxia problem acting only on discharge, without reducing the nutrient load and also containing invasive macrophytes.

Focusing on the specific case study of Mantua lakes and wetland, this thesis allowed the acquisition of a substantial body of environmental data within a context that previously had remained largely unexplored from an environmental engineering perspective. This information can now be employed by management agencies to guide and support their governance strategies and remediation plans.

Specifically, to slow the ongoing terrestrialization process, it is of paramount importance to reduce sediment input from the tributaries that drain agricultural areas, as was clear from the investigation in Section 5.3. This can be achieved through different technical solutions, such as buffer strips with riparian vegetation around agricultural fields to reduce runoff, sediment retention basins on the main Mincio River tributaries, or diversion of these channels towards a less critical portion of the riverine system (e.g., downstream of the lakes). In addition, increasing the discharge released into the Mincio River after heavy rainfall can increase its transport capacity, avoiding sediment deposition within the wetland. These types of lake flushing events can also have a positive impact on eutrophication thanks to dilution of nutrient

loads. Another advantage of increasing discharge in the Mincio River is the partial mitigation of anoxia problems, as shown in Section 6, due to better mixing of the water column. To improve anoxic conditions, the control of invasive vegetation is also of primary importance. For this purpose, frequent cutting operations or plant roots removal by dredging are fundamental.

As already mentioned, applying these solutions requires an integrated approach. In a system of this kind, addressing issues in a holistic manner is not merely a conceptual ideal, but an imperative operational necessity. This represents the most challenging aspect to implement, as it requires coordinated action among multiple governing bodies such as the hydraulic management agency (AIPo), the Mincio Park authority, Mantua Province and Municipality, Lombardy Region, and different agricultural consortia.

The topic of conservation of the natural value of the Mincio River has gained considerable public attention in recent years, especially for what concerns the Valli del Mincio wetland, as evidenced by the frequency of articles appearing in local newspapers. Unfortunately, the institutional debate on this topic has so far remained mainly confined to a political or economic level. This work provides a scientific basis to inform the discussion among policy makers in order to find an effective and shared solution.

For this reason, future developments of this work will focus on the publication of the available data on a website platform, where they can be openly accessed, with different levels of detail, from both the general public and experts in the field.

This will also provide a reference dataset for comparing similar case studies worldwide. For example, just to cite a few, Acton Lake, a hypereutrophic reservoir in Ohio (USA), has shown very similar problems, including sediment and nutrient inputs from agricultural land in the catchment, anoxia, reduced mixing, and algal blooms (Knoll et al., 2025). Another comparable context is the Mediterranean shallow Lake Stymfalia (Greece), as described by Papastergiadou et al. (2007), as well as Baiyangdian Lake in China (Zhang et al., 2012), and the shallow Pátka Reservoir in Hungary (Tombor et al., 2026). With regard to lotus flower, Lee et al. (2021) reported an analogous condition of *Nelumbo nucifera* invasiveness after its introduction in the Junam wetland (South Korea).

Appendix: ADCP configuration files

The following Appendix reports the Monitor ADCP configuration files used in VmDas software to deploy the instrument for the tests described in Section 4. StreamPro ADCP was managed with WinRiver II software, which offers a guided setup wizard and does not require a configuration file.

High resolution (Mode 11) configuration used in Lake Garda (Monitor ADCP)

```
;-----------------------------------------------------------
; ADCP Command File for use with VmDas software.
; ADCP type: 600 Khz Workhorse
; Setup name: default
; NOTE: Any line beginning with a semicolon in the first
; column is treated as a comment and is ignored by
; the VmDas software.
;-----------------------------------------------------------
; Restore factory default settings in the ADCP
cr1
; Set mode 11
WM11
WZ5
; Turning off the recorder
CF11110
; Make Workhorse not to sleep
CL0
```

```
; Set the data collection baud rate to 9600 bps (default),
; no parity, one stop bit, 8 data bits
; NOTE: VmDas sends baud rate change command after all other commands in
; this file, so that it is not made permanent by a CK command
cb411
; Set for broad bandwidth (better accuracy) profile mode (WB),
; single-ping ensembles (WP),
; 250 (WN) 50 cm bins (WS), 0.25 meter blanking distance (WF)
WB0
WP00001
WN250
WS050
WF0025
; Enable single-ping bottom track (BP),
; Set maximum bottom search depth to 150 meters (BX)
BP001
BX1500
; output velocity, correlation, echo intensity, percent good
WD111100000
; Three tenths of a second between bottom and water pings
TP000030
; Six tenths of a second between ensembles
; Since VmDas uses manual pinging, TE is ignored by the ADCP.
; You must set the time between ensemble in the VmDas Communication options
TE00000060
; Set to calculate speed-of-sound, use internal depth sensor (if available)
; use internal compass heading sensor, internal pitch or roll being used, no salinity
sensor,
; internal transducer temperature sensor
EZ1111101
; Output beam data (rotations are done in software)
EX00000
; Set magnetic compass offset or compass bias offset (hundredths of degrees)
EB00400
; Set transducer depth (decimeters)
ED00002
; Set Salinity (ppt)
ES0
```

; save this setup to non-volatile memory in the ADCP
CK

General purpose (Mode 1) configuration used in Lake Garda (Monitor ADCP)

;———————————————————————————————
; ADCP Command File for use with VmDas software.
; ADCP type: 600 Khz Workhorse
; Setup name: default
; NOTE: Any line beginning with a semicolon in the first
; column is treated as a comment and is ignored by
; the VmDas software.
;———————————————————————————————-
; Restore factory default settings in the ADCP
cr1
; Set mode 1
WM1
; Turning off the recorder
CF11110
; Make Workhorse not to sleep
CL0
; Set the data collection baud rate to 9600 bps (default),
; no parity, one stop bit, 8 data bits
; NOTE: VmDas sends baud rate change command after all other commands in
; this file, so that it is not made permanent by a CK command
cb411
; Set for broad bandwidth (better accuracy) profile mode (WB),
; single-ping ensembles (WP), 250 (WN) 50 cm bins (WS),
; 0.25 meter blanking distance (WF), 100 cm/s ambiguity velocity (WV)
WB0
WP00001
WN250
WS050
WF0025
WV100

; Enable single-ping bottom track (BP),
; Set maximum bottom search depth to 150 meters (BX)
BP001
BX1500
; output velocity, correlation, echo intensity, percent good
WD111100000
; Three tenths of a second between bottom and water pings
TP000030
; Six tenths of a second between ensembles
; Since VmDas uses manual pinging, TE is ignored by the ADCP.
; You must set the time between ensemble in the VmDas Communication options
TE00000060
; Set to calculate speed-of-sound, use internal depth sensor (if available)
; use internal compass heading sensor, internal pitch or roll being used, no salinity sensor,
; internal transducer temperature sensor
EZ1111101
; Output beam data (rotations are done in software)
EX00000
; Set magnetic compass offset or compass bias offset (hundredths of degrees)
EB00400
; Set transducer depth (decimeters)
ED00002
; Set Salinity (ppt)
ES0
; save this setup to non-volatile memory in the ADCP
CK

High resolution (Mode 11) configuration used in Lake Superiore (Monitor ADCP)

;———————————————————————————————
; ADCP Command File for use with VmDas software.
; ADCP type: 600 Khz Workhorse
; Setup name: default
; NOTE: Any line beginning with a semicolon in the first

```
; column is treated as a comment and is ignored by
; the VmDas software.
;-------------------------------------------------------------------
; Restore factory default settings in the ADCP
cr1
; Set mode 11
WM11
WZ5
; Turning off the recorder
CF11110
; Make Workhorse not to sleep
CL0
; Set the data collection baud rate to 9600 bps (default),
; no parity, one stop bit, 8 data bits
; NOTE: VmDas sends baud rate change command after all other commands in
; this file, so that it is not made permanent by a CK command
cb411
; Set for broad bandwidth (better accuracy) profile mode (WB),
; single-ping ensembles (WP),
; 60 (WN) 10 cm bins (WS), 0.25 meter blanking distance (WF)
WB0
WP00001
WN060
WS010
WF0025
; Enable single-ping bottom track (BP),
; Set maximum bottom search depth to 6.5 meters (BX)
BP001
BX65
; output velocity, correlation, echo intensity, percent good
WD111100000
; Three tenths of a second between bottom and water pings
TP000030
; Six tenths of a second between ensembles
; Since VmDas uses manual pinging, TE is ignored by the ADCP.
; You must set the time between ensemble in the VmDas Communication options
TE00000060
; Set to calculate speed-of-sound, use internal depth sensor (if available)
```

; use internal compass heading sensor, internal pitch or roll being used, no salinity sensor,
; internal transducer temperature sensor
EZ1111101
; Output beam data (rotations are done in software)
EX00000
; Set magnetic compass offset or compass bias offset (hundredths of degrees)
EB00400
; Set transducer depth (decimeters)
ED00002
; Set Salinity (ppt)
ES0
; save this setup to non-volatile memory in the ADCP
CK

Bibliography

Abd Rasid, N., Naim, M., Che Man, H., Abu Bakar, N., & Mokhtar, M. (2019). Evaluation of surface water treated with lotus plant; Nelumbo nucifera. *Journal of Environmental Chemical Engineering*, *7*(3), 103048. https://doi.org/10.1016/j.jece.2019.103048

Accordini, N. (2022). *Indagini di campo e modellazione numerica di un tratto di fiume Mincio in condizioni di stress idrico: Interazione fiume-falda*.

Adami, L., Bruno, M. C., Cerasino, L., De Vincenzi, M., & Tubino, M. (2024). *Attività di monitoraggio quali-quantitativo a supporto della definizione del deflusso ecologico nel fiume Mincio* (tech. rep.). Università di Trento.

Adami, L., Bruno, M. C., Cerasino, L., De Vincenzi, M., & Tubino, M. (2025). *Attività di monitoraggio quali-quantitativo a supporto della definizione del deflusso ecologico nel fiume Mincio* (tech. rep.). Università di Trento.

Adams, E. E., Asce, M., & Wells, S. A. (1984). Field Measurements on Side Arms of Lake Anna, Va. *Journal of Hydraulic Engineering*.

Al-Asadi, K., & Duan, J. G. (2017). Assessing methods for estimating roughness coefficient in a vegetated marsh area using Delft3D. *Journal of Hydroinformatics*, *19*(5), 766–783. https://doi.org/10.2166/HYDRO.2017.064

Alfasane, A., Khondker, M., & Tahmida Begum, Z. N. (2009). Effects of some limnological factors on the growth of *Nelumbo nucifera* Gaertner. *Bangladesh J. Bot.*, *38*(2), 133–138.

Ali, B., Anushka, & Mishra, A. (2022). Effects of dissolved oxygen concentration on freshwater fish: A review. *International Journal of Fisheries and Aquatic Studies*, *10*(4), 113–127. https://doi.org/10.22271/fish.2022.v10.i4b.2693

Alvarez, L. V., Moreno, H. A., Segales, A. R., Pham, T. G., Pillar-Little, E. A., & Chilson, P. B. (2018). Merging unmanned aerial systems (uas) imagery and echo soundings with an adaptive sampling technique for bathymetric surveys. *Remote Sensing*, *10*. https://doi.org/10.3390/rs10091362

ARPA Lombardia. (2020). *Stato delle acque superficiali in Lombardia. Laghi di Mantova. Aggiornamento 2014-2019.* (tech. rep.). Settore Monitoraggi Ambientali.

Bai, J., Guan, Y., Liu, P., Zhang, L., Cui, B., Li, X., & Liu, X. (2020). Assessing the safe operating space of aquatic macrophyte biomass to control the terrestrialization of a grass-type shallow lake in China. *Journal of Environmental Management*, *266*, 110479. https://doi.org/10.1016/J.JENVMAN.2020.110479

Bandini, F., Kooij, L., Mortensen, B. K., Caspersen, M. B., Thomsen, L. G., Olesen, D., & Bauer-Gottwein, P. (2023). Mapping inland water bathymetry with ground penetrating radar (gpr) on board unmanned aerial systems (uass). *Journal of Hydrology*, *616*. https://doi.org/10.1016/j.jhydrol.2022.128789

Bandini, F., Olesen, D., Jakobsen, J., Kittel, C. M. M., Wang, S., Garcia, M., & Bauer-Gottwein, P. (2018). Technical note: Bathymetry observations of inland water bodies using a tethered single-beam sonar controlled by an unmanned aerial vehicle. *Hydrology and Earth System Sciences*, *22*, 4165–4181. https://doi.org/10.5194/hess-22-4165-2018

Benjamin, T. B. (1968). Gravity currents and related phenomena. *Journal of Fluid Mechanics*, *31*(2), 209–248. https://doi.org/10.1017/S0022112068000133

Bhagowati, B., & Ahamad, K. U. (2019). A review on lake eutrophication dynamics and recent developments in lake modeling. *Ecohydrology and Hydrobiology*, *19*(1), 155–166. https://doi.org/10.1016/j.ecohyd.2018.03.002

Björk, S. (1972). Swedish lake restoration program gets results. *Ambio*, *1*(5), 153–165. Retrieved July 7, 2025, from http://www.jstor.org/stable/4311973

Bogoyavlensky, V., Bogoyavlensky, I., Nikonov, R., & Kishankov, A. (2020). Complex of geophysical studies of the seyakha catastrophic gas blowout crater on the yamal peninsula, russian arctic. *Geosciences (Switzerland)*, *10*. https://doi.org/10.3390/geosciences10060215

Bolpagni, R., Bresciani, M., Laini, A., Pinardi, M., Matta, E., Ampe, E. M., Giardino, C., Viaroli, P., & Bartoli, M. (2014). Remote sensing of phytoplankton-macrophyte coexistence in shallow hypereutrophic fluvial lakes. *Hydrobiologia*, *737*(1), 67–76. https://doi.org/10.1007/s10750-013-1800-6

Borrelli, P., Van Oost, K., Meusburger, K., Alewell, C., Lugato, E., & Panagos, P. (2018). A step towards a holistic assessment of soil degradation in Europe: Coupling on-site erosion with sediment transfer and carbon fluxes. *Environmental Research*, *161*, 291–298. https://doi.org/10.1016/j.envres.2017.11.009

Bouffard, D., Doda, T., Ramón, C. L., & Ulloa, H. N. (2025). Thermally driven cross-shore flows in stratified basins: A review on the thermal siphon dynamics. *Flow*, *5*, E1. https://doi.org/10.1017/flo.2024.31

Bresciani, M., Giardino, C., Fabbretto, A., Pellegrino, A., Mangano, S., Free, G., & Pinardi, M. (2022). Application of New Hyperspectral Sensors in the Remote Sensing of Aquatic Ecosystem Health: Exploiting PRISMA and DESIS for Four Italian Lakes. *Resources*, *11*(2). https://doi.org/10.3390/resources11020008

Bresciani, M., Pinardi, M., Free, G., Luciani, G., Ghebrehiwot, S., Laanen, M., Peters, S., Bella, V. D., Padula, R., & Giardino, C. (2020). The use of multisource optical sensors to study phytoplankton spatio-temporal variation in a Shallow Turbid Lake. *Water (Switzerland)*, *12*(1), 9–11. https://doi.org/10.3390/w12010284

Broere, S., van Emmerik, T., González-Fernández, D., Luxemburg, W., de Schipper, M., Cózar, A., & van de Giesen, N. (2021). Towards underwater macroplastic monitoring using echo sounding. *Frontiers in Earth Science*, *9*. https://doi.org/10.3389/feart.2021.628704

Brothers, S., Kazanjian, G., Köhler, J., Scharfenberger, U., & Hilt, S. (2017). Convective mixing and high littoral production established systematic errors in the diel oxygen curves of a shallow, eutrophic lake. *Limnology and Oceanography: Methods*, *15*(5), 429–435. https://doi.org/10.1002/lom3.10169

Brusa, G. (2018). *Monitoraggio di* Nelumbo nucifera *(Riserva Palude Brabbia) e di* Ludwigia hexapetala *(ZPS Lago di Varese) Relazione tecnica finale*. Progetto Rete Biodiversità.

Caraco, N., Cole, J., Findlay, S., & Wigand, C. (2006). Vascular Plants as Engineers of Oxygen in Aquatic Systems. *BioScience*, *56*(3), 219–225.

Caraco, N. F., & Cole, J. J. (2002). Contrasting impacts of a native and alien macrophyte on dissolved oxygen in a large river. *Ecological Applications*, *12*(5), 1496–1509. https://doi.org/10.1890/1051-0761(2002)012[1496:CIOANA]2.0.CO;2

Caroppi, G., Västilä, K., Järvelä, J., Lee, C., Ji, U., Kim, H. S., & Kim, S. (2022). Flow and wake characteristics associated with riparian vegetation patches: Results from field-scale experiments. *Hydrological Processes*, *36*(2). https://doi.org/10.1002/hyp.14506

Carpenter, S. R., Caraco, N. F., Correll, D. L., Howarth, R. W., Sharpley, A. N., & Smith, V. H. (1998). Nonpoint Pollution of Surface Waters With Phosphorus and Nitrogen. *Ecological Applications*, *8*(3), 559–568.

Carpenter, S. R., & Lodge, D. M. (1986). Effects of submersed macrophytes on ecosystem processes. *Aquatic Botany*, 341–370.

Cattaneo, A., Galanti, G., Gentinetta, S., & Susana, A. (1998). Epiphytic algae and macroinvertebrates on submerged and floating-leaved macrophytes in an

Italian lake. *Freshwater Biology*, *39*(4), 725–740. https://doi.org/10.1046/j.1365-2427.1998.00325.x

Clark, J. F., Simpson, H. J., Bopp, R. F., & Deck, B. L. (1995). Dissolved Oxygen in Lower Hudson Estuary: 1978–93. *Journal of Environmental Engineering*, *121*(10), 760–763. https://doi.org/10.1061/(ASCE)0733-9372(1995)121:10(760)

Conley, D. J., Paerl, H. W., Howarth, R. W., Boesch, D. F., Seitzinger, S. P., Havens, K. E., Lancelot, C., & Likens, G. E. (2009). Ecology - Controlling eutrophication: Nitrogen and phosphorus. *Science*, *323*(5917), 1014–1015. https://doi.org/10.1126/science.1167755

Cooke, G. D., Welch, E. B., Peterson, S., & Nichols, S. A. (2016). Restoration and management of lakes and reservoirs. https://doi.org/10.1201/9781420032109

Directive 2000/60/EC of the European Parliament and of the Council Establishing a Framework for the Community Action in the Field of Water Policy (2000). Retrieved December 13, 2022, from https://ec.europa.eu/environment/water/water-framework/index_en.html

Craig, H., Wharton, R. A., & McKay, C. P. (1992). Oxygen supersaturation in ice-covered antarctic lakes: Biological versus physical contributions. *Science*, *255*(5042), 318–321. https://doi.org/10.1126/science.11539819

Dale, H. M., & Gillespie, T. (1976). The influence of floating vascular plants on the diurnal fluctuations of temperature near the water surface in early spring. *Hydrobiologia*, *49*, 245–256.

Dale, H. M., & Gillespie, T. J. (1977). The influence of submersed aquatic plants on temperature gradients in shallow water bodies. *Can. J. Bot*, *55*, 2216–2225.

Dalmiglio, A., Grespi, F., Bonisoli, F., & Galbiati, M. (2005). *Laghi di Mantova: Studio della qualità di acque superficiali e sedimenti* (tech. rep.). ARPA Lombardia.

De Vincenzi, M. (2022). *Realizzazione della batimetria del Lago Superiore (MN) tramite misure di campo e successiva modellazione idraulica con la forzante meteorologica* [Master's thesis, Università di Trento].

Deepersonar. (2023). *Basics for boat and kayak fishing with deeper*. Retrieved April 20, 2025, from https://support.deeper.eu/925283-Basics-for-Boat-and-Kayak-fishing-with-Deeper-Deeper-PROCHIRP-models

Diaconu, D. C., Bretcan, P., Peptenatu, D., Tanislav, D., & Mailat, E. (2019). The importance of the number of points, transect location and interpolation techniques in the analysis of bathymetric measurements. *Journal of Hydrology*, *570*, 774–785. https://doi.org/10.1016/j.jhydrol.2018.12.070

Doda, T., Ramón, C. L., Ulloa, H. N., Wüest, A., & Bouffard, D. (2022). Seasonality of density currents induced by differential cooling. *Hydrology and Earth System Sciences*, *26*(2), 331–353. https://doi.org/10.5194/hess-26-331-2022

EPPO Global Database. (2022). *Invasive alien plants in romania* (tech. rep.). European and Mediterranean Plant Protection Organization.

ERSAF. (2004). *Suoli e paesaggi della provincia di mantova* (tech. rep.). Ente Regionale per i Servizi all'Agricoltura e alle Foreste.

Faggioli, M., Severini, E., Magri, M., Bolpagni, R., Pinardi, M., Ferrari, C., & Bartoli, M. (2022). *Analisi ecologiche e misure di portata per la definizione dei fattori correttivi nel calcolo dei deflussi nel Mincio e la calibrazione dei sistemi di misura* (tech. rep.). Università di Parma.

Fenocchi, A. (2015). *Circulation dynamics in a shallow fluvial lake - The case of the Superior Lake of Mantua* [Doctoral dissertation, Università di Pavia].

Folkard, A. M. (2011). Vegetated flows in their environmental context: A review. *Proceedings of the Institution of Civil Engineers - Engineering and Computational Mechanics*, *164*(1), 3–24. https://doi.org/10.1680/eacm.8.00006

Frodge, J. D., Thomas, G. L., & Pauley, G. B. (1991). Sediment Phosphorus Loading Beneath Dense Canopies of Aquatic Macrophytes. *Lake and Reservoir Management*, *7*(1), 61–71. https://doi.org/10.1080/07438149109354255

Giambastiani, Y., Giusti, R., Cecchi, S., Palomba, F., Manetti, F., Romanelli, S., & Bottai, L. (2020). Volume estimation of lakes and reservoirs based on aquatic drone surveys: The case study of Tuscany, Italy. *Journal of Water and Land Development*, *46*, 84–96. https://doi.org/10.24425/jwld.2020.134200

Gunawan, B., Sterling, M., & Knight, D. W. (2009). Using an acoustic Doppler current profiler in a small river. *Water and Environment Journal*, *24*(2), 147–158. https://doi.org/10.1111/j.1747-6593.2009.00170.x

Gunawan, B., & Neary, V. S. (2011, September). *ORNL ADCP post-processing guide and Matlab algorithms for MHK site flow and turbulence analysis* (tech. rep. No. ORNL/TM-2011/404, 1034379). https://doi.org/10.2172/1034379

Han, L., Zeng, Y., Chen, L., & Li, M. (2018). Modeling streamwise velocity and boundary shear stress of vegetation-covered flow. *Ecological Indicators*, *92*, 379–387. https://doi.org/10.1016/J.ECOLIND.2017.04.012

Harris, G. (1999). This is not the end of limnology (or of science): The world may well be a lot simpler than we think. *Freshwater Biology*, *42*(4), 689–706. https://doi.org/10.1046/j.1365-2427.1999.00486.x

Haygarth, P. M., Wood, F. L., Heathwaite, A. L., & Butler, P. J. (2005). Phosphorus dynamics observed through increasing scales in a nested headwater-to-river

channel study. *Science of the Total Environment*, *344*, 83–106. https://doi.org/10.1016/j.scitotenv.2005.02.007

Hilton, J., O'Hare, M., Bowes, M. J., & Jones, J. I. (2006). How green is my river? A new paradigm of eutrophication in rivers. *Science of The Total Environment*, *365*(1–3), 66–83. https://doi.org/10.1016/J.SCITOTENV.2006.02.055

Hinegk, L. (2022). *Long-term evolution of highly regulated basins and water management policies to support their ecosystem services* [Doctoral dissertation, University of Trento].

Hosper, H. (1997). *Clearing Lakes. An ecosystem approach to the restoration and management of shallow lakes in the Netherland*. Ministry of Transport, Public Works and Water Management. Institute for Inland Water Management and Waste Water Treatmente (RIZA). Leystad, the Netherlands.

ISPRA. (2009). *Valutazione dei risultati della caratterizzazione ambientale dell'area lacuale del Sito di Bonifica di Interesse Nazionale "Laghi di Mantova e Polo Chimico"*. Istituto Superiore per la Protezione e la Ricerca Ambientale (ISPRA).

Istituto Idrografico della Marina. (2023). *Disciplinare tecnico per l'esecuzione e la standardizzazione dei rilievi idrografici*.

James, F., Barko, J. W., & Eakin, H. L. (1994). Convective water exchanges during differential cooling and heating: Implications for dissolved constituent transport. *Hydrobiologia*, *294*, 167–176.

James, W. F., & Barko, J. W. (1991). Estimation of phosphorus exchange between littoral and pelagic zones during nighttime convective circulation. *Limnology and Oceanography*, *36*(1), 179–187. https://doi.org/10.4319/lo.1991.36.1.0179

Jane, S. F., Hansen, G. J. A., Kraemer, B. M., Leavitt, P. R., Mincer, J. L., North, R. L., Pilla, R. M., Stetler, J. T., Williamson, C. E., Woolway, R. I., Arvola, L., Chandra, S., DeGasperi, C. L., Diemer, L., Dunalska, J., Erina, O., Flaim, G., Grossart, H.-P., Hambright, K. D., ... Rose, K. C. (2021). Widespread deoxygenation of temperate lakes. *Nature*, *594*(7861), 66–70. https://doi.org/10.1038/s41586-021-03550-y

Jurgiel, B. (2022). *Point sampling tool plugin: Samples polygon attributes and raster values from multiple layers at specified sampling points*. Retrieved April 19, 2025, from https://github.com/borysiasty/pointsamplingtool

Kathleen A., D., Tom, J., & Adam, K. (1992). Dry-bulk density: Its use and determination. In B. Taylor & K. Fujioka (Eds.), *Proceedings of the ocean drilling program, scientific results* (Vol. 126). Ocean Drilling Program. https://doi.org/10.2973/odp.proc.sr.126.1992

Kellerer-Pirklbauer, A., Avian, M., Benn, D. I., Bernsteiner, F., Krisch, P., & Ziesler, C. (2021). Buoyant calving and ice-contact lake evolution at Pasterze Glacier (Austria) in the period 1998-2019. *Cryosphere*, *15*, 1237–1258. https://doi.org/10.5194/tc-15-1237-2021

Knoll, L. B., Fisher, T. J., Vanni, M. J., & Youngblade, E. G. (2025). Long-term Deepwater Dissolved Oxygen Dynamics in a Hypereutrophic Reservoir Following Shifts in Watershed Management and Lake Warming. *Ecosystems*, *28*(5), 48. https://doi.org/10.1007/s10021-025-00996-3

Koutalakis, P., & Zaimes, G. N. (2022). River flow measurements utilizing uav-based surface velocimetry and bathymetry coupled with sonar. *Hydrology*, *9*. https://doi.org/10.3390/hydrology9080148

Kumar, P., & Sharma, A. (2022). Experimental investigation of 3D flow properties around emergent rigid vegetation. *Ecohydrology*, *15*(8). https://doi.org/10.1002/eco.2474

Kunii, H., & Maeda, K. (1982). Seasonal and long-term changes in surface cover of aquatic plants in a shallow pond, Ojaga-ike, Chiba, Japan. *Hydrobiologia*, *87*(1), 45–55. https://doi.org/10.1007/BF00016661

Langone, L. (2009). *Studio radiochimico dei sedimenti inclusi nel SIN dei laghi di Mantova e Polo Chimico, volto a determinare le velocità di sedimentazione dell'area e l'evoluzione temporale dell'inquinamento antropico*. CNR-ISMAR.

Latinopoulos, D., Sidiropoulos, P., & Kagalou, I. (2018). Gap Analysis Targeting WFD Monitoring and Pressure Mapping: Lessons Learned from "EcoSUSTAIN", Interreg-MED Project. *EWaS3 2018*, 621. https://doi.org/10.3390/proceedings2110621

Lee, S.-D., Kim, H., Cho, B.-G., & Lee, G.-G. (2021). Characteristics and Management Plan for the Distribution of Nelumbo nucifera community in Junam Wetland. *Journal of People, Plants, and Environment*, *24*(5), 469–483. https://doi.org/10.11628/ksppe.2021.24.5.469

Lewis, W. M., & Wurtsbaugh, W. A. (2008). Control of lacustrine phytoplankton by nutrients: Erosion of the phosphorus paradigm. *International Review of Hydrobiology*, *93*(4–5), 446–465. https://doi.org/10.1002/iroh.200811065

Lin, Y. T., & Wu, C. H. (2014). The role of rooted emergent vegetation on periodically thermal-driven flow over a sloping bottom. *Environmental Fluid Mechanics*, *14*(6), 1303–1334. https://doi.org/10.1007/s10652-014-9336-5

Longhi, D., Bartoli, M., & Viaroli, P. (2008). Decomposition of four macrophytes in wetland sediments: Organic matter and nutrient decay and associated benthic processes. *Aquatic Botany*, *89*(3), 303–310. https://doi.org/10.1016/j.aquabot.2008.03.004

Lövstedt, C. B., & Bengtsson, L. (2008). Density-driven current between reed belts and open water in a shallow lake. *Water Resources Research*, *44*(10). https://doi.org/10.1029/2008WR006949

Marsden, M. (2006). Lake restoration by reducing external phosphorus loading: The influence of sediment phosphorus release. *Freshwater Biology*, *21*, 139–162. https://doi.org/10.1111/j.1365-2427.1989.tb01355.x

McArley, T. J., Sandblom, E., & Herbert, N. A. (2021). Fish and hyperoxia—From cardiorespiratory and biochemical adjustments to aquaculture and ecophysiology implications. *Fish and Fisheries*, *22*(2), 324–355. https://doi.org/10.1111/faf.12522

Michael, C., & John, F. (1994). The radiatively driven natural convection beneath a floating plant layer. *Limnology and Oceanography*, *39*(5), 1186–1194. https://doi.org/10.4319/lo.1994.39.5.1186

Moki, H., Taguchi, K., Nakagawa, Y., Montani, S., & Kuwae, T. (2020). Spatial and seasonal impacts of submerged aquatic vegetation (SAV) drag force on hydrodynamics in shallow waters. *Journal of Marine Systems*, *209*. https://doi.org/10.1016/j.jmarsys.2020.103373

Monismith, S. G., Imberger, J., & Morison, M. L. (1990). Convective motions in the sidearm of a small reservoir. *Limnology and Oceanography*, *35*(8), 1676–1702. https://doi.org/10.4319/lo.1990.35.8.1676

Moore, B. C., Funk, W. H., & Anderson, E. (1994). Water Quality, Fishery, and Biologic Characteristics in a Shallow, Eutrophic Lake with Dense Macrophyte Populations. *Lake and Reservoir Management*, *8*(2), 175–188. https://doi.org/10.1080/07438149409354469

Muste, M., Yu, K., Pratt, T., & Abraham, D. (2004a). Practical aspects of ADCP data use for quantification of mean river flow characteristics; Part II: Fixed-vessel measurements. *Flow Measurement and Instrumentation*, *15*(1), 17–28. https://doi.org/10.1016/j.flowmeasinst.2003.09.002

Muste, M., Yu, K., & Spasojevic, M. (2004b). Practical aspects of ADCP data use for quantification of mean river flow characteristics; Part I: Moving-vessel measurements. *Flow Measurement and Instrumentation*, *15*(1), 1–16. https://doi.org/10.1016/j.flowmeasinst.2003.09.001

Nepf, H. M. (1999). Drag, turbulence, and diffusion in flow through emergent vegetation. *Water Resources Research*, *35*(2), 479–489. https://doi.org/10.1029/1998WR900069

Nepf, H. M., & Vivoni, E. R. (2000). Flow structure in depth-limited, vegetated flow. *Journal of Geophysical Research: Oceans*, *105*(C12), 28547–28557. https://doi.org/10.1029/2000jc900145

Nepf, H. M. (2012). Hydrodynamics of vegetated channels. *Journal of Hydraulic Research*, *50*(3), 262–279. https://doi.org/10.1080/00221686.2012.696559

Nohara, S., & Tsuchiya, T. (1990). Effects of water level fluctuation on the growth of *Nelumbo nucifera* Gaertn. in Lake Kasumigaura, Japan. *Ecological Research*, *5*(2), 237–252. https://doi.org/10.1007/BF02346994

Oberg, K., & Mueller, D. S. (2007). Validation of Streamflow Measurements Made with Acoustic Doppler Current Profilers. *Journal of Hydraulic Engineering*, *133*(12), 1421–1432. https://doi.org/10.1061/(ASCE)0733-9429(2007)133:12(1421)

O'Donncha, F., Hartnett, M., & Plew, D. R. (2015). Parameterizing suspended canopy effects in a three-dimensional hydrodynamic model. *Journal of Hydraulic Research*, *53*(6), 714–727. https://doi.org/10.1080/00221686.2015.1093036

Oglesby, R. T., & Edmondson, W. T. (1966). Control of Eutrophication. *Journal (Water Pollution Control Federation)*.

Oldham, C. E., & Sturman, J. J. (2001). The effect of emergent vegetation on convective flushing in shallow wetlands: Scaling and experiments. *Limnology and Oceanography*, *46*(6), 1486–1493. https://doi.org/10.4319/lo.2001.46.6.1486

Ozan, A. Y., & Yilmazer, D. (2020). Near-wake flow structure of a suspended cylindrical canopy patch. *Water (Switzerland)*, *12*(1). https://doi.org/10.3390/w12010084

Pan, L., Jiang, R., Yang, X., Zhou, H., Cai, J., Li, N., & Wang, J. (2022). Experimental study on the disturbance effect of flexible vegetation patches of different shapes on slow-flow water body. *International Journal of Environmental Science and Technology*, 1–18. https://doi.org/10.1007/S13762-022-04166-Z/TABLES/2

Panagos, P., Borrelli, P., Poesen, J., Ballabio, C., Lugato, E., Meusburger, K., Montanarella, L., & Alewell, C. (2015). The new assessment of soil loss by water erosion in Europe. *Environmental Science & Policy*, *54*, 438–447. https://doi.org/10.1016/j.envsci.2015.08.012

Panagos, P., Matthews, F., Patault, E., De Michele, C., Quaranta, E., Bezak, N., Kaffas, K., Patro, E. R., Auel, C., Schleiss, A. J., Fendrich, A., Liakos, L., Van Eynde, E., Vieira, D., & Borrelli, P. (2024). Understanding the cost of soil erosion: An assessment of the sediment removal costs from the reservoirs of the European Union. *Journal of Cleaner Production*, *434*, 140183. https://doi.org/10.1016/j.jclepro.2023.140183

Papastergiadou, E. S., Retalis, A., Kalliris, P., & Georgiadis, T. (2007). Land use changes and associated environmental impacts on the Mediterranean shallow

Lake Stymfalia, Greece. *Hydrobiologia*, *584*(1), 361–372. https://doi.org/10.1007/s10750-007-0606-9

Pasinato, M. (2020). *Analisi per una gestione alternativa della risorsa idrica del nodo idraulico di Pozzolo (fiume Mincio)* [Master's thesis, Università di Trento].

Perera, D., Williams, S., & Smakhtin, V. (2023). Present and Future Losses of Storage in Large Reservoirs Due to Sedimentation: A Country-Wise Global Assessment. *Sustainability*, *15*, 219.

Peters, R. (1990). Pathologies in limnology. *Mem. Ist. Ital. Idrobiol*, *47*, 181–217.

Pinardi, M. (2008). *Autotrofia ed eterotrofia in un sistema fluviale e lacustre eutrofico: Bilanci di massa dei gas disciolti e dei nutrienti, ruolo della vegetazione macrofitica sommersa ed elofitica, del fitoplancton e dei tempi di residenza idraulica.* [Doctoral dissertation, Università di Parma].

Pinardi, M., Bartoli, M., Longhi, D., Marzocchi, U., Laini, A., Ribaudo, C., & Viaroli, P. (2009). Benthic metabolism and denitrification in a river reach: A comparison between vegetated and bare sediments. *J. Limnol*, *68*(1), 133–145.

Pinardi, M., Bresciani, M., Villa, P., Cazzaniga, I., Laini, A., Tóth, V., Fadel, A., Austoni, M., Lami, A., & Giardino, C. (2018). Spatial and temporal dynamics of primary producers in shallow lakes as seen from space: Intra-annual observations from Sentinel-2A. *Limnologica*, *72*, 32–43. https://doi.org/10.1016/j.limno.2018.08.002

Pinardi, M., Soana, E., Bresciani, M., Villa, P., & Bartoli, M. (2020). Upscaling nitrogen removal processes in fluvial wetlands and irrigation canals in a patchy agricultural watershed. *Wetlands Ecology and Management*, *28*(2), 297–313. https://doi.org/10.1007/s11273-020-09714-3

Pinardi, M., Villa, P., Free, G., Giardino, C., & Bresciani, M. (2021). Evolution of Native and Alien Macrophytes in a Fluvial-wetland System Using Long-term Satellite Data. *Wetlands*, *41*(1). https://doi.org/10.1007/s13157-021-01395-9

Pokorný, J., & Rejmánková, E. (1983). Oxygen regime in a fishpond with duckweeds (lemnaceae) and Ceratophyllum. *Aquatic Botany*, *17*(2), 125–137. https://doi.org/10.1016/0304-3770(83)90109-2

Provincia di Mantova. (2004). *Qualità delle acque superficiali nella provincia di Mantova: Dati misurati e considerazioni critiche sull'impatto delle attività antropiche* (tech. rep.). Area ambientale Servizio Acque e Suolo. Mantova.

Read, J. S., Hamilton, D. P., Jones, I. D., Muraoka, K., Winslow, L. A., Kroiss, R., Wu, C. H., & Gaiser, E. (2011). Derivation of lake mixing and stratification indices from high-resolution lake buoy data. *Environmental Modelling & Software*, *26*(11), 1325–1336. https://doi.org/10.1016/j.envsoft.2011.05.006

Rennella, A. M., & Quirós, R. (2006). The effects of hydrology on plankton biomass in shallow lakes of the Pampa Plain. *Hydrobiologia*, *556*(1), 181–191. https://doi.org/10.1007/s10750-005-0318-y

Ribaudo, C., Bartoli, M., Longhi, D., Castaldi, S., Neubauer, S. C., & Viaroli, P. (2012). CO2 and CH4 fluxes across a *nuphar* lutea (L.) Sm. stand. *Journal of Limnology*, *71*(1), 200–210. https://doi.org/10.4081/jlimnol.2012.e21

Robertson, D. M., & Imberger, J. (1994). Lake Number, a Quantitative Indicator of Mixing Used to Estimate Changes in Dissolved Oxygen. *Internationale Revue der gesamten Hydrobiologie und Hydrographie*, *79*(2), 159–176. https://doi.org/10.1002/iroh.19940790202

Rocha, S. M. G., Armstrong, A., Thackeray, S. J., Hernandez, R. R., & Folkard, A. M. (2024). Environmental impacts of floating solar panels on freshwater systems and their techno-ecological synergies. *Environmental Research: Infrastructure and Sustainability*, *4*(4), 042002. https://doi.org/10.1088/2634-4505/ad8e81

Ruffell, A., Lally, A., & Rocke, B. (2021). Dronar—geoforensic search sonar from a drone. *Forensic Sciences*, *1*, 202–212. https://doi.org/10.3390/forensicsci1030018

Salmaso, N., & Mosello, R. (2022). Limnological research in the deep southern subalpine lakes: Synthesis, directions and perspectives. *Advances in oceanography and limnology*, *1*(1), 29–66. https://doi.org/10.1080/19475721003735773

Sanjou, M., Kato, K., Aizawa, W., & Okamoto, T. (2022). Development of drone-type float for surface-velocity measurement in rivers. *Environmental Fluid Mechanics*, *22*, 955–969. https://doi.org/10.1007/s10652-022-09874-1

Scheffer, M. (2004). *Ecology of shallow lakes*. Springer Netherlands. https://doi.org/10.1007/978-1-4020-3154-0

Schindler, D. W. (1974). Eutrophication and recovery in experimental lakes: Implications for lake management. *Science*, *184*(4139), 897–899. https://doi.org/10.1126/science.184.4139.897

Schindler, D. W. (1978). Factors regulating phytoplankton production and standing crop in the world's freshwaters. *Limnology and Oceanography*, *23*(3), 478–486. https://doi.org/10.4319/lo.1978.23.3.0478

Schindler, D. W. (2006). Recent advances in the understanding and management of eutrophication. *Limnology and Oceanography*, *51*, 356–363.

Schindler, D. W., Hecky, R. E., Findlay, D. L., Stainton, M. P., Parker, B. R., Paterson, M. J., Beaty, K. G., Lyng, M., & Kasian, S. E. (2008). Eutrophication of lakes cannot be controlled by reducing nitrogen input: Results of a 37-year whole-ecosystem experiment. *Proceedings of the National Academy of Sciences of the United States of America*, *105*(32), 11254–11258. https:

//doi.org/10.1073/PNAS.0805108105/SUPPL_FILE/0805108105SI.PDF National Academy of Sciences.

Severini, E., Bartoli, M., Pinardi, M., & Celico, F. (2022). Short-Term Effects of the EU Nitrate Directive Reintroduction: Reduced N Loads to River from an Alluvial Aquifer in Northern Italy. *Hydrology*, *9*(3). https://doi.org/10.3390/hydrology9030044

Sharip, Z., Hipsey, M. R., Schooler, S. S., & Hobbs, R. J. (2012). Physical circulation and spatial exchange dynamics in a shallow floodplain wetland. *International Journal of Design and Nature and Ecodynamics*, *7*(3), 274–291. https://doi.org/10.2495/DNE-V7-N3-274-291

Søndergaard, M., Jensen, J. P., & Jeppesen, E. (2003). Role of sediment and internal loading of phosphorus in shallow lakes. *Hydrobiologia*, *506*, 135–145.

Stephan, U., & Gutknecht, D. (2002). Hydraulic resistance of submerged flexible vegetation. *Journal of Hydrology*, *269*(1–2), 27–43. https://doi.org/10.1016/S0022-1694(02)00192-0

Sturman, J. J., Oldham, C. E., & Ivey, G. N. (1999). Steady convective exchange flows down slopes. *Aquatic Sciences*.

Tallis, J. H. (1973). The Terrestrialization of Lake Basins in North Cheshire, with Special Reference to the Development of a 'Schwingmoor' Structure. *The Journal of Ecology*, *61*(2), 537. https://doi.org/10.2307/2259044

Teledyne RD Instruments. (2007). *Workhorse RioGrande Technical manual*.

Teledyne RD Instruments. (2011). Acoustic Doppler Current Profiler Principles of Operation. A Practical Primer.

Teledyne RD Instruments. (2013). *Workhorse RioGrande ADCP guide*.

Teledyne RD Instruments. (2021). *StreamPro ADCP Guide*.

Telò, R., & Menna, D. (2016). *Valli del Mincio un "EDEN" di natura d'Europa – interventi di ripristino idrodinamico per il potenziamento della navigazione turistica e dei percorsi in canoa*. Parco del Mincio.

Telò, R., Pinardi, M., Bartoli, M., Bodini, A., Viaroli, P., Racchetti, E., Cuizzi, D., Vannuccini, M., & Previdi, L. (2007). *Progetto " Da Agenda 21 ad Azione 21 " Caratterizzazione dello stato ambientale del fiume Mincio e analisi della strategia di riqualificazione integrata e partecipata* (tech. rep.). Parco del Mincio.

Temmerman, S., Bouma, T. J., Govers, G., Wang, Z. B., De Vries, M. B., & Herman, P. M. (2005). Impact of vegetation on flow routing and sedimentation patterns: Three-dimensional modeling for a tidal marsh. *Journal of Geophysical Research: Earth Surface*, *110*(4). https://doi.org/10.1029/2005JF000301

Toffolon, M., & Todeschini, I. (2006). Channel competition in tidal flats. *River, Coastal and Estuarine Morphodynamics: RCEM 2005 – Parker & García (eds)*, 653–661. https://doi.org/10.1201/9781439833896

Tombor, E., Korponai, J. L., Zsigmond, A.-R., Ofosu-Brakoh, A. A., Szalai, Z., Bede-Fazekas, Á., & Magyari, E. K. (2026). Response of a shallow water reservoir to anthropogenic stressors: Implications for the water supply of Lake Velence, a major recreational lake in Hungary. *Hydrobiologia*, *853*(9), 2769–2794. https://doi.org/10.1007/s10750-026-06111-4

Tóth, V. R., Villa, P., Pinardi, M., & Bresciani, M. (2019). Aspects of invasiveness of *Ludwigia* and *Nelumbo* in shallow temperate fluvial lakes. *Frontiers in Plant Science*, *10*, 1–13. https://doi.org/10.3389/fpls.2019.00647

Trapani, K., & Redón Santafé, M. (2015). A review of floating photovoltaic installations: 2007–2013. *Progress in Photovoltaics: Research and Applications*, *23*(4), 524–532. https://doi.org/10.1002/pip.2466

Ulloa, H. N., Ramón, C. L., Doda, T., Wüest, A., & Bouffard, D. (2022). Development of overturning circulation in sloping waterbodies due to surface cooling. *Journal of Fluid Mechanics*, *930*, A18. https://doi.org/10.1017/jfm.2021.883

Valerio, C. (2017). *Uso della risorsa idrica e gestione dei manufatti idraulici nel bilancio idrico del fiume Mincio*.

Van Haren, H. (2009). Using high sampling-rate ADCP for observing vigorous processes above sloping [deep] ocean bottoms. *Journal of Marine Systems*, *77*(4), 418–427. https://doi.org/10.1016/j.jmarsys.2008.10.012

Vannuccini, M., Pinardi, M., & Bartoli, M. (2011). Valutazione dello stato di qualità ambientale del fiume Mincio con il metodo STRARIFLU modificato. *Biologia Ambientale*, *25*(2), 33–46.

Verstraeten, G., & Poesen, J. (2002). Using sediment deposits in small ponds to quantify sediment yield from small catchments: Possibilities and limitations. *Earth Surface Processes and Landforms*, *27*(13), 1425–1439. https://doi.org/10.1002/esp.439

Villa, P., Pinardi, M., Bolpagni, R., Gillier, J. M., Zinke, P., Nedelcuţ, F., & Bresciani, M. (2018). Assessing macrophyte seasonal dynamics using dense time series of medium resolution satellite data. *Remote Sensing of Environment*, *216*, 230–244. https://doi.org/10.1016/j.rse.2018.06.048

Villa, P., Pinardi, M., Tóth, V. R., Hunter, P. D., Bolpagni, R., & Bresciani, M. (2017). Remote sensing of macrophyte morphological traits: Implications for the management of shallow lakes. *Journal of Limnology*, *76*(S1), 109–126. https://doi.org/10.4081/jlimnol.2017.1629

Vollenweider, R. A. (1968). *Scientific fundamentals of the eutrophication of lakes and flowing waters, with particular reference to nitrogen and phosphorus as factors in eutrophication* (No. 35). Organisation for Economic Co-operation and Development.

Vozza, G., Costantino, D., Pepe, M., & Alfio, V. S. (2023). Smart sensors system based on smartphones and methodology for 3d modelling in shallow water scenarios. *Applied System Innovation*, *6*. https://doi.org/10.3390/asi6010028

Walker, D., Shutler, J. D., Morrison, E. H., Harper, D. M., Hoedjes, J. C., & Laing, C. G. (2022). Quantifying water storage within the north of lake naivasha using sonar remote sensing and landsat satellite data. *Ecohydrology and Hydrobiology*, *22*, 12–20. https://doi.org/10.1016/j.ecohyd.2021.07.011

Welch, E., & Patmont, C. (1980). Lake restoration by dilution: Moses lake, washington. *Water Research*, *14*(9), 1317–1325. https://doi.org/https://doi.org/10.1016/0043-1354(80)90192-X

Woolway, R. I., Zhao, G., Rocha, S. M. G., Thackeray, S. J., & Armstrong, A. (2024). Decarbonization potential of floating solar photovoltaics on lakes worldwide. *Nature Water*, *2*(6), 566–576. https://doi.org/10.1038/s44221-024-00251-4

Xu, Z., & Xu, Y. J. (2015). Determination of Trophic State Changes with Diel Dissolved Oxygen: A Case Study in a Shallow Lake. *Water Environment Research*, *87*(11), 1970–1979. https://doi.org/10.2175/106143015X14362865226716

Yang, H., He, S., Feng, Q., Liu, Z., Xia, S., Zhou, Q., Wu, Z., & Zhang, Y. (2024). Lotus (*nelumbo nucifera*): A multidisciplinary review of its cultural, ecological, and nutraceutical significance. *Bioresources and Bioprocessing*, *11*(1), 18. https://doi.org/10.1186/s40643-024-00734-y

Yang, P., Chua, L. H., Irvine, K. N., Nguyen, M. T., & Low, E. W. (2022). Impacts of a floating photovoltaic system on temperature and water quality in a shallow tropical reservoir. *Limnology*, *23*(3), 441–454. https://doi.org/10.1007/s10201-022-00698-y

Zarrinabadi, E., Lobb, D. A., Enanga, E., Badiou, P., & Creed, I. F. (2023a). Agricultural activities lead to sediment infilling of wetlandscapes in the Canadian Prairies: Assessment of soil erosion and sedimentation fluxes. *Geoderma*, *436*. https://doi.org/10.1016/j.geoderma.2023.116525

Zarrinabadi, E., Lobb, D. A., Li, S., Koiter, A. J., & Badiou, P. (2023b). Agricultural activities lead to sediment infilling of wetlandscapes in the Canadian Prairies: Assessment of contributions by tillage, water and wind erosion. *Geoderma*, *438*. https://doi.org/10.1016/j.geoderma.2023.116621

Zhang, X., & Nepf, H. M. (2009). Thermally driven exchange flow between open water and an aquatic canopy. *Journal of Fluid Mechanics*, *632*, 227–243. https://doi.org/10.1017/S0022112009006491

Zhang, X., & Nepf, H. M. (2011). Exchange flow between open water and floating vegetation. *Environmental Fluid Mechanics*, *11*(5), 531–546. https://doi.org/10.1007/s10652-011-9213-4

Zhang, Y., Cui, B., Lan, Y., Han, Z., Wang, T., & Guo, A. (2012). Four terrestrialization characteristics of Baiyangdian Lake, China. *Procedia Environmental Sciences*, *13*, 645–654. https://doi.org/10.1016/j.proenv.2012.01.056

Zhou, X., Feng, D., Wen, C., & Liu, D. (2018). Decomposition dynamic of two aquatic macrophytes *Trapa bispinosa* Roxb. and *Nelumbo nucifera* detritus. *Environmental Science and Pollution Research*, *25*(16), 16177–16191. https://doi.org/10.1007/s11356-018-1754-3